

NASA Contractor Report 3553

NASA
CR
3553
c. 1

TECH LIBRARY KAFB, NM
0062190

Mathematical Models for the Synthesis and Optimization of Spiral Bevel Gear Tooth Surfaces

F. L. Litvin, Pernez Rahman,
and Robert N. Goldrich

THIS COPY, DESIGN OR
DRAWING IS THE PROPERTY OF
NASA AND IS TO BE RETURNED TO
NASA

GRANT NAG-348
JUNE 1982

NASA





NASA Contractor Report 3553

Mathematical Models for the Synthesis and Optimization of Spiral Bevel Gear Tooth Surfaces

F. L. Litvin, Pernez Rahman,
and Robert N. Goldrich

*University of Illinois at Chicago Circle
Chicago, Illinois*

Prepared for
Lewis Research Center
under Grant NAG-348



National Aeronautics
and Space Administration

**Scientific and Technical
Information Office**

1982

TABLE OF CONTENTS

	Page
SUMMARY.....	1
1. BASIC METHODS OF INVESTIGATION.....	4
1.1 General Kinematic Relations.....	4
1.2 Transfer Velocity.....	10
1.3 Relative Velocity of Contact Points.....	14
1.4 The General Law of Gearings.....	18
1.5 Contact Lines, Surface of Action, The Enveloped Surface.....	24
1.6 Relations Between Principal Curvatures and Directions of Two Surfaces Being in Meshing.....	37
1.7 Contact Ellipse.....	50
2. GEOMETRY OF SPIRAL BEVEL GEARS.....	61
2.1 Introduction.....	61
2.2 Geometry I: The Line of Action.....	62
2.3 Geometry I: Contact Point Path on Surface Σ_i ($i=1,2$).....	71
2.4 Geometry I: The Instantaneous Contact Ellipse.....	76
2.5 Geometry II: Generating Surfaces.....	80
2.6 Geometry II: The Line of Action.....	84
2.7 Geometry II: The Instantaneous Contact Ellipse.....	85
3. METHODS TO CALCULATE GEAR-DRIVE KINEMATICAL ERRORS.....	88
3.1 Introduction.....	88
3.2 The Computer Method.....	88
3.3 Approximate Method.....	93
3.4 Kinematical Errors of Spiral Bevel Gears Induced by Their Eccentricity.....	99
3.5 Kinematical Errors Induced by Misalignment.....	106
4. CONCLUSION.....	112
LIST OF SYMBOLS.....	113
REFERENCES.....	118

SUMMARY

Spiral bevel gears have widespread applications in the transmission systems of helicopters, airplanes, trucks, automobiles, tanks and many other machines. Major requirements in the field of helicopter transmissions are: (a) improved life and reliability, (b) reduction in overall weight (i.e., a large power to weight ratio) without compromising the strength and efficiency during the service life, (c) reduction in the transmission noise.

Spiral bevel gears which used in practice are normally generated with approximately conjugate tooth surfaces by using special machine and tool settings. Therefore, designers and researchers cannot solve the Hertzian contact stress problem and define the dynamic capacity and contact fatigue life until these settings are calculated. The geometry of gear tooth surfaces is very complicated and the determination of principal curvatures and principal directions of tooth surfaces for Hertzian problem is a very hard problem.

The first two parts of this report deal with tooth contact geometry. In this report, a novel approach to the study of the geometry of spiral bevel gears and to their rational design is proposed. The nonconjugate tooth surfaces of spiral bevel gears are, in theory, replaced (or approximated) by conjugated tooth surfaces. These surfaces can be generated: (a) by two conical surfaces which are rigidly connected with each other and are in linear tangency along a common generatrix of tool cones and (b) by a conical surface and a surface of revolution which are in linear tangency along a circle.

We can imagine that four surfaces are in mesh: two of them are tool surfaces Σ_1 and Σ_2 , G_1 and G_2 are gear tooth surfaces. Surfaces Σ_1 and G_1 are in linear contact and the contact line moves along the surfaces Σ_1 and G_1 in the process of meshing. Surfaces Σ_2 and G_2 are rigidly connected and move in the process of meshing as a whole body. Surfaces G_1 and G_2 are in point contact and the point of their contact moves along the surfaces in the process of meshing. Surfaces G_1 and G_2 are hypothetical conjugate tooth surfaces which approximate the actual nonconjugate tooth surfaces to within manufacturing tolerances in the neighborhood of any path contact point. It is important to note that these conjugate tooth surfaces are not practical to use and, due to a constant tooth depth, may be undercut partly. However, the dynamic design of the gears is primarily dependent upon the nature of tooth surfaces in the neighborhood of the path of contact, and we propose to use these hypothetical conjugate surfaces for this purpose.

Although these hypothetical conjugate surfaces are simpler than the actual ones, the determination of their principal curvatures and directions is still a complicated problem. Therefore, a new approach to the solution of these is proposed in this report. In this approach, direct relationships between the principal curvatures and directions of the tool surface and those of the generated gear surface are obtained. Therefore, the principal curvatures and directions of gear tooth surface are obtained without using the complicated equations of these surfaces.

The proposed report utilizes effective methods of kinematic and analytic geometry (e.g., matrices for coordinate transformation, kinematic relations between motions of contact point and unit normal vector of two surfaces, etc.). With the aid of these analytical tools, the Hertzian

contact problem for conjugate tooth surfaces can be solved. These results are eventually useful in determining compressive load capacity and surface fatigue life of spiral bevel gears.

In the third part of this report, a general theory of kinematical errors exerted by manufacturing and assembly errors is developed. This theory is used to determine the analytical relationship between gear misalignments and kinematical errors. In the past, the influence of manufacturing errors and assembly errors on two surfaces in contact could be determined only by using numerical methods.

1. BASIC METHODS OF INVESTIGATION

1.1 General Kinematic Relations

Three coordinate systems rigidly connected with mechanism links are considered. One of these - $S_f(x_f, y_f, z_f)$ - is rigidly connected with the frame. The other two - $S_i(x_i, y_i, z_i)$ ($i=1,2$) are rigidly connected with the driving and driven gears.

The tooth surface is represented by vector-function

$$\underline{r}_i(u_i, \theta_i) \in C^1 \quad (u, \theta) \in G \quad (1.1.1)$$

where (u_i, θ_i) are surface coordinates. The symbol C^1 means that function (1.1.1) has continuous partial derivatives of first order with respect to all its arguments. The designation $\in G$ means that surface coordinates belong to the area G .

The normal vector \underline{N}_i and unit normal vector \underline{n}_i are represented by the following equations:

$$\underline{N}_i = \frac{\partial \underline{r}_i}{\partial u_i} \times \frac{\partial \underline{r}_i}{\partial \theta_i} \quad (1.1.2)$$

$$\underline{n}_i = \frac{\underline{N}_i}{|\underline{N}_i|} \quad (1.1.3)$$

It is assumed that surface Σ_i is a regular one and $\underline{N}_i \neq 0$.

Surface Σ_i and its unit normal vector may be represented in coordinate system S_f by equations

$$\underline{r}_f^{(i)} = \underline{r}_f^{(i)}(u_i, \theta_i, \phi_i) \quad (i=1,2) \quad (u_i, \theta_i) \in G, \quad \phi_i^{(1)} < \phi_i < \phi_i^{(2)} \quad (1.1.4)$$

$$\underline{n}_f^{(i)} = \underline{n}_f^{(i)}(u_i, \theta_i, \phi_i) \quad (i=1,2) \quad (1.1.5)$$

Equations (1.1.4) and (1.1.5) can be obtained with the matrix equations

$$[\underline{r}_f^{(i)}] = [M_{fi}] [\underline{r}_i] \quad (1.1.6)$$

$$[\underline{n}_f^{(i)}] = [L_{fi}] [\underline{n}_i] \quad (1.1.7)$$

Matrix $[M_{fi}]$ is represented by

$$\begin{aligned}
[M_{fi}] &= \begin{bmatrix} a_{11} & a_{12} & a_{13} & a_{14} \\ a_{21} & a_{22} & a_{23} & a_{24} \\ a_{31} & a_{32} & a_{33} & a_{34} \\ 0 & 0 & 0 & 1 \end{bmatrix} = \\
&= \begin{bmatrix} \cos(x_f, \hat{x}_i) & \cos(x_f, \hat{y}_i) & \cos(x_f, \hat{z}_i) & x_f^{(0_i)} \\ \cos(y_f, \hat{x}_i) & \cos(y_f, \hat{y}_i) & \cos(y_f, \hat{z}_i) & y_f^{(0_i)} \\ \cos(z_f, \hat{x}_i) & \cos(z_f, \hat{y}_i) & \cos(z_f, \hat{z}_i) & z_f^{(0_i)} \\ 0 & 0 & 0 & 1 \end{bmatrix} \quad (1.1.8)
\end{aligned}$$

where $x_f^{(0_i)}$, $y_f^{(0_i)}$ and $z_f^{(0_i)}$ are "new" coordinates of the "old" origin-- the coordinates of origin 0_i of the coordinate system S_i as defined in coordinate system S_f .

The column matrix $[r_i]$ is represented by

$$[r_i] = \begin{bmatrix} x_i \\ y_i \\ z_i \\ 1 \end{bmatrix} \quad (1.1.9)$$

Here the coordinates of a point M are homogeneous coordinates: $M(x_i, y_i, z_i, 1)$

Matrix $[L_{fi}]$ is a sub-matrix of $[M_{fi}]$

$$\begin{aligned}
[L_{fi}] &= \\
= \begin{bmatrix} a_{11} & a_{12} & a_{13} \\ a_{21} & a_{22} & a_{23} \\ a_{31} & a_{32} & a_{33} \end{bmatrix} &= \begin{bmatrix} \cos(x_f, \hat{x}_i) & \cos(x_f, \hat{y}_i) & \cos(x_f, \hat{z}_i) \\ \cos(y_f, \hat{x}_i) & \cos(y_f, \hat{y}_i) & \cos(y_f, \hat{z}_i) \\ \cos(z_f, \hat{x}_i) & \cos(z_f, \hat{y}_i) & \cos(z_f, \hat{z}_i) \end{bmatrix} \quad (1.1.10)
\end{aligned}$$

The column matrix $[n_i]$ is represented by

$$[n_i] = \begin{bmatrix} n_{ix} \\ n_{iy} \\ n_{iz} \end{bmatrix} \quad (1.1.11)$$

In the process of motion tooth surfaces Σ_1 and Σ_2 must be in continuous tangency. Therefore, the following equations are to be observed

$$\underline{r}_f^{(1)}(u_1, \theta_1, \phi_1) = \underline{r}_f^{(2)}(u_2, \theta_2, \phi_2) \quad (1.1.12)$$

$$\underline{n}_f^{(1)}(u_1, \theta_1, \phi_1) = \underline{n}_f^{(2)}(u_2, \theta_2, \phi_2), \quad (1.1.13)$$

where ϕ_1 and ϕ_2 are the angles of rotation of the driving and driven gears, respectively. Equation (1.1.12) expresses that surfaces Σ_1 and Σ_2 have common points. Equation (1.1.13) expresses that surfaces Σ_1 and Σ_2 have common unit normals at their common points. Together, equation systems (1.1.12) and (1.1.13) express that surfaces Σ_1 and Σ_2 are in tangency. Figure 1.1.1 shows surfaces Σ_1 and Σ_2 which are in tangency at point M. Plane T is tangent to these surfaces at their point of tangency, point M. Position vectors $\underline{r}_f^{(1)}$ and $\underline{r}_f^{(2)}$ drawn from the origin O_f of coordinate system $S_f(x_f, y_f, z_f)$ coincide with each other at point M. At this point the unit normal vectors $\underline{n}_f^{(1)}$ and $\underline{n}_f^{(2)}$ coincide, too.

Vector equations (1.1.12) and (1.1.13) yield the following six scalar equations

$$x_f^{(1)}(u_1, \theta_1, \phi_1) = x_f^{(2)}(u_2, \theta_2, \phi_2) \quad (1.1.14)$$

$$y_f^{(1)}(u_1, \theta_1, \phi_1) = y_f^{(2)}(u_2, \theta_2, \phi_2) \quad (1.1.15)$$

$$z_f^{(1)}(u_1, \theta_1, \phi_1) = z_f^{(2)}(u_2, \theta_2, \phi_2) \quad (1.1.16)$$

$$n_x^{(1)}(u_1, \theta_1, \phi_1) = n_x^{(2)}(u_2, \theta_2, \phi_2) \quad (1.1.17)$$

$$n_y^{(1)}(u_1, \theta_1, \phi_1) = n_y^{(2)}(u_2, \theta_2, \phi_2) \quad (1.1.18)$$

$$n_z^{(1)}(u_1, \theta_1, \phi_1) = n_z^{(2)}(u_2, \theta_2, \phi_2) \quad (1.1.19)$$

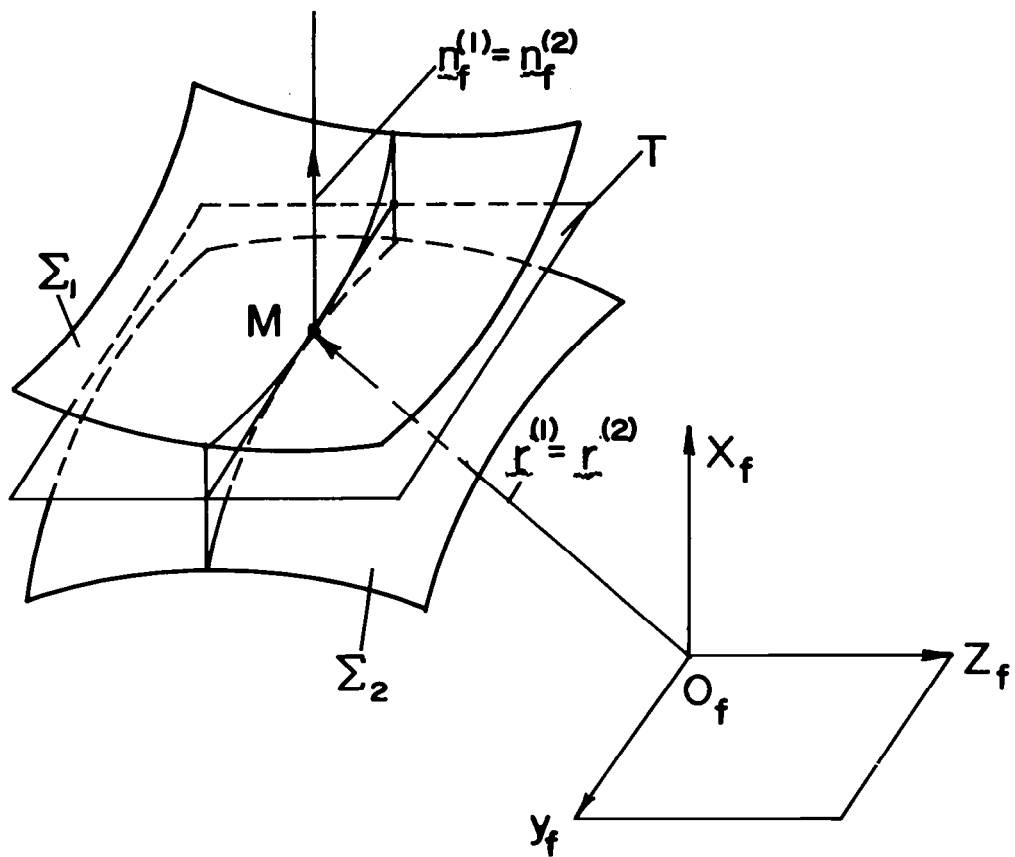


FIG. I.I.1

Contacting Tooth Surfaces

Scalar equations (1.1.14) - (1.1.19) can be represented as

$$f_k(u_1, \theta_1, \phi_1, u_2, \theta_2, \phi_2) = 0 \quad (k=1,2,\dots,6) \quad (1.1.20)$$

But three equations (1.1.17) - (1.1.19) of the system (1.1.14) - (1.1.19) can provide only two independent equations because $\underline{n}_f^{(1)}$ and $\underline{n}_f^{(2)}$ are unit vectors. Therefore, $|\underline{n}_f^{(1)}| = |\underline{n}_f^{(2)}|$ and if two projections of each unit vector are equal then the third projections must be equal, too. Consequently, vector equations (1.1.12) and (1.1.13) yield a system of only five independent equations:

$$f_i(u_1, \theta_1, \phi_1, u_2, \theta_2, \phi_2) = 0 \quad (i=1,2,3,4,5) \quad (1.1.21)$$

It is assumed that

$$\{f_1, f_2, f_3, f_4, f_5\} \in C^1 \quad (1.1.22)$$

In other words, it is assumed that functions $f_i (i=1,\dots,5)$ have with respect to all arguments continuous partial derivatives of first order at least.

It is known that the instantaneous contact of tooth surfaces can be a linear contact (along a spatial curve, in general) or a point contact. Let us suppose that the system of equations (1.1.20) is satisfied at a point M_0 by a set of parameters

$$P = (u_1^\circ, \theta_1^\circ, \phi_1^\circ, u_2^\circ, \theta_2^\circ, \phi_2^\circ) \quad (1.1.23)$$

If link 1 is the input and tooth surfaces are in contact point in the neighborhood of M_0 a system of functions

$$\{\phi_2(\phi_1), u_1(\phi_1), \theta_1(\phi_1), u_2(\phi_1), \theta_2(\phi_1)\} \in C^1$$

must exist in the neighborhood of M_0 . This requirement will be satisfied

if at point M_0 the following inequality is observed

$$\frac{D(f_1, f_2, f_3, f_4, f_5)}{D(u_1, \theta_1, u_2, \theta_2, \phi_2)} \neq 0 \quad (1.1.24)$$

Here:

$$\frac{D(f_1, f_2, f_3, f_4, f_5)}{D(u_1, \theta_1, u_2, \theta_2, \phi_2)} = \left| \begin{array}{ccccc} \frac{\partial f_1}{\partial u_1} & \frac{\partial f_1}{\partial \theta_1} & \frac{\partial f_1}{\partial u_2} & \frac{\partial f_1}{\partial \theta_2} & \frac{\partial f_1}{\partial \phi_2} \\ \frac{\partial f_2}{\partial u_1} & \frac{\partial f_2}{\partial \theta_1} & \frac{\partial f_2}{\partial u_2} & \frac{\partial f_2}{\partial \theta_2} & \frac{\partial f_2}{\partial \phi_2} \\ \frac{\partial f_3}{\partial u_1} & \frac{\partial f_3}{\partial \theta_1} & \frac{\partial f_3}{\partial u_2} & \frac{\partial f_3}{\partial \theta_2} & \frac{\partial f_3}{\partial \phi_2} \\ \frac{\partial f_4}{\partial u_1} & \frac{\partial f_4}{\partial \theta_1} & \frac{\partial f_4}{\partial u_2} & \frac{\partial f_4}{\partial \theta_2} & \frac{\partial f_4}{\partial \phi_2} \\ \frac{\partial f_5}{\partial u_1} & \frac{\partial f_5}{\partial \theta_1} & \frac{\partial f_5}{\partial u_2} & \frac{\partial f_5}{\partial \theta_2} & \frac{\partial f_5}{\partial \phi_2} \end{array} \right| \quad (1.1.25)$$

is the Jacobian of system (1.1.20)

Inequality (1.1.24) indicates that the tooth surfaces are in contact at a point. If the inequality (1.1.24) becomes an equality this indicates that surfaces contact each other along a line.

It results from the continuity of surface contact that

$$\frac{dr_{\sim f}^{(1)}}{dt}(u_1, \theta_1, \phi_1) = \frac{dr_{\sim f}^{(2)}}{dt}(u_2, \theta_2, \phi_2) \quad (1.1.26)$$

$$\frac{dn_{\sim f}^{(1)}}{dt}(u_1, \theta_1, \phi_1) = \frac{dn_{\sim f}^{(2)}}{dt}(u_2, \theta_2, \phi_2) \quad (1.1.27)$$

or that

$$\frac{dr_{\sim f}^{(1)}}{dt}(u_1, \theta_1, \phi_1) = \frac{dr_{\sim f}^{(2)}}{dt}(u_2, \theta_2, \phi_2) \quad (1.1.28)$$

$$\frac{dn_{\sim f}^{(1)}}{dt}(u_1, \theta_1, \phi_1) = \frac{dn_{\sim f}^{(2)}}{dt}(u_2, \theta_2, \phi_2) \quad (1.1.29)$$

Let us designate $\frac{dr_{\sim f}^{(i)}}{dt}$ by $v_{\sim abs}^{(i)}$ and $\frac{dn_{\sim f}^{(i)}}{dt}$ by $\dot{n}_{\sim abs}^{(i)}$ ($i=1,2$). Here: $v_{\sim abs}^{(i)}$ is the velocity of contact point in the absolute motion (with respect to the frame); $\dot{n}_{\sim abs}$ is the velocity of the end of unit normal in absolute motion (with respect to the frame).

The velocity of absolute motion can be represented as a sum of two components: (a) velocity of transfer motion - together with the surface; and (b) velocity of a relative motion - relative to the surface. Consequently,

$$v_{\sim abs}^{(1)} = v_{\sim tr}^{(1)} + v_{\sim r}^{(1)}, \quad v_{\sim abs}^{(2)} = v_{\sim tr}^{(2)} + v_{\sim r}^{(2)} \quad (1.1.30)$$

$$\dot{n}_{\sim abs}^{(1)} = \dot{n}_{\sim tr}^{(1)} + \dot{n}_{\sim r}^{(1)}, \quad \dot{n}_{\sim abs}^{(2)} = \dot{n}_{\sim tr}^{(2)} + \dot{n}_{\sim r}^{(2)} \quad (1.1.31)$$

Equations (1.1.12), (1.1.13), (1.1.30) and (1.1.31) yield

$$v_{\sim tr}^{(i)} = \frac{\partial r_{\sim f}^{(i)}}{\partial \phi_i} \frac{d\phi_i}{dt}, \quad v_{\sim r}^{(i)} = \frac{\partial r_{\sim f}^{(i)}}{\partial u_i} \frac{du_i}{dt} + \frac{\partial r_{\sim f}^{(i)}}{\partial \theta_i} \frac{d\theta_i}{dt} \quad (1.1.32)$$

$$\dot{\tilde{n}}_{tr}^{(i)} = \frac{\partial n^{(i)}}{\partial \phi_i} \frac{d\phi_i}{dt}, \quad \dot{\tilde{n}}_r^{(i)} = \frac{\partial n^{(i)}}{\partial u_i} \frac{du_i}{dt} + \frac{\partial n^{(i)}}{\partial \theta_i} \frac{d\theta_i}{dt} \quad (1.1.33)$$

Due to continuity of tangency

$$\tilde{v}_{abs}^{(1)} = \tilde{v}_{abs}^{(2)}, \quad \dot{\tilde{n}}_{abs}^{(1)} = \dot{\tilde{n}}_{abs}^{(2)} \quad (1.1.34)$$

Equations (1.1.30), (1.1.31) and (1.1.34) yield

$$\tilde{v}_{tr}^{(1)} + \tilde{v}_r^{(1)} = \tilde{v}_{tr}^{(2)} + \tilde{v}_r^{(2)} \quad (1.1.35)$$

$$\dot{\tilde{n}}_{tr}^{(1)} + \dot{\tilde{n}}_r^{(1)} = \dot{\tilde{n}}_{tr}^{(2)} + \dot{\tilde{n}}_r^{(2)} \quad (1.1.36)$$

Equations (1.1.34) and (1.1.35) were proposed by F. Litvin. On the basis of these equations important problems in the theory of gearings, such as problem of tooth-nonundercutting, relations between curvatures of two surfaces in mesh, and the problem of kinematical errors of gear drives caused by errors of manufacturing and assemblage, were solved.

1.2 Transfer Velocity

In addition to equation (1.1.32), transfer velocity may be defined in a kinematical way, too.

Figure 1.2.1 shows a tooth surface Σ_i of gear i . The gear rotates with angular velocity $\omega_f^{(i)}$ about axis j - j . Generally, the axis of rotation does not pass through the origin O_f of coordinate system S_f .

The sliding vector $\omega_f^{(i)}$ directed along j - j may be substituted by the same vector which passes through O_f and a vector-moment $R_f^{(i)} \times \omega_f^{(i)}$, where $R_f^{(i)}$ is a position vector drawn from O_f to an arbitrary point on the line of action of $\omega_f^{(i)}$ (of axis j - j). Figure 2.1 shows vector $R_f^{(i)} = \overline{O_f N}^{(i)}$.

The reduction of the sliding vector $\omega_f^{(i)}$ passing through point $N^{(i)}$ by the same vector $\omega_f^{(i)}$ passing through O_f and vector-moment $R_f^{(i)} \times \omega_f^{(i)}$ is based on the opportunity to represent the transfer velocity by the following two equations:

$$\tilde{v}_{tr}^{(i)} = \omega_f^{(i)} \times \rho_f^{(i)} \quad (1.2.1)$$

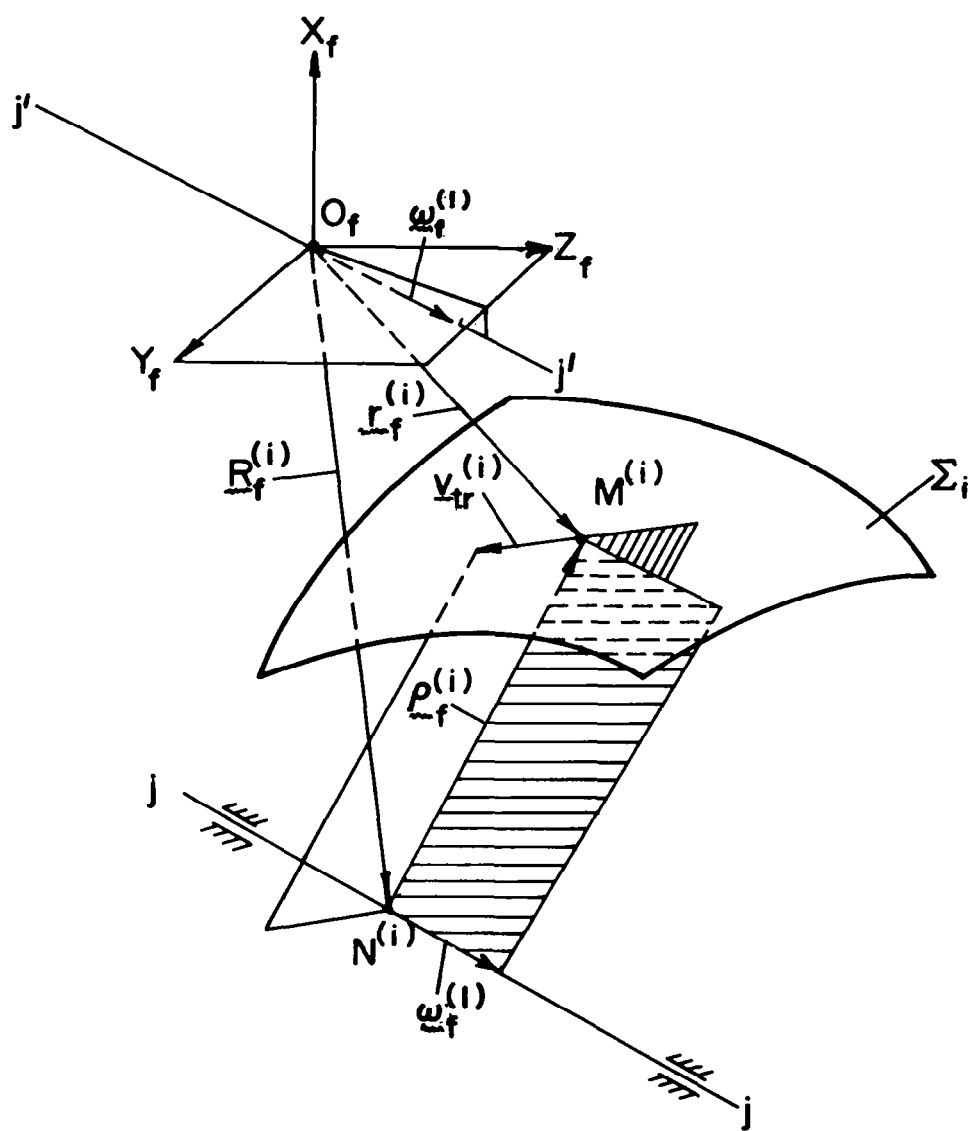


FIG 1.2.1

Rotation of Tooth Surface About Axis Not Passing Through Origin

$$\underline{v}_{tr}^{(i)} = \underline{\omega}_f^{(i)} \times \underline{r}_f^{(i)} + \underline{R}_f^{(i)} \times \underline{\omega}_f^{(i)} \quad (1.2.2)$$

It is easy to verify that

$$\underline{\omega}_f^{(i)} \times \underline{r}_f^{(i)} + \underline{R}_f^{(i)} \times \underline{\omega}_f^{(i)} = \underline{\omega}_f^{(i)} \times \underline{\rho}_f^{(i)}, \quad (1.2.3)$$

taking into account that

$$\underline{\rho}_f^{(i)} = \overline{N^{(i)}O_f} + \overline{O_fM^{(i)}} = \overline{O_fM^{(i)}} - \overline{O_fN^{(i)}} = \underline{r}_f^{(i)} - \underline{R}_f^{(i)} \quad (1.2.4)$$

Consequently,

$$\underline{\omega}_f^{(i)} \times \underline{r}_f^{(i)} + \underline{R}_f^{(i)} \times \underline{\omega}_f^{(i)} = \underline{\omega}_f^{(i)} \times (\underline{r}_f^{(i)} - \underline{R}_f^{(i)}) = \underline{\omega}_f^{(i)} \times \underline{\rho}_f^{(i)}$$

The velocity of transfer motion represented by equation (1.2.2) can be considered as a resultant velocity of two motions: (a) translation with the velocity $\underline{R}_f^{(i)} \times \underline{\omega}_f^{(i)}$; and (b) rotation with angular velocity $\underline{\omega}_f^{(i)}$ about axis $j'-j'$ drawn through O_f parallel to axis $j-j$.

Now, let us define the transfer velocity of the unit normal vector.

Fig. 1.2.2 shows point $M^{(i)}$ of the tooth surface Σ_i ($i=1,2$), the unit normal $\underline{n}_f^{(i)}$, and the tangent plane T to the surface at point $M^{(i)}$. The surface rotates about axis $j-j$ with angular velocity $\underline{\omega}_f^{(i)}$.

Unlike the previous case, shown in Fig. 1.2.1, let us move the sliding vector $\underline{\omega}_f^{(i)}$ not to point O_f but to point $M^{(i)}$. Then, the transfer motion may be represented as a resultant motion with two components: (a) of translation with velocity $\overline{M^{(i)}N^{(i)}} \times \underline{\omega}_f^{(i)}$; and (b) of rotation about axis $j'-j'$ with angular velocity $\underline{\omega}_f^{(i)}$. Axis $j'-j'$ is drawn through point $M^{(i)}$ parallel to $j-j$ (Fig. 1.2.2); point $N^{(i)}$ is an arbitrarily chosen point on axis $j-j$.

By translation the unit normal vector $\underline{n}^{(i)}$ will be moved with the surface point $M^{(i)}$ parallel to its original direction. So, when surface Σ_i with point $M^{(i)}$ and unit normal $\underline{n}^{(i)}$ is translated with velocity $\overline{M^{(i)}N^{(i)}} \times \underline{\omega}_f^{(i)}$ vector $\underline{n}_f^{(i)}$ does not change its original direction. But the direction of $\underline{n}^{(i)}$ will be changed by rotation about axis $j'-j'$.

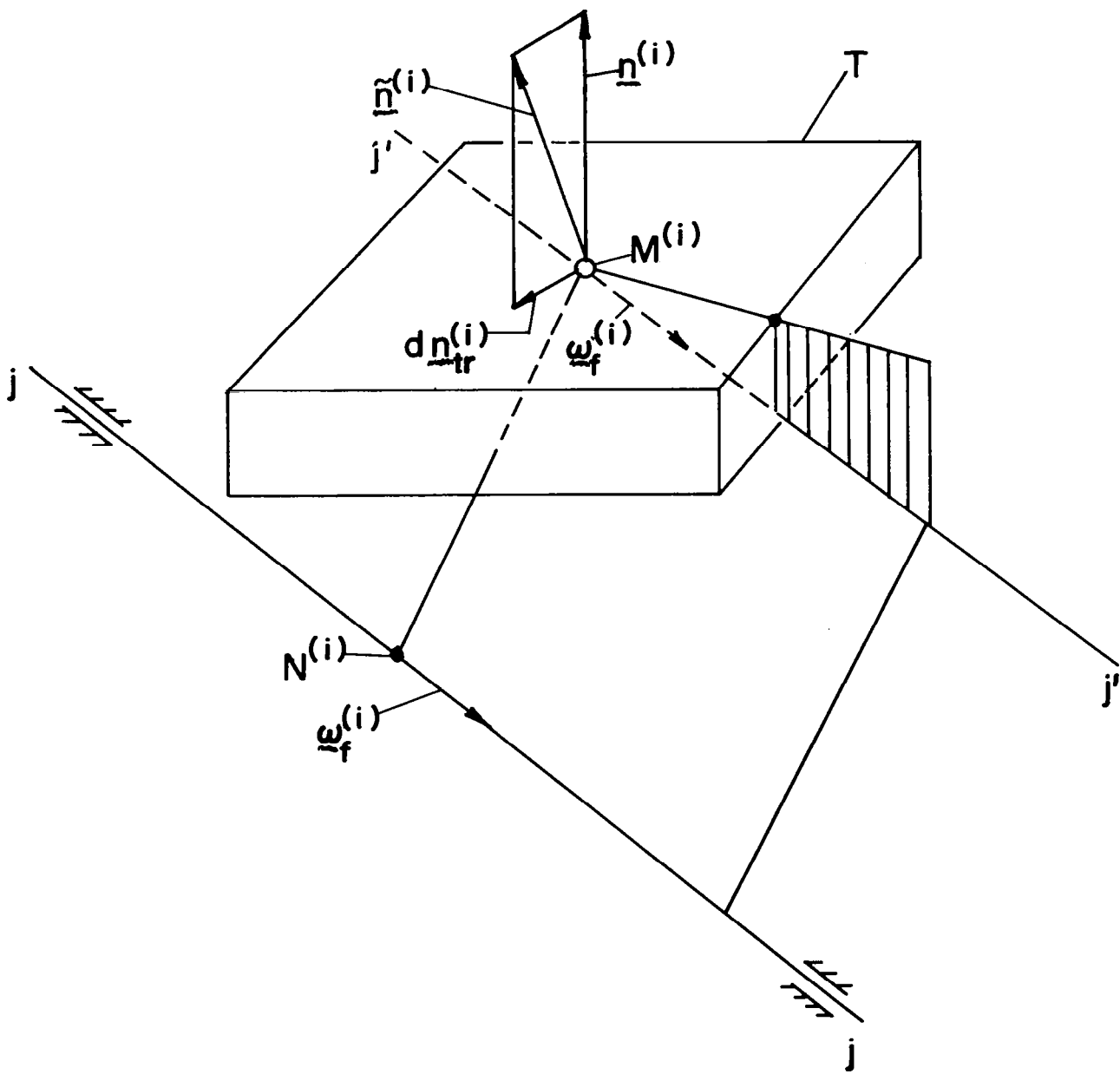


FIG. 1.2.2

Transfer Velocity of Unit Normal Vector

Fig. 1.2.2 shows two positions of the unit vector: $\underline{n}^{(i)}$ is the initial position and $\underline{\tilde{n}}^{(i)}$ is the changed position after rotation about axis $j'-j'$ by the angle $d\phi^{(i)} = \underline{\omega}_f^{(i)} dt$. The difference

$$\underline{\tilde{n}}^{(i)} - \underline{n}^{(i)} = d\underline{n}_{tr}^{(i)} \quad (1.2.5)$$

represents the displacement of unit normal by rotation about axis $j'-j'$.

Vector $d\underline{n}_{tr}$ is represented by the equation

$$d\underline{n}_{tr} = d\phi^{(i)} \times \underline{n}^{(i)} = (\underline{\omega}_f^{(i)} \times \underline{n}^{(i)}) dt \quad (1.2.6)$$

Accordingly, the velocity $\dot{\underline{n}}_{tr}^{(i)}$ of transfer motion may be represented by equation

$$\dot{\underline{n}}_{tr}^{(i)} = \frac{d\underline{n}_{tr}}{dt} = \underline{\omega}_f^{(i)} \times \underline{n}^{(i)} \quad (1.2.7)$$

1.3 Relative Velocity of Contact Points

Consider tooth surfaces Σ_1 and Σ_2 which are in mesh. Points $M^{(1)}$ and $M^{(2)}$ are rigidly connected with their respective surfaces and coincide with each other at the point of surface contact.

Let us designate by $\underline{v}_1^{(1)}$ and $\underline{v}_1^{(2)}$ the transfer velocities of points $M^{(1)}$ and $M^{(2)}$; the subscript "1" means that $\underline{v}_1^{(1)}$ and $\underline{v}_1^{(2)}$ are represented in terms of components of coordinate system S_1 rigidly connected with surface Σ_1 . The relative velocity

$$\underline{v}_1^{(21)} = \underline{v}_1^{(2)} - \underline{v}_1^{(1)} \quad (1.3.1)$$

expresses the velocity of point $M^{(2)}$ with respect to point $M^{(1)}$ defined by an observer located at the system S_1 at point $M^{(1)}$.

Sample problem 1.3.1

Gears 1 and 2 rotate about crossed axes z_1 and z_2 with angular velocities $\underline{\omega}^{(1)}$ and $\underline{\omega}^{(2)}$ (Fig. 1.3.1); axes z_1 and z_2 make an angle γ ; the shortest distance between z_1 and z_2 is C . Points $M^{(1)}$ and $M^{(2)}$ of surfaces Σ_1 and Σ_2 coincide with each other at the point of contact M .

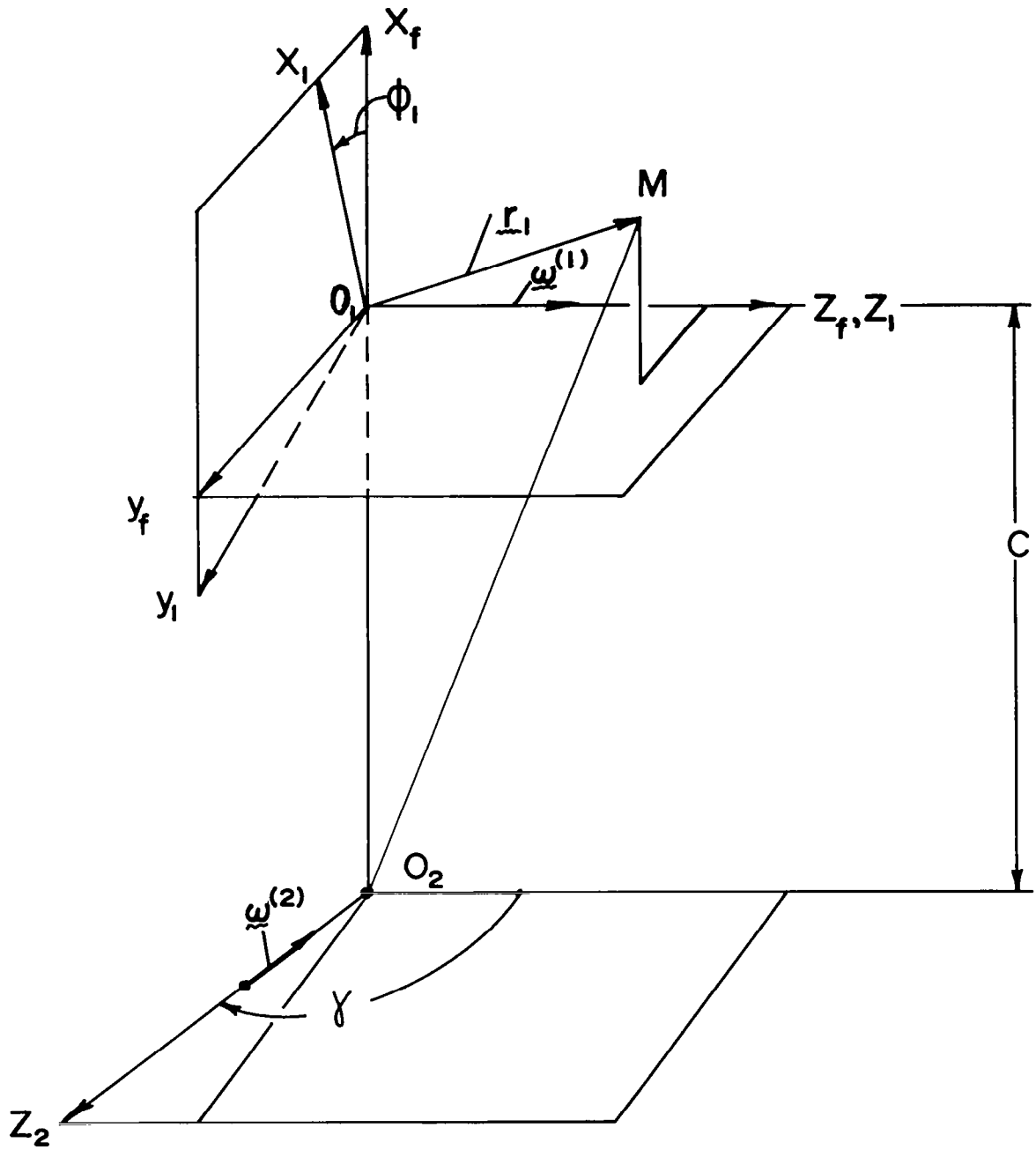


FIG. 1.3.1

Vectors for Computing Relative Velocity at Point M

The transfer velocities of points $M^{(1)}$ and $M^{(2)}$ are represented by the equations

$$\vec{v}_1^{(1)} = \vec{\omega}_1^{(1)} \times \overline{O_1 M} = \begin{vmatrix} \tilde{i}_1 & \tilde{j}_1 & \tilde{k}_1 \\ \omega_{x1}^{(1)} & \omega_{y1}^{(1)} & \omega_z^{(1)} \\ x_1 & y_1 & z_1 \end{vmatrix} \quad (1.3.2)$$

$$\vec{v}_1^{(2)} = \omega_1^{(2)} \times \overline{O_1 M} + \overline{O_1 O_2} \times \omega_{z1}^{(2)} = \begin{vmatrix} \tilde{i}_1 & \tilde{j}_1 & \tilde{k}_1 \\ \omega_{x1}^{(2)} & \omega_{y1}^{(2)} & \omega_{z1}^{(2)} \\ x_1 & y_1 & z_1 \end{vmatrix} + \begin{vmatrix} \tilde{i}_1 & \tilde{j}_1 & \tilde{k}_1 \\ x_1^{(O_2)} & y_1^{(O_2)} & z_1^{(O_2)} \\ \omega_{x1}^{(2)} & \omega_{y1}^{(2)} & \omega_{z1}^{(2)} \end{vmatrix} \quad (1.3.3)$$

Here: (x_1, y_1, z_1) are coordinates of point $M^{(1)} \equiv M^{(2)} \equiv M$, $\omega_{x1}^{(i)}$, $\omega_{y1}^{(i)}$, $\omega_{z1}^{(i)}$ are projections of angular velocity $\vec{\omega}^{(i)}$ ($i=1,2$); $x_1^{(O_2)}$, $y_1^{(O_2)}$, $z_1^{(O_2)}$ are coordinates of point O_2 in terms of coordinate system S_1 .

Surface Σ_1 rotates about z_1 and

$$\omega_{x1}^{(1)} = \omega_{y1}^{(1)} = 0, \quad \omega_{z1}^{(1)} = \omega^{(1)} \quad (1.3.4)$$

It is easy to express $\omega_f^{(2)}$ in terms of components of coordinate system S_f rigidly connected with the frame

$$\begin{bmatrix} \omega_f^{(2)} \end{bmatrix} = \begin{bmatrix} 0 \\ -\omega^{(2)} \sin \gamma \\ -\omega^{(2)} \cos \gamma \end{bmatrix} \quad (1.3.5)$$

The angular velocity $\omega_1^{(2)}$ can be expressed in terms of components of coordinate system S_1 with the aid of the matrix equation

$$[\omega_1^{(2)}] = [L_{1f}] [\omega_f^{(2)}] \quad (1.3.6)$$

Here: matrix

$$[L_{1f}] = \begin{bmatrix} \cos\phi_1 & \sin\phi_1 & 0 \\ -\sin\phi_1 & \cos\phi_1 & 0 \\ 0 & 0 & 1 \end{bmatrix} \begin{bmatrix} 0 \\ -\omega^{(2)} \sin\gamma \\ -\omega^{(2)} \cos\gamma \end{bmatrix} \quad (1.3.7)$$

describes transformation of vector projections by transition from S_f to S_1 .

It results from expressions (1.3.5)-(1.3.7) that

$$[\omega_1^{(2)}] = \begin{bmatrix} -\omega^{(2)} \sin\gamma \sin\phi_1 \\ -\omega^{(2)} \sin\gamma \cos\phi_1 \\ -\omega^{(2)} \cos\gamma \end{bmatrix} \quad (1.3.8)$$

Transformation of coordinates of some point given in system S_f to S_1 is represented by matrix equation

$$[r_1] = [M_{1f}] [r_f], \quad (1.3.9)$$

where

$$[M_{1f}] = \begin{bmatrix} \cos\phi_1 & \sin\phi_1 & 0 & 0 \\ -\sin\phi_1 & \cos\phi_1 & 0 & 0 \\ 0 & 0 & 1 & 0 \\ 0 & 0 & 0 & 1 \end{bmatrix} \quad (1.3.10)$$

For point O_2 the column matrix is given by

$$[r_f] = [R_f] = \begin{bmatrix} -C \\ 0 \\ 0 \\ 1 \end{bmatrix} \quad (R_f = \overline{0_1 0_2}) \quad (1.3.11)$$

Expressions (1.3.9)-(1.3.14) yield

$$[R_1] = \begin{bmatrix} x_1^{(0_2)} \\ y_1^{(0_2)} \\ z_1^{(0_2)} \\ 1 \end{bmatrix} = \begin{bmatrix} -C \cos\phi_1 \\ C \sin\phi_1 \\ 0 \\ 1 \end{bmatrix} \quad (R_1 = \overline{0_1 0_2}) \quad (1.3.12)$$

The subscripts "f" and "1" for $[R_f]$ and $[R_1]$ denote that the same vector $R = \overline{0_1 0_2}$ is expressed in terms of components of two coordinate systems: S_f and S_1 .

Equations (1.3.2)-(1.3.4), (1.3.8) and (1.3.12) yield

$$\begin{aligned}
 [v_1^{(21)}] &= [v_1^{(2)}] - [v_1^{(1)}] = \\
 &= \begin{bmatrix} y_1(\omega^{(2)} \cos \gamma + \omega^{(1)}) - z_1 \omega^{(2)} \sin \gamma \cos \phi_1 - C \omega^{(2)} \cos \gamma \sin \phi_1 \\ -x_1(\omega^{(2)} \cos \gamma + \omega^{(1)}) + z_1 \omega^{(2)} \sin \gamma \sin \phi_1 - C \omega^{(2)} \cos \gamma \cos \phi_1 \\ \omega^{(2)} \sin \gamma (x_1 \cos \phi_1 - y_1 \sin \phi_1 + C) \end{bmatrix} \quad (1.3.13)
 \end{aligned}$$

To express the relative velocity $v^{(21)}$ in terms of components of coordinate system S_f it is sufficient to put in matrix (1.3.13) $\phi_1 = 0$ and $x_1 = x_f$, $y_1 = y_f$, $z_1 = z_f$ because with $\phi_1 = 0$ the coordinate system S_1 coincides with S_f .

$$[v_f^{(21)}] = \begin{bmatrix} y_f(\omega^{(2)} \cos \gamma + \omega^{(1)}) - z_f \omega^{(2)} \sin \gamma \\ -x_f(\omega^{(2)} \cos \gamma + \omega^{(1)}) - C \omega^{(2)} \cos \gamma \\ \omega^{(2)} \sin \gamma (x_f + C) \end{bmatrix} \quad (1.3.14)$$

For the case when motion is transformed between parallel axes the crossing angle γ must be put equal to zero in matrices (1.3.13) and (1.3.14). For gear drives with intersecting axes, such as bevel gears, the shortest distance C must be put equal to zero in the same matrices; the angle γ is made by intersected axes.

1.4. The General Law of Gearings

Let us suppose that tooth surfaces Σ_1 and Σ_2 which are in linear or point contact must transform motion with prescribed angular velocity ratio $R_{21} = \omega^{(2)} : \omega^{(1)}$ with prescribed location of the axes of rotation. Because the contact of surfaces must be a continuous one the surfaces should not interfere each other or lose their contact. Therefore, at a point of contact

the relative velocity $\tilde{v}_1^{(21)}$ must belong to the common tangent plane T to the surfaces at their contact point M (Fig. 1.4.1). Consequently, at a point of contact the following equation

$$N_1 \cdot \tilde{v}_1^{(21)} = 0 \quad (1.4.1)$$

must be observed. Here: N_1 is the common surface normal at the contact point M , $\tilde{v}_1^{(21)}$ is the relative velocity represented by equations (1.3.13).

For a surface Σ_1 represented by vector-function

$$\tilde{r}_1(u, \theta) \in C^1, \quad (u, \theta) \in G \quad (1.4.2)$$

the surface normal is defined by equation

$$N_1 = \frac{\partial \tilde{r}_1}{\partial u} \times \frac{\partial \tilde{r}_1}{\partial \theta} \quad (1.4.3)$$

Equations (1.4.1) and (1.4.3) yield that the scalar triple product $\left[\frac{\partial \tilde{r}_1}{\partial u} \frac{\partial \tilde{r}_1}{\partial \theta} \tilde{v}_1^{(21)} \right]$ is equal to zero. The equation

$$\left[\frac{\partial \tilde{r}_1}{\partial u} \frac{\partial \tilde{r}_1}{\partial \theta} \tilde{v}_1^{(21)} \right] = 0 \quad (1.4.4)$$

provides an equation of meshing

$$f(u, \theta, \phi_1) = 0 \quad (1.4.5)$$

because $\frac{\partial \tilde{r}_1}{\partial u}$ and $\frac{\partial \tilde{r}_1}{\partial \theta}$ are functions of surface coordinates (u, θ) and $\tilde{v}_1^{(12)}(x_1, y_1, z_1, \phi_1)$ is a function of (u, θ, ϕ_1) .

Surface Σ_1 can be represented in coordinate system Σ_f by the vector-function

$$\tilde{r}_f(u, \theta, \phi_1) \in C^1, \quad (u, \theta) \in G, \quad \phi_1^{(1)} < \phi_1 < \phi_1^{(2)} \quad (1.4.6)$$

Different values of ϕ_1 correspond to different positions of Σ_1 in coordinate system Σ_f . For a definite position of Σ_1 the motion parameter ϕ_1 must be considered as a fixed one.

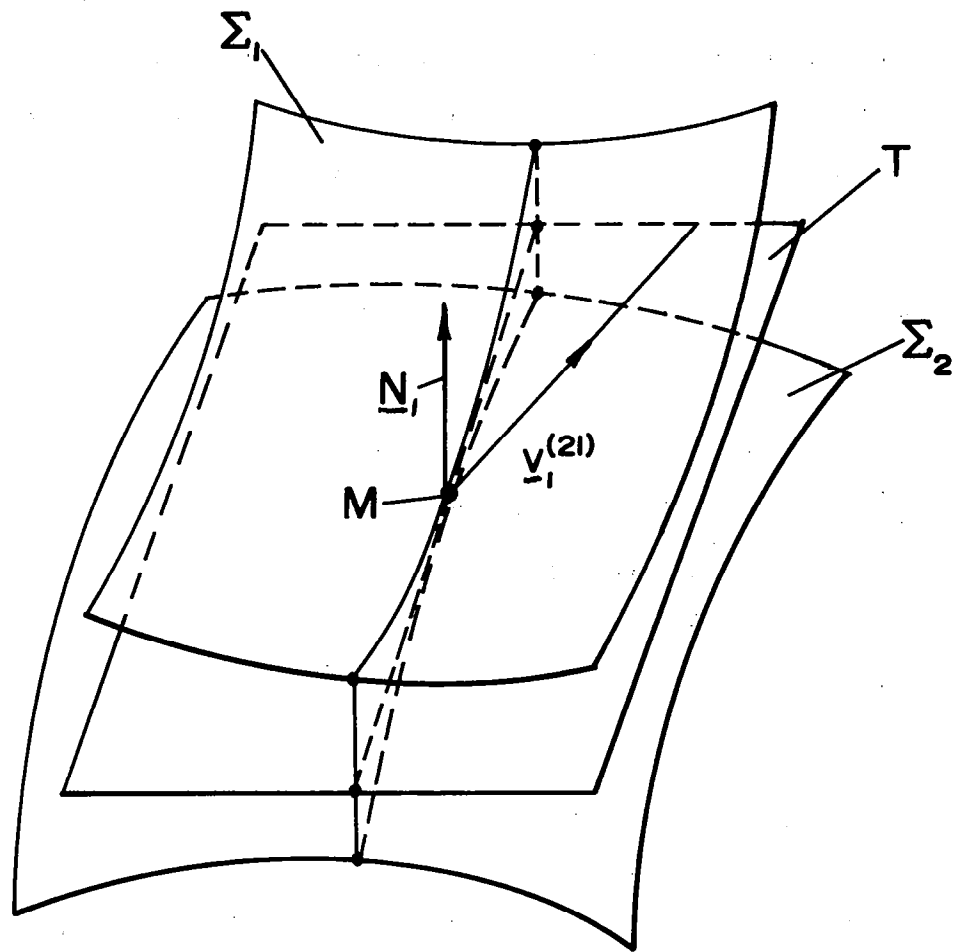


FIG 1.4.1

Contacting Tooth Surfaces and Common Tangent Plane

The equation of meshing (1.4.5) can be obtained by

$$\left[\frac{\partial \tilde{r}_f}{\partial u} \frac{\partial \tilde{r}_f}{\partial \theta} \tilde{v}_f^{(21)} \right] = f(u, \theta, \phi_1) = 0 \quad (1.4.7)$$

Here:

$$\frac{\partial \tilde{r}_f}{\partial u} \times \frac{\partial \tilde{r}_f}{\partial \theta} = \tilde{N}_f \quad (1.4.8)$$

is the surface normal; the relative velocity $\tilde{v}_f^{(21)}$ is represented by equations (1.3.14).

For gearings with parallel and intersecting axes the law of meshing can be expressed in another form.

For gears with parallel axes the relative motion can be represented as a rotation about the instantaneous axis of rotation I-I (Fig. 1.4.2). By a given ratio

$$R_{21} = \frac{\omega^{(2)}}{\omega^{(1)}} \quad (1.4.9)$$

the relative motion is rolling of two cylinders with operating radii r_2' and r_1' defined by equations

$$\frac{r_1'}{r_2'} = \frac{\omega^{(2)}}{\omega^{(1)}} = R_{21}, \quad r_1' + r_2' = C, \quad (1.4.10)$$

where $C = O_1O_2$ is the distance between the axes of rotation.

With cylinder 1 fixed, cylinder 2 rotates about axis I-I with angular velocity $\tilde{\omega}^{(21)} = \tilde{\omega}^{(2)} - \tilde{\omega}^{(1)}$. The relative velocity $\tilde{v}_1^{(21)}$ is represented by equation

$$\tilde{v}_1^{(21)} = \tilde{\omega}^{(21)} \times \overline{MM'}, \quad (1.4.11)$$

where M is the point of contact of surfaces Σ_1 and Σ_2 ; $\overline{MM'}$ is a perpendicular to axis I-I drawn from point M.

Equations (1.4.1) and (1.4.11) yield

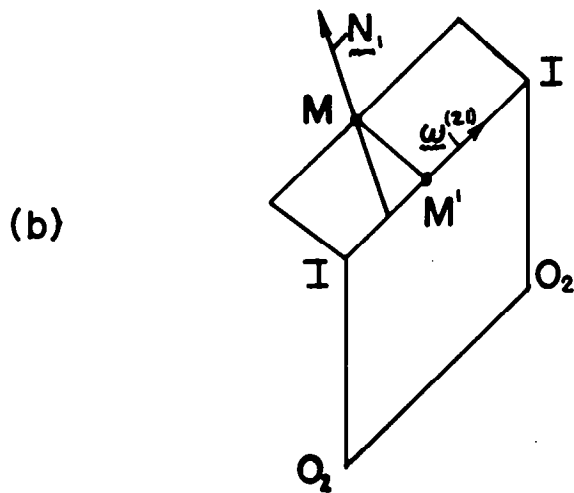
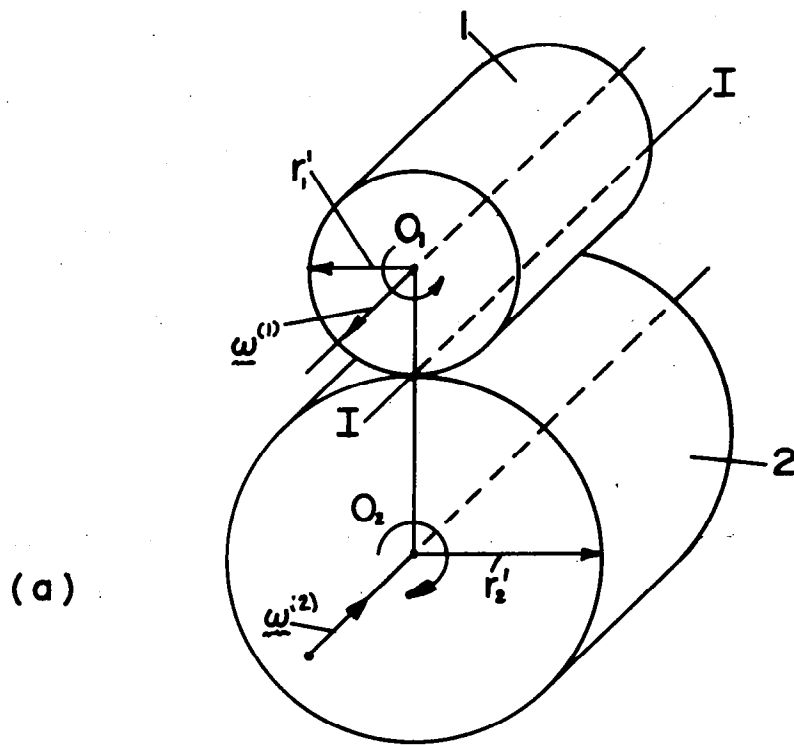


FIG 1.4.2

Pitch Cylinders and Instantaneous Axis of Rotation

$$\vec{N}_1 \cdot (\vec{\omega}^{(21)} \times \vec{M} M) = [\vec{N}_1 \vec{\omega}^{(21)} \vec{M} M] = 0 \quad (1.4.12)$$

Because the scalar triple product is equal to zero, all three vectors must belong to the same plane and the surface normal \vec{N}_1 must intersect the instantaneous axis of rotation I-I (Fig. 1.4.2,B). This fact results in the following theorem:

The contact line of tooth surfaces of gears with parallel axes of rotation must be such that common normal to tooth surfaces at any point of contact intersects the instantaneous axis I-I of rotation (the line of tangency of operating pitch cylinders).

According to this theorem the law of meshing may be defined with the following equations

$$\frac{X_1 - x_1(u, \theta)}{N_{x1}} = \frac{Y_1 - y_1(u, \theta)}{N_{y1}} = \frac{Z_1 - z_1(u, \theta)}{N_{z1}} \quad (1.4.13)$$

Here: $x_1(u, \theta)$, $y_1(u, \theta)$, $z_1(u, \theta)$ are coordinates of a point of surface Σ_1 ; $X_1(\phi_1)$, $Y_1(\phi_1)$, $Z_1(l_1)$ are coordinates of a point which belongs to axis I-I (Fig. 1.4.2). It is assumed that axis Z_1 is the rotation axis of gear 1 and l_1 is a coordinate of a point of this axis.

The first equation (1.4.13)

$$\frac{X_1(\phi_1) - x_1(u, \theta)}{N_{x1}(u, \theta)} = \frac{Y_1(\phi_1) - y_1(u, \theta)}{N_{y1}(u, \theta)} \quad (1.4.14)$$

yields the equation of meshing (1.4.5).

Equations (1.4.13) can be applied for bevel gears, too.

The equation of meshing can also be defined another way, if instead of (1.4.14) the following equation is used

$$\frac{X_f - x_f(u, \theta, \phi_1)}{N_{fx}(u, \theta, \phi_1)} = \frac{Y_f - y_f(u, \theta, \phi_1)}{N_{fy}(u, \theta, \phi_1)} \quad (1.4.15)$$

Subscript "f" denotes that all vectors are represented in terms of components of coordinate system $S_f(x_f, y_f, z_f)$ rigidly connected with the

frame; X_f, Y_f, Z_f are coordinates of a point which belongs to the axis of instantaneous rotation; x_f, y_f, z_f are coordinates of a point of surface Σ_1 ; N_{xf}, N_{yf}, N_{zf} are projection of surface normal.

1.5 Contact Lines, Surface of Action, The Enveloped Surface

The same three coordinate systems mentioned in item 1.1 are considered. The problem to be solved can be formulated as follows: The surface Σ_1 of gear 1 teeth is given; surface Σ_2 of gear 2 teeth, the surface of action Σ_f and lines of contact of surfaces Σ_1 and Σ_2 must be defined. Let us take Σ_1 as the generating surface and Σ_2 as the surface generated by Σ_1 .

Let us suppose that surface Σ_1 is represented by vector-function

$$\vec{r}_1(u, \theta) \in C^1, \quad (u, \theta) \in G \quad (1.5.1)$$

Then, contact lines on surface Σ_1 can be represented by the following equations

$$\begin{aligned} x_1 &= x_1(u, \theta) \\ y_1 &= y_1(u, \theta) \\ z_1 &= z_1(u, \theta) \\ \vec{n}_1 \cdot \vec{v}_1^{(21)} &= f(u, \theta, \phi_1) = 0 \end{aligned} \quad (1.5.2)$$

The first three equations represent surface Σ_1 , the fourth one represents the equation of meshing; ϕ_1 is a fixed value for every contact line.

Fig. 1.5.1 shows surface Σ_1 covered with contact lines $CL(\phi_1^{(i)})$ ($i=1, 2, 3, \dots$), where $\phi_1^{(i)}$ are fixed values. By a definite value of $\phi_1^{(i)}$ line $CL(\phi_1^{(i)})$ will become the line of instantaneous tangency of Σ_1 and Σ_2 .

The to-be-defined surface Σ_2 can be represented as the locus of contact lines in coordinate system $S_2(x_2, y_2, z_2)$. Consequently, surface Σ_2 can be represented by equations

$$\begin{aligned} x_2 &= x_2(u, \theta, \phi_1), \quad y_2 = y_2(u, \theta, \phi_1), \\ z_2 &= z_2(u, \theta, \phi_1), \quad f(u, \theta, \phi_1) = 0 \end{aligned} \quad (1.5.3)$$

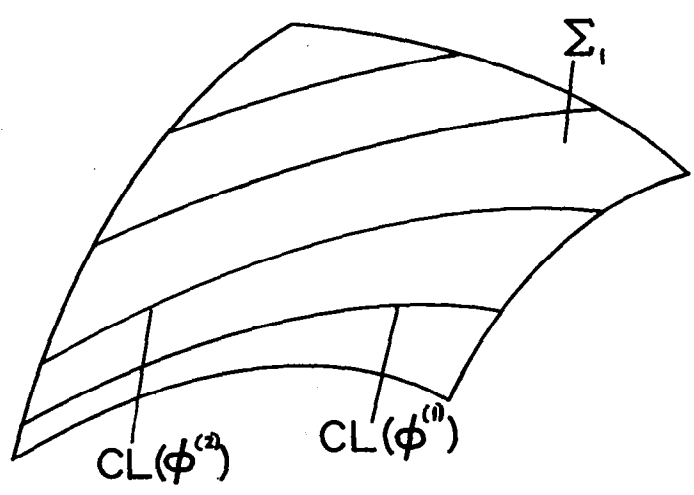


FIG. 1.5.1

Surface Covered with Contact Lines

The first of these three equations can be obtained through the matrix equation

$$\begin{bmatrix} r_2 \end{bmatrix} = \begin{bmatrix} M_{21}(\phi_1) \end{bmatrix} \begin{bmatrix} r_1(u, \theta) \end{bmatrix}, \quad (1.5.4)$$

where

$$\begin{bmatrix} r_2 \end{bmatrix} = \begin{bmatrix} x_2 \\ y_2 \\ z_2 \\ 1 \end{bmatrix}, \quad \begin{bmatrix} r_1 \end{bmatrix} = \begin{bmatrix} x_1(u, \theta) \\ y_1(u, \theta) \\ z_1(u, \theta) \\ 1 \end{bmatrix};$$

matrix $\begin{bmatrix} M_{21} \end{bmatrix}$ describes coordinate transformation by transition from S_1 to S_2 .

The surface of action is a locus of contact lines represented in the coordinate system S_f by equations

$$\begin{aligned} x_f &= x_f(u, \theta, \phi_1), & y_f &= y_f(u, \theta, \phi_1), & z_f &= z_f(u, \theta, \phi_1), \\ f(u, \theta, \phi_1) &= 0 \end{aligned} \quad (1.5.5)$$

The first three equations are obtained by using the matrix equation

$$\begin{bmatrix} r_f \end{bmatrix} = \begin{bmatrix} M_{f1}(\phi_1) \end{bmatrix} \begin{bmatrix} r_1(u, \theta) \end{bmatrix} \quad (1.5.6)$$

Sample problem 1.5.1.

The generating process of spiral bevel gears is shown in Fig. 1.5.2. The tool is a head-cutter with blades mounted in it. Both shapes of a blade are straight lines. By rotation about head-cutter axis C the straight-lined side of the blade describes a cone surface with vertex angle $2\psi_c$ (Fig. 1.5.3,a). The angular velocity of the head-cutter rotation is not related to the kinematics of tooth generation.

The head cutter is mounted on the cradle of the cutting machine (Fig. 1.5.2). In the process of cutting the cradle and the to-be-generated gear rotate about intersecting axes $0-0$ and $a-a$ with angular velocities $\omega^{(1)}$ and $\omega^{(2)}$, respectively. The generating surface Σ_1 and the generating gear are shown in Fig. 1.5.3.

The conic surface Σ_1 is represented in coordinate system S_c

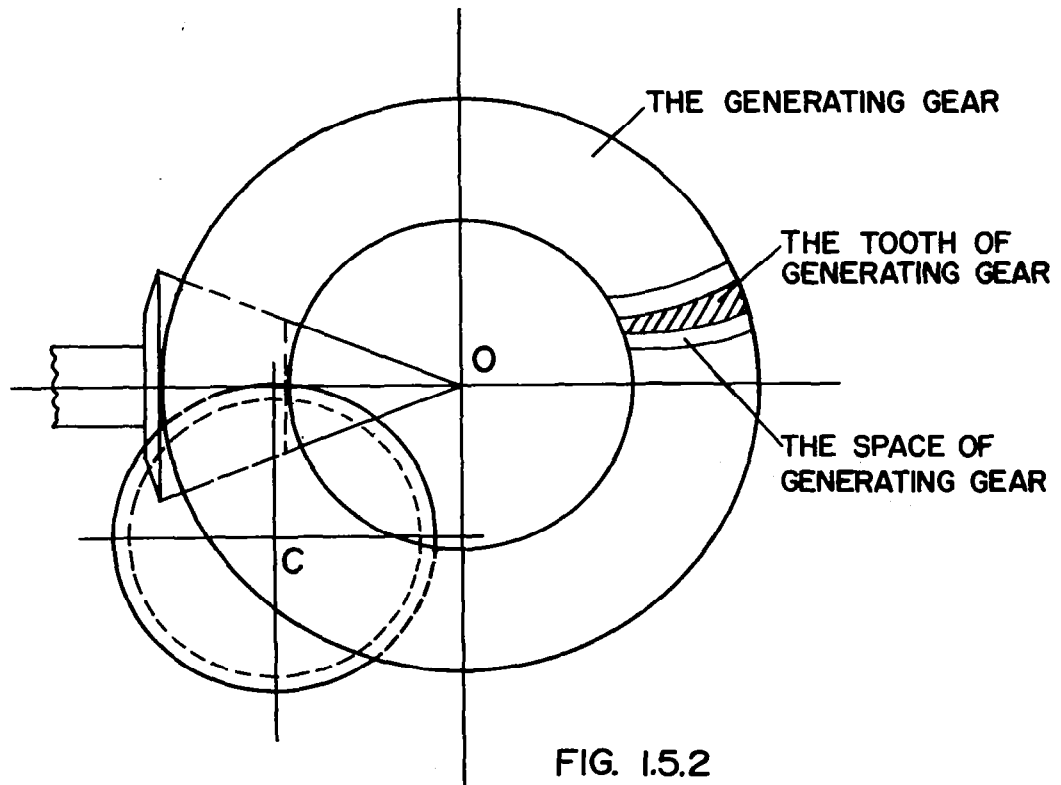
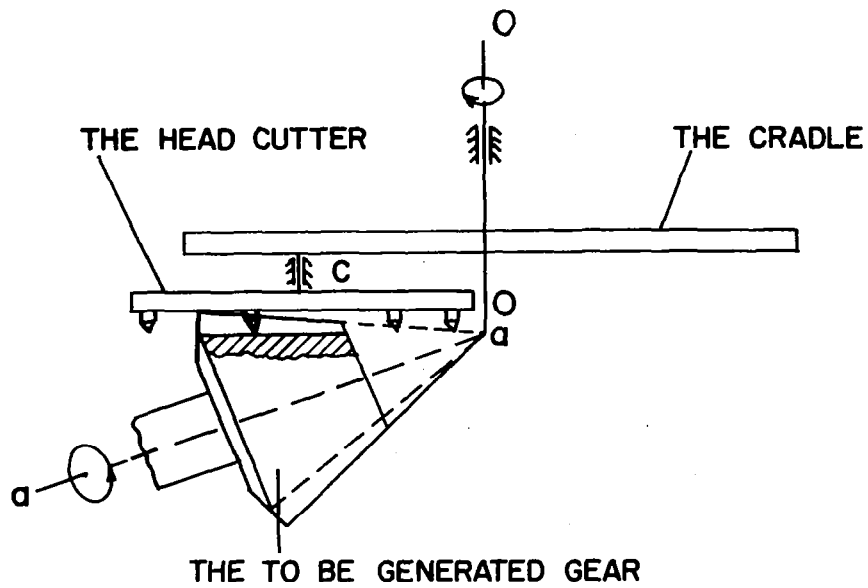


FIG. I.5.2

Schematic of Cutting Process for Spiral Bevel Gears

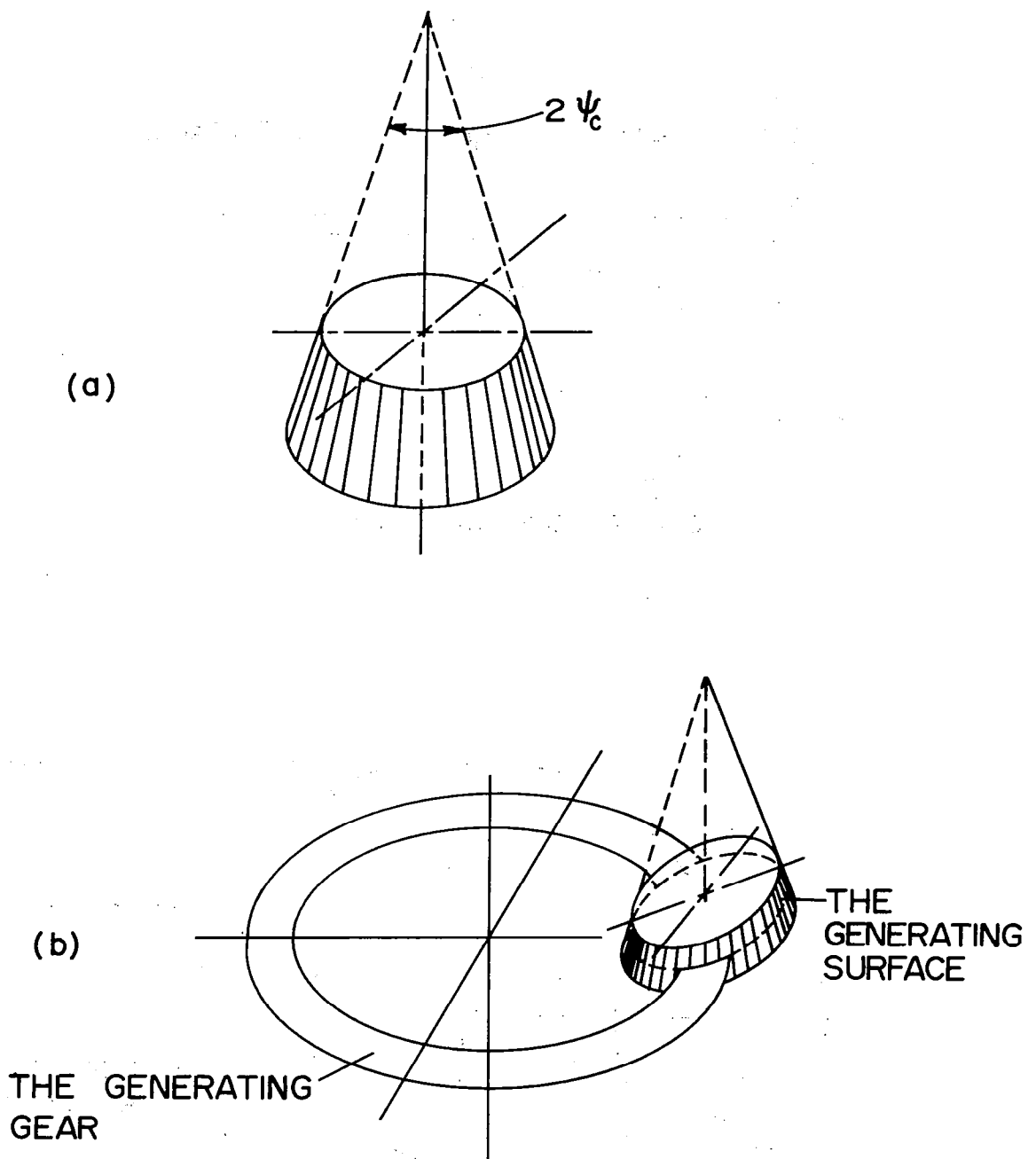


FIG. 1.5.3

Generating Surface and Generating Gear

(Fig. 1.5.4,a) by the equation

$$\begin{aligned}x_c &= r_c \cot \psi_c - u \cos \psi_c, \\y_c &= u \sin \psi_c \sin \theta, \\z_c &= u \sin \psi_c \cos \theta.\end{aligned}\tag{1.5.7}$$

Here: $u = \overline{O_1 N}$ and θ are surface coordinates, ψ_c is the angle made by the cone generatrix and cone axis and r_c is the mean radius of the head cutter measured in plane $x_c = 0$.

Coordinate systems S_c and S_1 are rigidly connected with the generating gear. Axis x_1 is the axis of rotation of the generating gear by cutting. The location of the head cutter (or of system S_c) is defined by the distance $O_1 O_c = b$ and by the angle q (Fig. 1.5.4,b and Fig. 1.5.4,c); β is the mean spiral angle; M is the point of intersection of the cone surface and axis z_1 .

The coordinate transformation from system S_c to S_1 is represented by matrix equation

$$[r_1] = [M_{1c}] [r_c],\tag{1.5.8}$$

where (Fig. 1.5.4)

$$[M_{1c}] = \begin{bmatrix} 1 & 0 & 0 & 0 \\ 0 & \cos q & -\sin q & -b \sin q \\ 0 & \sin q & \cos q & b \cos q \\ 0 & 0 & 0 & 1 \end{bmatrix}\tag{1.5.9}$$

Equations (1.5.7)-(1.5.9) yield

$$\begin{aligned}x_1 &= r_c \cot \psi_c - u \cos \psi_c \\y_1 &= u \sin \psi_c \sin(\theta - q) - b \sin q \\z_1 &= u \sin \psi_c \cos(\theta - q) + b \cos q.\end{aligned}\tag{1.5.10}$$

Equations (1.5.10) represent the generating surface in coordinate system S_1 , represent the generating gear.

The surface normal is represented by the equation

$$\underline{N}_1 = \frac{\partial \underline{r}_1}{\partial \theta} \times \frac{\partial \underline{r}_1}{\partial u} =$$

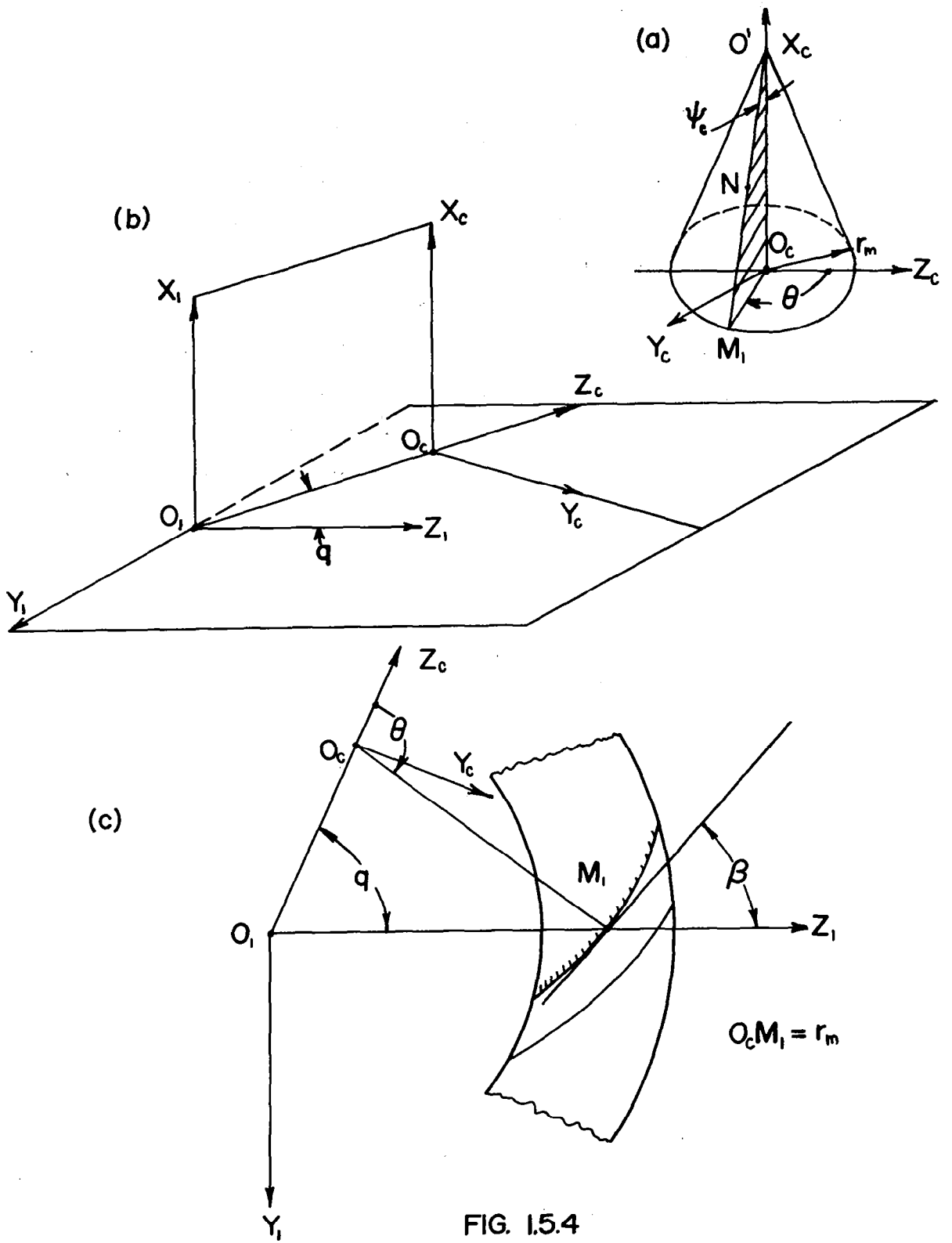


FIG. I.5.4

$$\begin{aligned}
&= \begin{vmatrix} \underline{i}_1 & \underline{j}_1 & \underline{k}_1 \\ 0 & u \sin \psi_c \cos(\theta-q) & -u \sin \psi_c \sin(\theta-q) \\ -\cos \psi_c & \sin \psi_c \sin(\theta-q) & \sin \psi_c \cos(\theta-q) \end{vmatrix} = \\
&= u \sin^2 \psi_c \underline{i}_1 + u \sin \psi_c \cos \psi_c \sin(\theta-q) \underline{j}_1 + u \sin \psi_c \cos \psi_c \cos(\theta-q) \underline{k}_1
\end{aligned} \tag{1.5.11}$$

The surface unit normal is represented by the equations (it is assumed that $u \sin \psi_c \neq 0$):

$$\underline{n}_1 = \sin \psi_c \underline{i}_1 + \cos \psi_c \sin(\theta-q) \underline{j}_1 + \cos \psi_c \cos(\theta-q) \underline{k}_1 \tag{1.5.12}$$

In the process of cutting the generating gear 1 rotates about axis x_f (of coordinate system S_f) rigidly connected with the frame, while the generated gear 2 rotates about axis z_p of the auxiliary coordinate system S_p which is rigidly connected with $S_f(x_f, y_f, z_f)$ (Fig. 1.5.5). The angular velocities $\omega^{(1)}$ and $\omega^{(2)}$ are related such that $O_p M^{(p)}$ is the instantaneous axis of rotation ($O_p M^{(p)}$ is the generatrix of the pitch cone of gear 2). A coordinate system S_2 (see below) is rigidly connected with gear 2.

The coordinate transformation is represented by matrix equations

$$[r_f] = [M_{f1}] [r_1] \tag{1.5.12}$$

$$[r_p] = [M_{pf}] [r_f] \tag{1.5.13}$$

$$[r_2] = [M_{2p}] [r_p] \tag{1.5.14}$$

According to the drawings of Figs. 1.5.5-7, the mentioned matrices are given by

$$[M_{f1}] = \begin{bmatrix} 1 & 0 & 0 & 0 \\ 0 & \cos \phi_1 & \sin \phi_1 & 0 \\ 0 & -\sin \phi_1 & \cos \phi_1 & 0 \\ 0 & 0 & 0 & 1 \end{bmatrix} \tag{1.5.15}$$

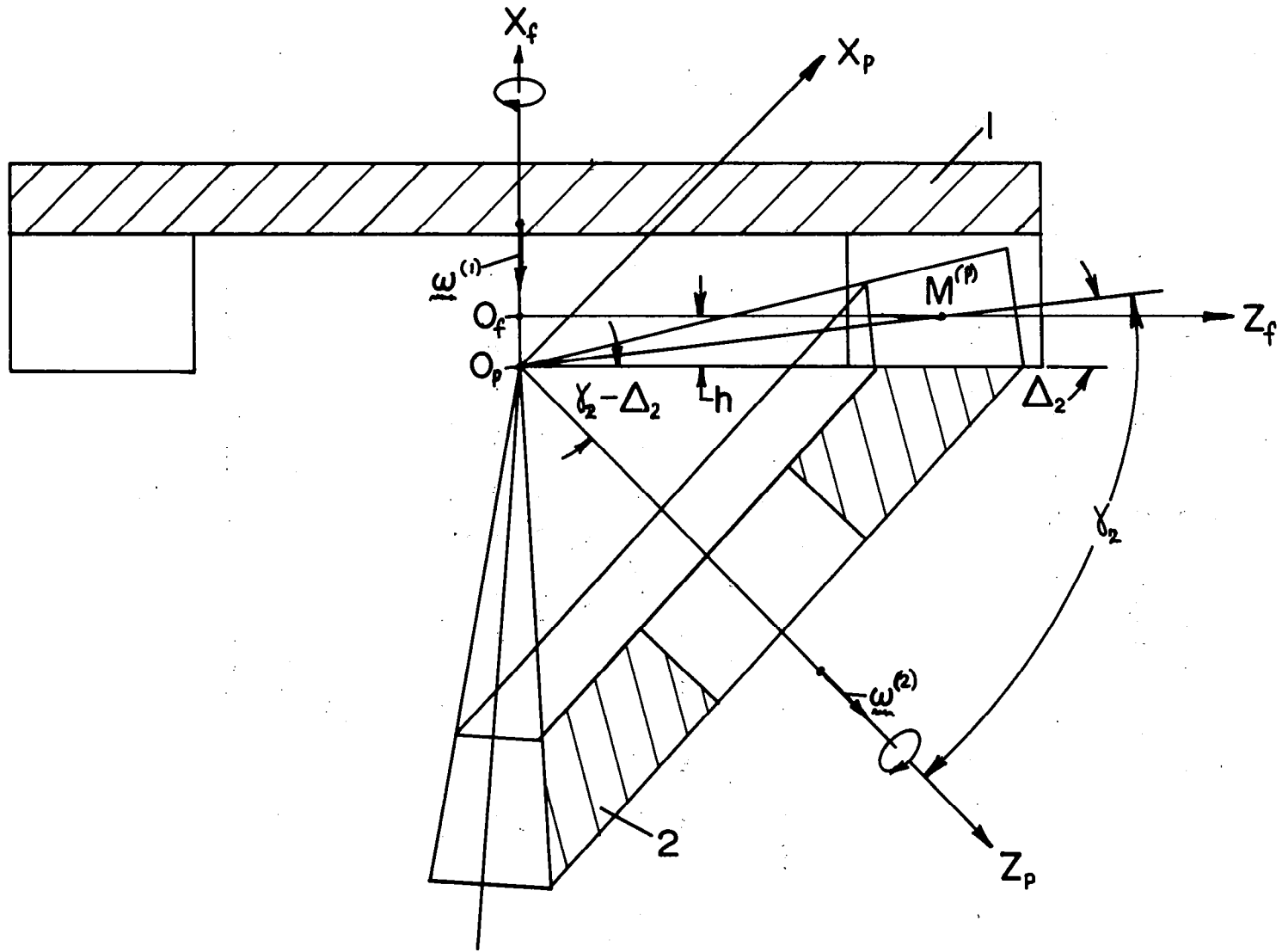


FIG I.5.5

Positioning of Generating Gear and Generated Gear During Cutting

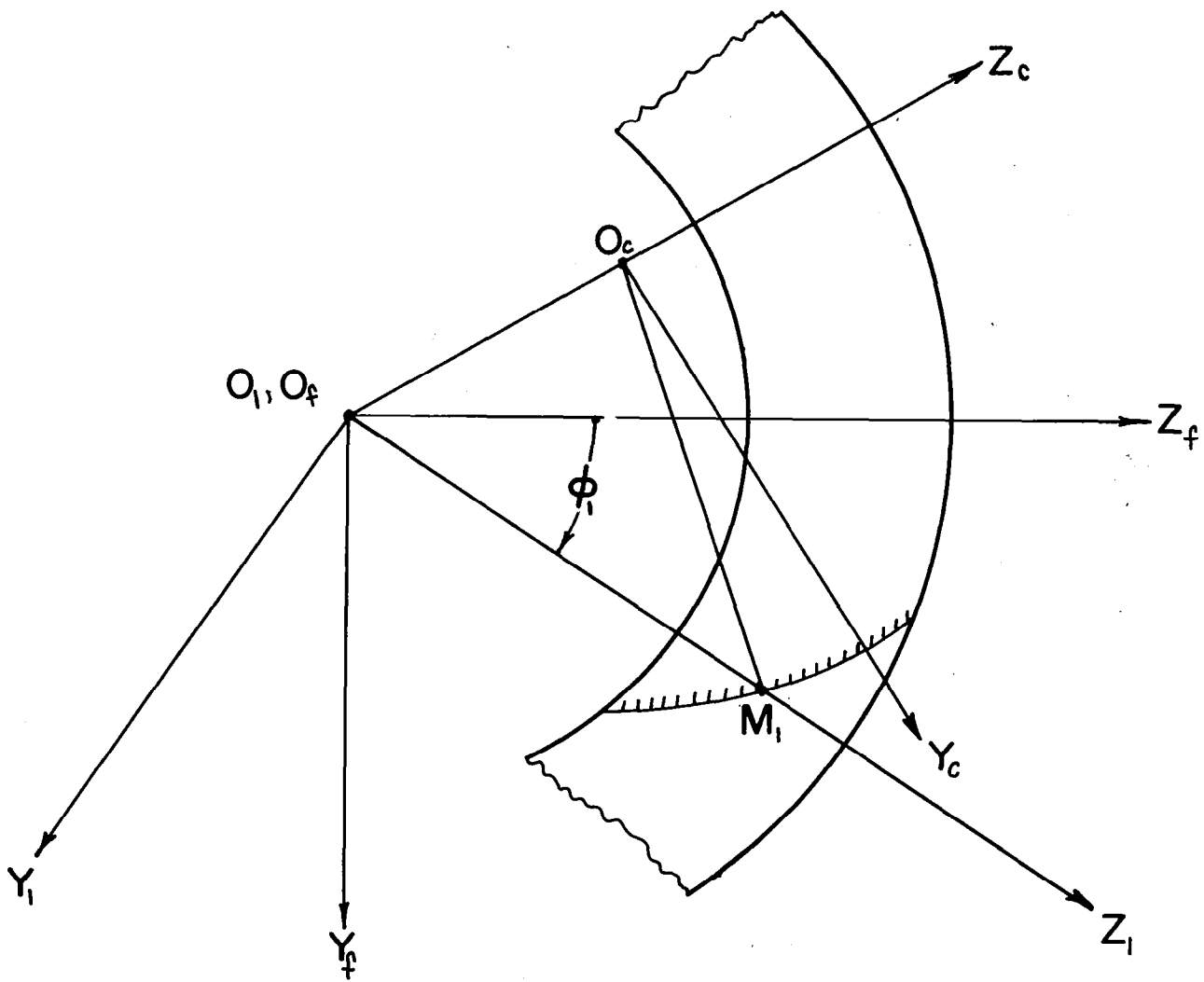


FIG. 1.5.6

Applied Coordinate Systems (Top View)

$$[M_{pf}] = \begin{bmatrix} \cos(\gamma_2 - \Delta_2) & 0 & \sin(\gamma_2 - \Delta_2) & h \cos(\gamma_2 - \Delta_2) \\ 0 & 1 & 0 & 0 \\ -\sin(\gamma_2 - \Delta_2) & 0 & \cos(\gamma_2 - \Delta_2) & -h \sin(\gamma_2 - \Delta_2) \\ 0 & 0 & 0 & 1 \end{bmatrix} \quad (1.5.16)$$

$$[M_{2p}] = \begin{bmatrix} \cos\phi_2 & \sin\phi_2 & 0 & 0 \\ -\sin\phi_2 & \cos\phi_2 & 0 & 0 \\ 0 & 0 & 1 & 0 \\ 0 & 0 & 0 & 1 \end{bmatrix} \quad (1.5.17)$$

Let us define the equation of meshing (1.4.7). The relative velocity $\underline{v}_f^{(21)}$ is represented by equation

$$\begin{aligned} \underline{v}_f^{(21)} &= \underline{v}_f^{(2)} - \underline{v}_f^{(1)} = \underline{\omega}_f^{(2)} \times \underline{r}_f + \overline{0_1 0_p} \times \underline{\omega}_f^{(2)} - \underline{\omega}_f^{(1)} \times \underline{r}_f = \\ &(\underline{\omega}_f^{(2)} - \underline{\omega}_f^{(1)}) \times \underline{r}_f + \overline{0_1 0_p} \times \underline{\omega}_f^{(2)} = \end{aligned}$$

$$\begin{vmatrix} \underline{i}_f & \underline{j}_f & \underline{k}_f \\ -\omega^{(2)} \sin(\gamma_2 - \Delta_2) + \omega^{(1)} & 0 & \omega^{(2)} \cos(\gamma_2 - \Delta_2) \\ x_f & y_f & z_f \end{vmatrix} + \begin{vmatrix} \underline{i}_f & \underline{j}_f & \underline{k}_f \\ -h & 0 & 0 \\ -\omega^{(2)} \sin(\gamma_2 - \Delta_2) & 0 & \omega^{(2)} \cos(\gamma_2 - \Delta_2) \end{vmatrix} \quad (1.5.17)$$

Vectors $\underline{\omega}^{(2)}$ and $\underline{\omega}^{(1)}$ are related such that $\underline{\omega}^{(2)} - \underline{\omega}^{(1)} = \underline{\omega}^{(21)}$ coincides with the generatrix of the pitch cone. Consequently (Fig. 1.5.5),

$$\omega^{(2)} \sin\gamma_2 = \omega^{(1)} \cos\Delta_2 \quad (1.5.18)$$

Equations (1.5.17) and (1.5.18) yield

$$\underline{v}_f^{(21)} = \omega^{(2)} \cos(\gamma_2 - \Delta_2) [-y_f \underline{i}_f + (x_f + h) \underline{j}_f] \quad (1.5.19)$$

It results from equation of meshing (1.4.7) that $N_f \cdot \underline{v}_f^{(21)} = 0$ and from (1.5.19) that

$$-y_f N_{fx} + (x_f + L \sin\Delta_2) N_{fy} = 0 \quad (1.5.20)$$

Here $L \sin \Delta_2 = h$ (Fig. 1.5.5), where $l = 0_2 M^{(p)}$ is the mean length of the generatrix of pitch cone.

Equation (1.5.20) can be obtained another way, on the basis of equation (1.4.14), which was represented above by

$$\frac{X_f - x_f}{N_{fx}} - \frac{Y_f - y_f}{N_{fy}} = 0 \quad (1.5.21)$$

Here X_f and Y_f are coordinates of an arbitrary point on instantaneous axis of rotation - generatrix $O_p M^{(p)}$. In the discussed case putting into equation (1.5.21) coordinates $X_f = h, Y_f = 0$ of point O_p (Fig. 1.5.7), equation (1.5.20) will be found.

Equation (1.5.10) and matrix equation (1.5.12) with matrix (1.5.15) yield that

$$\begin{aligned} x_f &= r_c \cot \psi_c - u \cos \psi_c \\ y_f &= u \sin \psi_c \sin(\theta - q + \phi_1) - b \sin(q - \phi_1) \\ z_f &= u \sin \psi_c \cos(\theta - q + \phi_1) + b \cos(q - \phi_1) \end{aligned} \quad (1.5.22)$$

Equation (1.5.11) and matrix equation

$$[n_f] = [L_{f1}] [n_1] \quad (1.5.23)$$

yield

$$\begin{aligned} n_{fx} &= \sin \psi_c, \quad n_{fy} = \cos \psi_c \sin(\theta - q + \phi_1), \\ n_{fz} &= \cos \psi_c \cos(\theta - q + \phi_1) \end{aligned} \quad (1.5.24)$$

Matrix $[L_{f1}]$ is a submatrix of $[M_{f1}]$ which is found from $[M_{f1}]$ by elimination of the fourth row and fourth column. Projections of N_{fx} and of N_{fy} contained in equation (1.5.20) can be substituted by proportional projections of n_f .

Equations (1.5.20), (1.5.22) and (1.5.24) yield

$$\begin{aligned} & (r_c \cot \psi_c - u \cos \psi_c + L \sin \Delta_2) \cos \psi_c \sin(\theta - q + \phi_1) - \\ & [u \sin \psi_c \sin(\theta - q + \phi_1) - b \sin(q - \phi_1)] \sin \psi_c = \\ & [(r_c \cot \psi_c + L \sin \Delta_2) \cos \psi_c - u] \sin(\theta - q + \phi_1) + \\ & b \sin \psi_c \sin(q - \phi_1) = f(u, \theta, \phi_1) = 0 \end{aligned} \quad (1.5.25)$$

Equation (1.5.25) is the equation of meshing.

Equations (1.5.10) and (1.5.25) represent the set of contact lines covering surface Σ_1 . Each contact line of the set is defined by fixed value of ϕ . Surface Σ_2 is represented by equations

$$\begin{aligned} x_2 &= x_2(u, \theta, \phi_1), \quad y_2 = y_2(u, \theta, \phi_1), \quad z_2 = z_2(u, \theta, \phi_1), \\ f(u, \theta, \phi_1) &= 0 \end{aligned} \quad (1.5.26)$$

The first three equations are defined by equations (1.5.10) and matrix equality

$$[r_2] = [M_{2p}] [M_{pf}] [M_{f1}] [r_1] \quad (1.5.27)$$

1.6 Relations Between Principal Curvatures and Directions of Two Surfaces Being in Meshing

Generally, equations of the enveloped surface are considerably more complicated than of the enveloping one. Therefore a direct way to obtain the principal curvatures and directions of the enveloped surface is a very hard problem. The solution of this problem can be significantly simplified if relations between the principal curvatures and directions of two surfaces which are in mesh are known. Such relations were worked out first by F. L. Litvin. It is necessary to emphasize that the principal curvatures and directions of two contacting surfaces are necessary to define the size and direction of contact ellipse at the contact point.

Let us suppose that surfaces Σ_1 and Σ_2 contact each other at point M given in the coordinate system S_f rigidly connected with the frame. Principal directions of surface Σ_1 are represented by unit vectors \tilde{i}_I and \tilde{i}_{II} and principal curvatures κ_I and κ_{II} of Σ_1 are known. At the point of contact the equation of meshing

$$\tilde{n}_f^{(1)} \cdot \tilde{v}_f^{(12)} = \tilde{n}_f^{(1)} \cdot \left[(\omega_f^{(1)} - \omega_f^{(2)}) \tilde{x}_{r_f}^{(1)} - (R_f \times \omega_f^{(2)}) \right] = 0 \quad (1.6.1)$$

is satisfied

Here: $\underline{n}_f^{(1)}$ is the surface Σ_1 unit normal; $\underline{v}_f^{(12)}$ is the relative velocity ($\underline{v}_f^{(12)} = \underline{v}_f^{(1)} - \underline{v}_f^{(2)}$); $\underline{v}_f^{(i)}$ ($i=1,2$) is the transfer velocity of a point rigidly connected with surface Σ_i ; \underline{R}_f is a vector-radius drawn from the origin of coordinate system S_f to an arbitrary point of the line of action of angular velocity $\underline{\omega}_f^{(2)}$; vector $\underline{v}_f^{(12)} = -\underline{v}_f^{(21)} = -(\underline{v}_f^{(2)} - \underline{v}_f^{(1)})$ where $\underline{v}_f^{(21)}$ is the vector represented by equations (1.3.14).

Equation of meshing (1.6.1) must be observed not only at the point of contact M, but in the neighborhood of M, too. Therefore, equation (1.6.1) can be differentiated which yields:

$$\dot{\underline{n}}^{(1)} \underline{v}^{(12)} + \underline{n}^{(1)} (\underline{\omega}^{(12)} \times \dot{\underline{r}}^{(1)}) = 0 \quad (1.6.2)$$

It is assumed that $\underline{\omega}^{(1)} = \text{const}$, $R^{(21)} = \frac{\omega^{(2)}}{\omega^{(1)}} = \text{const}$, $R = \text{const}$. Lower subscript "f" is eliminated for simplification.

According to results demonstrated in items (1.1) and (1.2) by equations (1.1.31) and (1.2.7) it yields that

$$\dot{\underline{n}}^{(1)} = \underline{\omega}^{(1)} \times \underline{n}^{(1)} + \dot{\underline{n}}_r^{(1)} \quad (1.6.3)$$

Equation (1.1.30) yields

$$\dot{\underline{r}}^{(1)} = \underline{v}_{tr}^{(1)} + \underline{v}_r^{(1)} \quad (1.6.4)$$

It results from equations (1.6.2), (1.6.3) and (1.6.4) that

$$\left[\underline{\omega}^{(1)} \underline{n}^{(1)} \underline{v}^{(12)} \right] + \dot{\underline{n}}_r^{(1)} \cdot \underline{v}^{(12)} + \left[\underline{n}^{(1)} \underline{\omega}^{(12)} \underline{v}_{tr}^{(1)} \right] + \left[\underline{n}^{(1)} \underline{\omega}^{(12)} \underline{v}_r^{(1)} \right] = 0 \quad (1.6.5)$$

where

$$\underline{v}^{(12)} = \underline{v}_{tr}^{(1)} - \underline{v}_{tr}^{(2)} \quad (1.6.6)$$

$$\underline{\omega}^{(12)} = \underline{\omega}^{(1)} - \underline{\omega}^{(2)} \quad (1.6.7)$$

Equations (1.6.5)-(1.6.7) yield

$$\begin{aligned} & \dot{\underline{n}}_r^{(1)} \underline{v}^{(12)} - \underline{v}_r^{(1)} (\underline{\omega}^{(12)} \times \underline{n}^{(1)}) + \underline{n}^{(1)} \cdot (\underline{\omega}^{(1)} \times \underline{v}_{tr}^{(1)} - \underline{\omega}^{(2)} \times \underline{v}_{tr}^{(1)}) \\ & = 0 \end{aligned} \quad (1.6.8)$$

Two other equations

$$\underline{v}_r^{(2)} = \underline{v}_r^{(1)} + \underline{v}^{(12)} \quad (1.6.9)$$

$$\dot{\underline{n}}_r^{(2)} = \dot{\underline{n}}_r^{(1)} + \omega^{(12)} \chi \underline{n}^{(1)} \quad (1.6.10)$$

were represented before in item (1.1) by equations (1.1.35) and (1.1.36).

Relations between the principal curvatures and principal directions of surfaces Σ_1 and Σ_2 will be composed on the basis of equations (1.6.8) - (1.6.10). Before this, let us recall the following equations from differential geometry. The normal curvature of a surface is represented by equation

$$\kappa = - \frac{\dot{\underline{n}}_r \cdot \underline{v}_r}{\underline{v}_r \cdot \underline{v}_r} \quad (1.6.11)$$

Along the principal direction, vectors $\dot{\underline{n}}_r$ and \underline{v}_r are co-linear and the principal curvature is represented by equation

$$\dot{\underline{n}}_r \cdot \underline{i} = - \kappa_i (\underline{v}_r \cdot \underline{i}), \quad (1.6.12)$$

where \underline{i} is the unit vector directed along the principal direction.

Now, let us place two right trihedrons at the contact point M (Fig. 1.6.1): $S_a(\underline{i}_I, \underline{i}_{II}, \underline{n})$ and $S_b(\underline{i}_{III}, \underline{i}_{IV}, \underline{n})$. Here: $\underline{i}_I, \underline{i}_{II}$ are unit vectors directed along principal directions of surface Σ_1 ; \underline{i}_{III} and \underline{i}_{IV} are unit vectors directed along principal directions of surface Σ_2 ; \underline{n} is the common unit normal of surfaces Σ_1 and Σ_2 . It is assumed that unit vectors \underline{i}_I and \underline{i}_{III} make an angle σ (Fig. 1.6.1). Vectors $\underline{v}_r^{(1)}, \dot{\underline{n}}_r^{(1)}$ and $\underline{v}_r^{(2)}, \dot{\underline{n}}_r^{(2)}$ can be expressed in terms of components of coordinate systems S_a and S_b by following equations

$$\underline{v}_r^{(1)} = v_{rI}^{(1)} \underline{i}_I + v_{rII}^{(1)} \underline{i}_{II} \quad (1.6.13)$$

$$\dot{\underline{n}}_r^{(1)} = \dot{n}_{rI}^{(1)} \underline{i}_I + \dot{n}_{rII}^{(1)} \underline{i}_{II} \quad (1.6.14)$$

$$\underline{v}_r^{(2)} = v_{rIII}^{(2)} \underline{i}_{III} + v_{rIV}^{(2)} \underline{i}_{IV} \quad (1.6.15)$$

$$\dot{\underline{n}}_r^{(2)} = \dot{n}_{rIII}^{(2)} \underline{i}_{III} + \dot{n}_{rIV}^{(2)} \underline{i}_{IV} \quad (1.6.16)$$

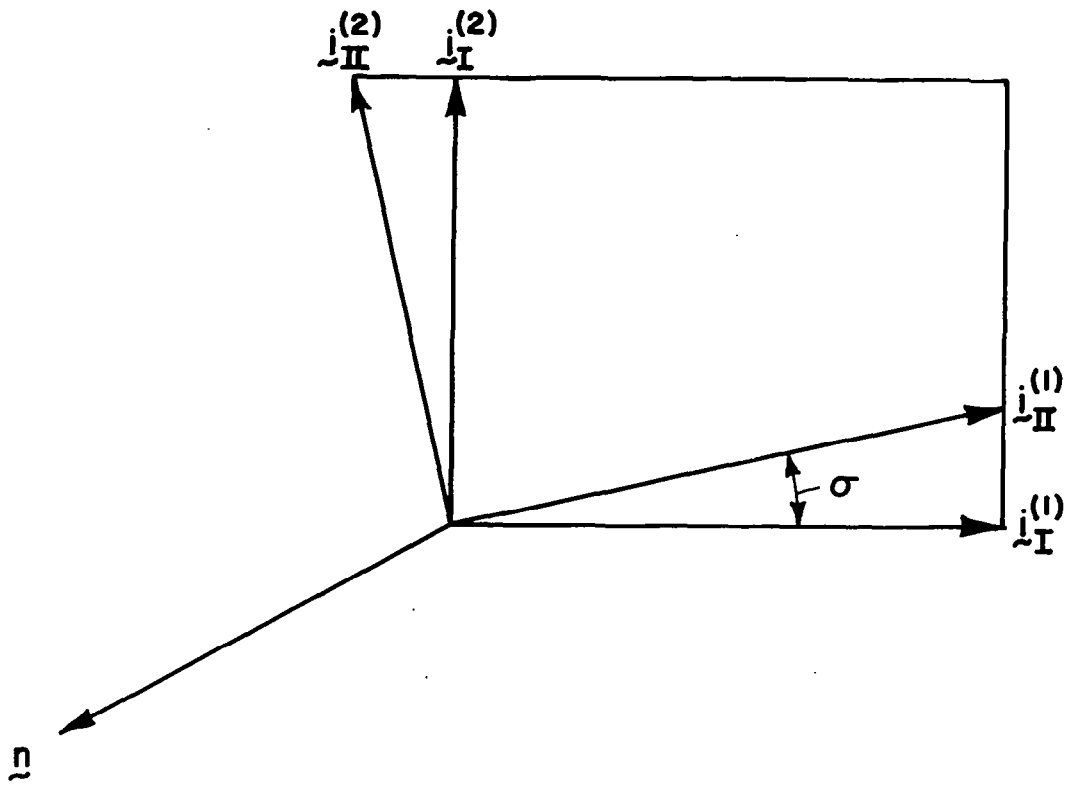


Fig. 1.6.1

Principal Directions of Surfaces Σ_1 and Σ_2

Vectors $v_r^{(2)}$ and $\dot{n}_r^{(2)}$ can be expressed in terms of components of coordinate system $S_a(i_I, i_{II}, n)$ by the following equations

$$v_{rI}^{(2)} = v_r^{(2)} \cdot i_I = v_{rIII}^{(2)} i_{III} \cdot i_I + v_{riv}^{(2)} i_{iv} \cdot i_I \quad (1.6.17)$$

$$v_{rII}^{(2)} = v_r^{(2)} \cdot i_{II} = v_{rIII}^{(2)} i_{III} \cdot i_{II} + v_{riv}^{(2)} i_{iv} \cdot i_{II} \quad (1.6.18)$$

$$\dot{n}_{rI}^{(2)} = \dot{n}_r^{(2)} \cdot i_I = \dot{n}_{rIII}^{(2)} i_{III} \cdot i_I + \dot{n}_{riv}^{(2)} i_{iv} \cdot i_I \quad (1.6.19)$$

$$\dot{n}_{rII}^{(2)} = \dot{n}_r^{(2)} \cdot i_{II} = \dot{n}_{rIII}^{(2)} i_{III} \cdot i_{II} + \dot{n}_{riv}^{(2)} i_{iv} \cdot i_{II} \quad (1.6.20)$$

Here (Fig. 1.6.1):

$$i_{III} \cdot i_I = \cos \sigma, \quad i_{iv} \cdot i_I = -\sin \sigma, \quad i_{III} \cdot i_{II} = \sin \sigma, \quad i_{iv} \cdot i_{II} = \cos \sigma \quad (1.6.21)$$

Equations (1.6.17)-(1.6.21) yield

$$v_{rI}^{(2)} = v_{rIII}^{(2)} \cos \sigma - v_{riv}^{(2)} \sin \sigma \quad (1.6.22)$$

$$v_{rII}^{(2)} = v_{rIII}^{(2)} \sin \sigma + v_{riv}^{(2)} \cos \sigma \quad (1.6.22, a)$$

$$\dot{n}_{rI}^{(2)} = \dot{n}_{rIII}^{(2)} \cos \sigma - \dot{n}_{riv}^{(2)} \sin \sigma \quad (1.6.23)$$

$$\dot{n}_{rII}^{(2)} = \dot{n}_{rIII}^{(2)} \sin \sigma + \dot{n}_{riv}^{(2)} \cos \sigma \quad (1.6.24)$$

Equations (1.6.8)-(1.6.10), (1.6.12) and (1.6.22)-(1.6.24) yield the following system of 9 linear equations in 8 unknowns $v_{rI}^{(1)}$, $v_{rII}^{(1)}$, $\dot{n}_{rI}^{(1)}$, $\dot{n}_{rII}^{(1)}$, $v_{rIII}^{(2)}$, $v_{riv}^{(2)}$, $\dot{n}_{rIII}^{(2)}$, $\dot{n}_{riv}^{(2)}$:

$$\dot{n}_{rI}^{(1)} v_I^{(12)} + \dot{n}_{rII}^{(1)} v_{II}^{(12)} - v_{rI}^{(1)} \left[\omega^{(12)} n^{(1)} i_I \right] - v_{rII}^{(1)} \left[\omega^{(12)} n^{(1)} i_{II} \right] = \left[n^{(1)} \omega^{(2)} v_{tr}^{(1)} \right] - \left[n^{(1)} \omega^{(1)} v_{tr}^{(2)} \right] \quad (1.6.25)$$

$$v_{rIII}^{(2)} \cos \sigma - v_{riv}^{(2)} \sin \sigma - v_{rI}^{(1)} = v_I^{(12)} \quad (1.6.26)$$

$$v_{rIII}^{(2)} \sin \sigma + v_{riv}^{(2)} \cos \sigma - v_{rII}^{(1)} = v_{II}^{(12)} \quad (1.6.27)$$

$$\dot{n}_{rIII}^{(2)} \cos \sigma - \dot{n}_{riv}^{(2)} \sin \sigma - \dot{n}_{rI}^{(1)} = \left[\omega^{(12)} n^{(1)} i_I \right] \quad (1.6.28)$$

$$\dot{n}_{rIII}^{(2)} \sin \sigma + \dot{n}_{riv}^{(2)} \cos \sigma - \dot{n}_{rII}^{(1)} = \left[\omega^{(12)} n^{(1)} i_{II} \right] \quad (1.6.29)$$

$$\dot{n}_{rI}^{(1)} + \kappa_I v_{rI}^{(1)} = 0 \quad (1.6.30)$$

$$\dot{n}_{rII}^{(2)} + \kappa_{II} v_{rII}^{(1)} = 0 \quad (1.6.31)$$

$$\dot{n}_{rIII}^{(2)} + \kappa_{III} v_{rIII}^{(2)} = 0 \quad (1.6.32)$$

$$\dot{n}_{riv}^{(2)} + \kappa_{iv} v_{riv}^{(2)} = 0 \quad (1.6.33)$$

Here: κ_I and κ_{II} , κ_{III} and κ_{iv} are principal curvatures of surfaces Σ_1 and Σ_2 at contact point M.

After eliminating 6 unknowns a system of 3 linear equations in two unknowns $x_1 = v_{rI}^{(1)}$, $x_2 = v_{rII}^{(1)}$ can be got:

$$\begin{aligned} a_{11}x_1 + a_{12}x_2 &= b_1 \\ a_{21}x_1 + a_{22}x_2 &= b_2 \\ a_{31}x_1 + a_{32}x_2 &= b_3 \end{aligned} \quad (1.6.34)$$

Here:

$$\begin{aligned} a_{11} &= -\kappa_I + 1/2 \left[(\kappa_{III} + \kappa_{iv}) + (\kappa_{III} - \kappa_{iv}) \cos 2\sigma \right]; \\ a_{12} &= a_{21} = 1/2 \left[(\kappa_{III} - \kappa_{iv}) \sin 2\sigma \right]; \\ a_{22} &= -\kappa_{II} + 1/2 \left[(\kappa_{III} + \kappa_{iv}) - (\kappa_{III} - \kappa_{iv}) \cos 2\sigma \right]; \\ a_{31} &= \left[\tilde{n}^{(1)} \tilde{\omega}^{(12)} \tilde{i}_I \right] - \kappa_I v_I^{(12)} \\ a_{32} &= \left[\tilde{n}^{(1)} \tilde{\omega}^{(12)} \tilde{i}_{II} \right] - \kappa_{II} v_{II}^{(12)} \\ b_1 &= \left[\tilde{n}^{(1)} \tilde{\omega}^{(12)} \tilde{i}_I \right] - \frac{v_I^{(12)}}{2} \left[(\kappa_{III} + \kappa_{iv}) + (\kappa_{III} - \kappa_{iv}) \cos 2\sigma \right] - \\ &\quad \frac{v_{II}^{(12)}}{2} (\kappa_{III} - \kappa_{iv}) \sin 2\sigma \\ b_2 &= \left[\tilde{n}^{(1)} \tilde{\omega}^{(12)} \tilde{i}_{II} \right] - \frac{v_I^{(12)}}{2} (\kappa_{III} - \kappa_{iv}) \sin 2\sigma - \\ &\quad \frac{v_{II}^{(12)}}{2} \left[(\kappa_{III} + \kappa_{iv}) - (\kappa_{III} - \kappa_{iv}) \cos 2\sigma \right] \end{aligned}$$

$$b_3 = \left[\begin{matrix} \tilde{n}^{(1)} \tilde{\omega}^{(2)} \tilde{v}_{tr}^{(1)} \end{matrix} \right] - \left[\begin{matrix} \tilde{n}^{(1)} \tilde{\omega}^{(1)} \tilde{v}_{tr}^{(2)} \end{matrix} \right]$$

The number of equations (1.6.34) is not equal to the number of unknowns. Therefore, requirements to this system by which the system will have a solution must be discussed.

Let us consider two cases: (a) the instantaneous contact of surfaces Σ_1 and Σ_2 is a linear-contact; (b) the instantaneous contact of surfaces is a point contact.

In the first case surface Σ_1 is covered with instantaneous contact lines (Fig. 1.6.2,a) and the direction of $\tilde{v}_R^{(1)}$ from point M to the neighboring one is an indefinite one and the system (1.6.34) must have an infinite number of solutions. In the second case contact points makes on surface Σ_1 a line (Fig. 1.6.2,b), the direction of $\tilde{v}_R^{(1)}$ to the neighboring point is a definite one, and the system (1.6.34) must possess one solution.

It is known from linear algebra that system (1.6.34) possesses an infinite number of solutions if the rank of matrix

$$\begin{bmatrix} a_{11} & a_{12} & b_1 \\ a_{21} & a_{22} & b_2 \\ a_{31} & a_{32} & b_3 \end{bmatrix} \quad (1.6.35)$$

is equal to one

That yields

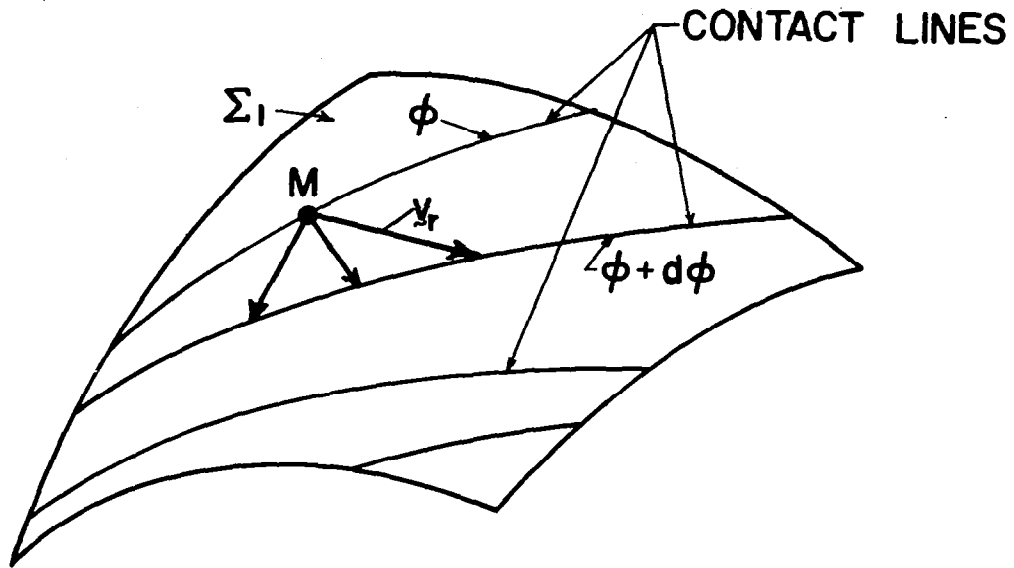
$$\frac{a_{11}}{a_{21}} = \frac{a_{12}}{a_{22}} = \frac{b_1}{b_2}, \quad \frac{a_{21}}{a_{31}} = \frac{a_{22}}{a_{32}} = \frac{b_2}{b_3} \quad (1.6.36)$$

Taking into account that $a_{21} = a_{12}$ equalities (1.6.36) can be represented as:

$$\frac{a_{11}}{a_{21}} = \frac{a_{12}}{a_{22}} = \frac{a_{31}}{a_{32}} = \frac{b_1}{b_2}, \quad (1.6.37)$$

$$\frac{a_{21}}{a_{31}} = \frac{b_2}{b_3} \quad (1.6.38)$$

(a)



(b)

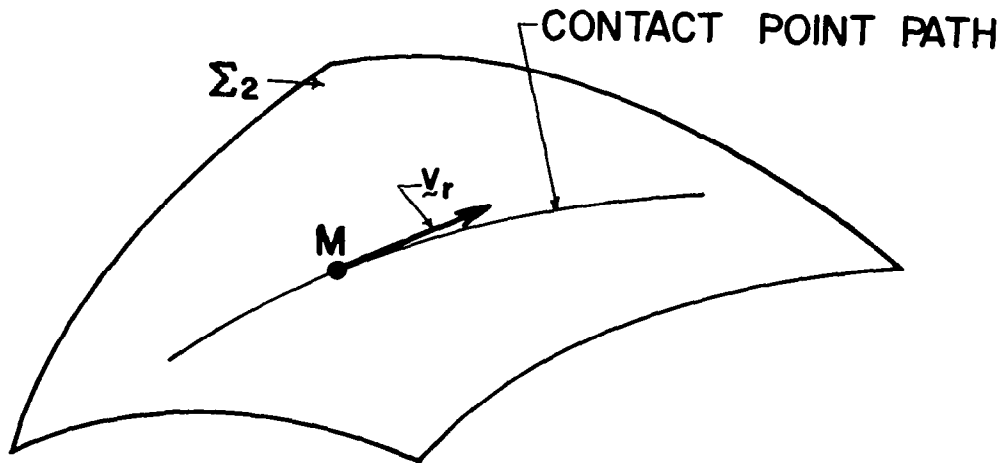


Fig: 1.6.2

Directions of Velocity of Contact Point

The system of equalities (1.6.37) provides only two independent equations because

$$b_1 = a_{31} - v_I^{(12)} a_{11} - v_{II}^{(12)} a_{12}, \quad b_2 = a_{32} - v_I^{(12)} a_{12} - v_{II}^{(12)} a_{22}$$

Equality (1.6.38) and

$$\frac{a_{11}}{a_{21}} = \frac{a_{12}}{a_{22}} = \frac{a_{31}}{a_{32}} \quad (1.6.39)$$

provide three equations for definition of κ_{III} , κ_{iv} and σ :

$$\tan 2\sigma = \frac{2F}{\kappa_I - \kappa_{II} + G} \quad (1.6.40)$$

$$\kappa_{III} + \kappa_{iv} = \kappa_I + \kappa_{II} + S \quad (1.6.41)$$

$$\kappa_{III} - \kappa_{iv} = \frac{\kappa_I - \kappa_{II} + G}{\cos 2\sigma} \quad (1.6.42)$$

Here:

$$F = \frac{a_{31} a_{32}}{b_3 + v_I^{(12)} a_{31} + v_{II}^{(12)} a_{32}}$$

$$G = \frac{a_{31}^2 - a_{32}^2}{b_3 + v_I^{(12)} a_{31} + v_{II}^{(12)} a_{32}}$$

$$S = \frac{a_{31}^2 + a_{32}^2}{b_3 + v_I^{(12)} a_{31} + v_{II}^{(12)} a_{32}}$$

For the case when surfaces Σ_1 and Σ_2 are in point contact and the system (1.6.34) possesses one solution the rank of matrix (1.6.35) must be equal to two. That yields that the determinant of matrix (1.6.35) must be equal to zero. Consequently,

$$\begin{vmatrix} a_{11} & a_{12} & b_1 \\ a_{21} & a_{22} & b_2 \\ a_{31} & a_{32} & b_3 \end{vmatrix} = 0 \quad (1.6.43)$$

Equality (1.6.43) provides an equation

$$f(\kappa_I, \kappa_{II}, \kappa_{III}, \kappa_{IV}, \sigma) = 0 \quad (1.6.44)$$

which relates the principal curvatures and directions of two surfaces in point contact.

Sample problem 1.6.1. Let us compose equations to define principal curvatures and directions of a spiral bevel gear generated by a cone surface (sample problem 1.5.1). The generating surface Σ_1 is represented by equation (1.5.22).

The relative velocity $\underline{v}_R^{(1)}$ is represented by the following equations

$$\left[\underline{v}_R^{(1)} \right] = \begin{bmatrix} \frac{\partial x_f}{\partial u} \frac{du}{dt} + \frac{\partial x_f}{\partial \theta} \frac{d\theta}{dt} \\ \frac{\partial y_f}{\partial u} \frac{du}{dt} + \frac{\partial y_f}{\partial \theta} \frac{d\theta}{dt} \\ \frac{\partial z_f}{\partial u} \frac{du}{dt} + \frac{\partial z_f}{\partial \theta} \frac{d\theta}{dt} \end{bmatrix} \quad (1.6.45)$$

Equation (1.5.22) and equality (1.6.45) yield

$$\left[\underline{v}_R^{(1)} \right] = \begin{bmatrix} -\cos \psi_c \frac{du}{dt} \\ \sin \psi_c \sin(\theta - q + \phi_1) \frac{du}{dt} + u \sin \psi_c \cos(\theta - q + \phi_1) \frac{d\theta}{dt} \\ \sin \psi_c \cos(\theta - q + \phi_1) \frac{du}{dt} - u \sin \psi_c \sin(\theta - q + \phi_1) \frac{d\theta}{dt} \end{bmatrix} \quad (1.6.46)$$

The unit normal of generating surface was represented by equations (1.5.24).

It results from (1.5.24) that

$$\left[\underline{\dot{n}}_R^{(1)} \right] = \begin{bmatrix} 0 \\ \cos \psi_c \cos(\theta - q + \phi_1) \frac{d\theta}{dt} \\ -\cos \psi_c \sin(\theta - q + \phi_1) \frac{d\theta}{dt} \end{bmatrix} \quad (1.6.47)$$

Vectors (1.6.46) and (1.6.47) are co-linear for principal directions of surface Σ_1 . Consequently,

$$\frac{\dot{n}_{xr}^{(1)}}{v_{xr}^{(1)}} = \frac{\dot{n}_{yr}^{(1)}}{v_{yr}^{(1)}} = \frac{\dot{n}_{zr}^{(1)}}{v_{zr}^{(1)}} \quad (1.6.48)$$

Equalities (1.6.46) - (1.6.48) yield that

$$\frac{du}{dt} \frac{d\theta}{dt} = 0 \quad (1.6.49)$$

One of the principal directions with unit vector \tilde{i}_I corresponds to $\frac{du}{dt} = 0$. The principal curvature

$$\kappa_I = -\frac{\dot{n}_{yr}^{(1)}}{v_{yr}^{(1)}} = -\frac{\dot{n}_{zr}^{(1)}}{v_{zr}^{(1)}} = -\frac{1}{u \tan \psi_c} \quad (1.6.50)$$

The unit vector \tilde{i}_I can be represented by equation

$$\tilde{i}_I = \left[\frac{v_r^{(1)}}{v_r^{(1)}} \right] \text{ by } \frac{du}{dt} = 0 \quad (1.6.51)$$

Equations (1.6.46) and (1.6.51) yield

$$[\tilde{i}_{II}] = \begin{bmatrix} 0 \\ \cos(\theta - q + \phi_1) \\ -\sin(\theta - q + \phi_1) \end{bmatrix} \quad (1.6.52)$$

The second principal direction corresponds to $\frac{d\theta}{dt} = 0$. The principal curvature is

$$\kappa_{II} = 0 \quad (1.6.53)$$

and the unit vector of the principal direction is

$$[\tilde{i}_{II}] = \begin{bmatrix} -\cos \psi_c \\ \sin \psi_c \sin(\theta - q + \phi_1) \\ \sin \psi_c \cos(\theta - q + \phi_1) \end{bmatrix} \quad (1.6.54)$$

A case is suggested when $\Delta_2 = 0$, $\omega^{(1)} = 1 \frac{\text{rad}}{\text{sec}}$. Then:

$$\omega^{(2)} = \frac{1}{\sin \gamma_2},$$

$$\begin{aligned} \left[\omega^{(1)} \right] &= \begin{bmatrix} -1 \\ 0 \\ 0 \end{bmatrix}, \\ \left[\omega^{(2)} \right] &= \frac{1}{\sin \gamma_2} \begin{bmatrix} -\sin \gamma_2 \\ 0 \\ \cos \gamma_2 \end{bmatrix} \\ \left[v^{(12)} \right] &= -\cot \gamma_2 \begin{bmatrix} y \\ -x \\ 0 \end{bmatrix}, \end{aligned}$$

where (x,y,z) are represented by equations (1.5.22), the lower subscript "F" is eliminated. Equations (1.6.40)-(1.6.42) define principal curvatures and directions of tooth surface Σ_2 of the generated gear.

Let us define principal curvatures and directions at the mean contact point M with coordinates $x=y=0, z=L$. It results from equations (1.5.22) and (1.5.24) that point M is generated by $\phi_1=0, \theta-q=90^\circ-\beta$. By $x=0, y=0$ vector $v^{(12)}$ is equal to zero. Coefficients a_{31}, a_{32}, b_3, F and S are represented by equations:

$$a_{31} = \left[\tilde{n}^{(1)} \tilde{\omega}^{(12)} \tilde{i}_I \right] = \sin \psi_c \sin \beta \cot \gamma_2 \quad (1.6.55)$$

Here:

$$\begin{aligned} \left[\tilde{n}^{(1)} \right] &= \begin{bmatrix} \sin \psi_c \\ \cos \psi_c \cos \beta \\ \cos \psi_c \sin \beta \end{bmatrix} \\ \left[\tilde{\omega}^{(12)} \right] &= \begin{bmatrix} 0 \\ 0 \\ -\cot \gamma_2 \end{bmatrix} \\ \left[\tilde{i}_I \right] &= \begin{bmatrix} 0 \\ \sin \beta \\ -\cos \beta \end{bmatrix} \end{aligned}$$

$$a_{32} = \left[\begin{matrix} \tilde{n}^{(1)} \omega^{(12)} \\ \tilde{\omega}^{(12)} i_{II} \end{matrix} \right] = \cos \beta \cot \gamma_2 \quad (1.6.56)$$

Here:

$$[i_{II}] = \begin{bmatrix} -\cos \psi_c \\ \sin \psi_c \cos \beta \\ \sin \psi_c \sin \beta \end{bmatrix}$$

$$b_3 = \left[\begin{matrix} \tilde{n}^{(1)} \omega^{(2)} \\ \tilde{\omega}^{(2)} v_{tr}^{(1)} \end{matrix} \right] - \left[\begin{matrix} \tilde{n}^{(1)} \omega^{(1)} \\ \tilde{\omega}^{(1)} v_{tr}^{(2)} \end{matrix} \right] = -L \sin \psi_c \cot \gamma_2 \quad (1.6.56,a)$$

Here:

$$[\omega^{(1)}] = \begin{bmatrix} -1 \\ 0 \\ 0 \end{bmatrix}; \quad [v_{tr}^{(2)}] = [v_{tr}^{(1)}] = \omega^{(1)} \times \overline{O_F M} =$$

$$\begin{bmatrix} i_f & j_f & k_f \\ -1 & 0 & 0 \\ 0 & 0 & L \end{bmatrix} = \begin{bmatrix} 0 \\ L \\ 0 \end{bmatrix}; \quad [\omega^{(2)}] = \begin{bmatrix} -1 \\ 0 \\ \cot \gamma_2 \end{bmatrix}$$

$$2F = \frac{2a_{31} a_{32}}{b_3} = -\frac{\sin 2\beta \cot \gamma_2}{L} \quad (1.6.57)$$

$$G = \frac{a_{31}^2 - a_{32}^2}{b_3} = -\frac{(\sin^2 \psi_c \sin^2 \beta - \cos^2 \beta) \cot \gamma_2}{L \sin \psi_c} \quad (1.6.58)$$

$$S = \frac{a_{31}^2 + a_{32}^2}{b_3} = -\frac{(\sin^2 \psi_c \sin^2 \beta + \cos^2 \beta) \cot \gamma_2}{L \sin \psi_c} \quad (1.6.59)$$

Equation (1.6.50) yields that at point M

$$\kappa_I = -\frac{1}{u \tan \psi_c} = -\frac{\cos \psi_c}{r_c} \quad (1.6.60)$$

It results from equations (1.6.40)-(1.6.42) and (1.6.57)-(1.6.59) that

$$\tan 2\sigma = \frac{2F}{\kappa_I - \kappa_{II} + G} =$$

$$\frac{\sin 2\beta \cot \gamma_2}{\frac{L}{r_c} \cos \psi_c + \frac{(\sin^2 \psi_c \sin^2 \beta - \cos^2 \beta) \cot \gamma_2}{\sin \psi_c}} \quad (1.6.61)$$

$$\kappa_{III} + \kappa_{iv} = \kappa_I + \kappa_{II} + S =$$

$$-\frac{\cos \psi_c}{r_c} - \frac{(\sin^2 \psi_c \sin^2 \beta + \cos^2 \beta) \cot \gamma_2}{L \sin \psi_c} \quad (1.6.62)$$

$$\kappa_{III} - \kappa_{iv} = \frac{\kappa_I - \kappa_{II} + G}{\cos 2\sigma} =$$

$$-\frac{\cos \psi_c}{r_c} - \frac{(\sin^2 \psi_c \sin^2 \beta - \cos^2 \beta) \cot \gamma_2}{L \sin \psi_c}$$

$$= \frac{\cos 2\sigma}{\cos 2\sigma} \quad (1.6.63)$$

Equations (1.6.61)-(1.6.63) define the principal curvatures and directions of the generated surface of spiral bevel gear at the main contact point M.

These equations may be applied for bevel gears with straight teeth, too. For this case $\beta=0$, $\frac{1}{r_c}=0$, $\kappa_I = \kappa_{II} = 0$ because the generating surface is a plane. Equations (1.6.61)-(1.6.63) yield

$$\tan 2\sigma = 0, \kappa_{III} = 0, \kappa_{iv} = -\frac{\cot \gamma_2}{L \sin \psi_c} \quad (1.6.64)$$

1.7. Contact Ellipse

The bearing contact of spiral bevel and hypoid gears is checked on a test-machine under a small load. The bearing contact depends on the contact ellipse of tooth surfaces which are considered as elastic ones.

There is a typical problem in the theory of elasticity: (a) the magnitudes of contact forces and mechanical properties of surface materials are given; (b) the principal curvatures and directions of surfaces at their contact point are known. Methods known from the theory of elasticity permit to define the approach of surfaces, the size and location of contact ellipse.

To appraise conditions of tooth contact it is more reasonable to consider as given the approach of surfaces under the action of load. Then, the size and location of instantaneous contact ellipse can be defined as a result of a simple geometric solution. The magnitude of surface approach is known from experiments.

Fig. 1.7.1 shows surfaces Σ_1 and Σ_2 in tangency at point M. The unit normal and the tangent plane are designated by \underline{n} and t-t. The deformed surfaces are shown by dotted lines. The areas of deformation are K_1ML_1 for surface Σ_1 and K_2ML_2 for surface Σ_2 .

Let us choose points $N(\rho, \ell^{(1)})$ and $N'(\rho, \ell^{(2)})$ where ρ is the distance from M and $\ell^{(i)}$ ($i=1,2$) is the distance from the tangent plane. As a result of deformation, body 1 will be displaced in a direction opposite the unit normal \underline{n} by δ_1 (Fig. 1.7.1, Fig. 1.7.2); body 2 will be displaced in the opposite direction by δ_2 . The approach of both bodies is $\delta = \delta_1 + \delta_2$.

The approach of bodies is accompanied with their elastic deformation. It is necessary to distinguish the displacement of a body point with the body given by δ_i ($i=1,2$), and a displacement relative to the body resulting from elastic deformation.

Let us define the new location N_2 of point N. With the body point 1 will displace by δ_1 and get the position N_1 . Due to elastic deformation which is equal to f_1 point N will be displaced from N_1 to N_2 . The distance ℓ between point N_2 and the tangent plane t-t is represented by the following equation

$$\ell = \ell^{(1)} - \delta_1 + f_1 \quad (1.7.1)$$

The resulting position of point N' of body 2 is N_2' . The distance ℓ between point N_2' and the tangent plane t-t is represented by equation

$$\ell = \ell^{(2)} + \delta_2 - f_2 \quad (1.7.2)$$

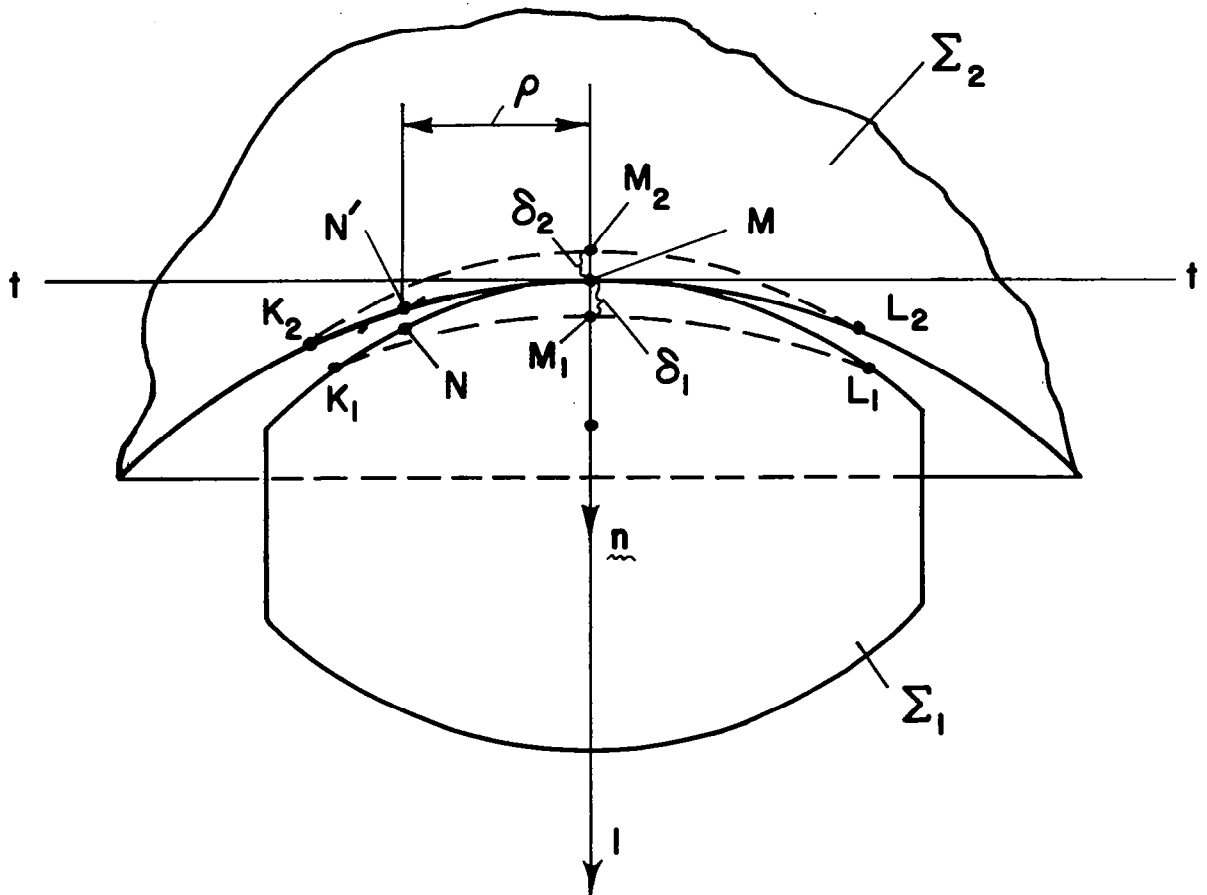
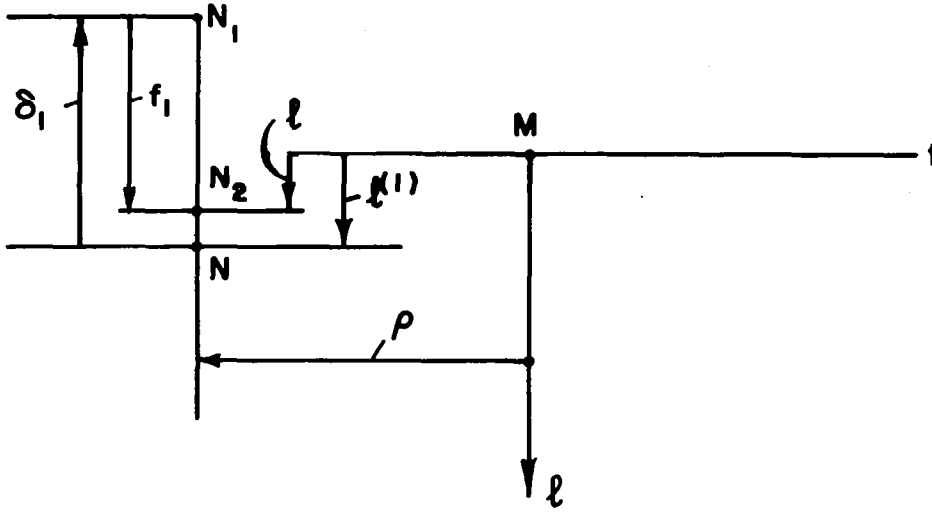


Fig. 1.7.1

Surfaces Σ_1 and Σ_2 in Tangency - Before and After Deformation

(a)



(b)

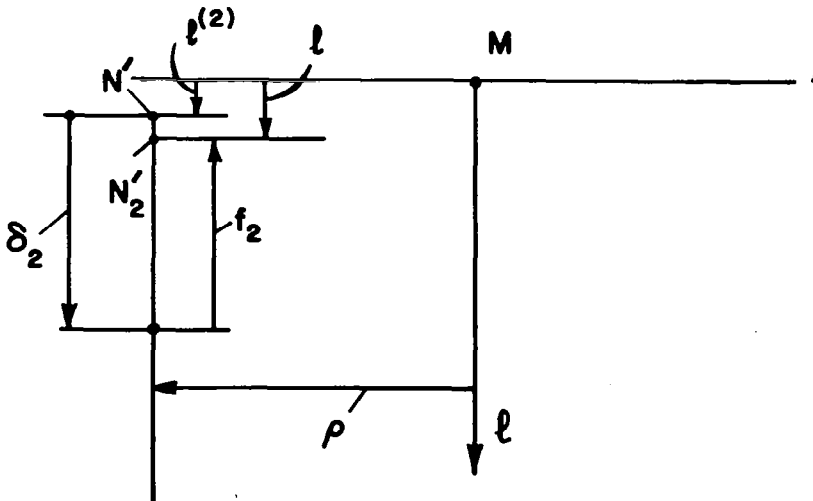


Fig. I.7.2

Displacements of Surfaces Σ_1 and Σ_2

Due to the approach of bodies and their deformation, points N and N' must coincide and

$$\varrho^{(1)} - \delta_1 + f_1 = \varrho^{(2)} + \delta_2 - f_2 \quad (1.7.3)$$

Equality (1.7.3) yields

$$\left| \varrho^{(1)} - \varrho^{(2)} \right| = \delta_1 + \delta_2 - (f_1 + f_2) \quad (1.7.4)$$

Equation (1.7.4) is observed at all points of the area of deformation. Without this area

$$\left| \varrho^{(1)} - \varrho^{(2)} \right| > \delta = \delta_1 + \delta_2 \quad (1.7.5)$$

The right part of equation (1.7.4) is larger than zero because $\delta_1 > f_1$, $\delta_2 > f_2$. Therefore the left part of equation (1.7.4) represents the absolute magnitude of the difference between $\varrho^{(1)}$ and $\varrho^{(2)}$.

Within the area of deformation

$$\left| \varrho^{(1)} - \varrho^{(2)} \right| \leq \delta \quad (1.7.6)$$

Equation

$$\left| \varrho^{(1)} - \varrho^{(2)} \right| = \delta \quad (1.7.7)$$

corresponds to the edge of deformation area. Equation (1.7.7) defines the line which limits the area of deformation.

Let us correlate $\varrho^{(i)}$ with surface Σ_i curvatures. Surface Σ_i is represented by equation

$$\underline{r} = \underline{r}(u, \theta) \quad (1.7.8)$$

Curve MM' (Fig. 1.7.3) on a surface Σ is represented by equation

$$\underline{r} = \underline{r}[u(s), \theta(s)] \quad (1.7.9)$$

where s is the length of an arc.

Let us designate by $\Delta s = \overline{MM'}$ the arc length and by $\Delta \underline{r} = \overline{MM'}$ the increment of vector-radius \underline{r} . The increment $\Delta \underline{r}$ can be expressed by Taylor-Series Expansion.

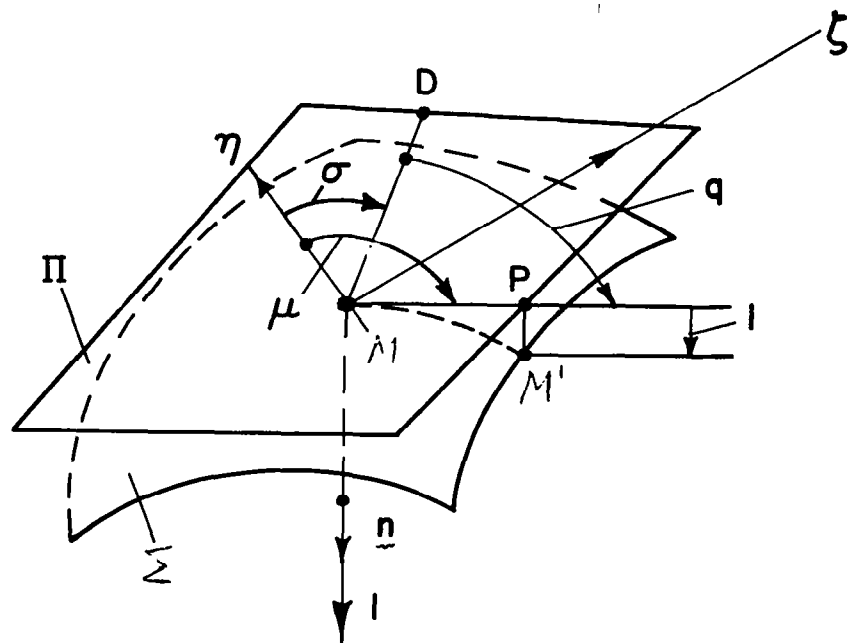


Fig. 1.7.3

Tooth Surface and Tangent Plane

$$\overline{MM'} = \Delta \underline{r} = \frac{d\underline{r}}{ds} \Delta s + \frac{d^2 \underline{r}}{ds^2} \frac{(\Delta s)^2}{2!} + \frac{d^3 \underline{r}}{ds^3} \frac{(\Delta s)^3}{3!} + \dots, \quad (1.7.10)$$

where

$$\begin{aligned} \frac{d\underline{r}}{ds} &= \frac{\partial \underline{r}}{\partial u} \frac{du}{ds} + \frac{\partial \underline{r}}{\partial \theta} \frac{d\theta}{ds}, \quad \frac{d^2 \underline{r}}{ds^2} = \frac{\partial^2 \underline{r}}{\partial u^2} \left(\frac{du}{ds} \right)^2 + \\ & 2 \frac{\partial^2 \underline{r}}{\partial u \partial \theta} \frac{du}{ds} \frac{d\theta}{ds} + \frac{\partial^2 \underline{r}}{\partial \theta^2} \left(\frac{d\theta}{ds} \right)^2 \quad \text{and so on.} \end{aligned}$$

Let us draw a plane Π tangent to the surface Σ at point M and then draw from point M' a perpendicular $M'P$ to Π . Vector $\overline{PM'}$ which is parallel to surface unit normal \underline{n} represents the deflexion of point M' from the tangent plane Π . This deflexion is

$$\overline{PM'} = \ell \underline{n} \quad (1.7.11)$$

Here: $\ell > 0$ if directions of $\overline{PM'}$ and \underline{n} coincide.

Equalities

$$\overline{MM'} = \Delta \underline{r}, \quad \overline{MM'} = \overline{MP} + \overline{PM'} = MP + \ell \underline{n}$$

yield

$$\overline{MP} + \ell \underline{n} = \frac{d\underline{r}}{ds} \Delta s + \frac{d^2 \underline{r}}{ds^2} \frac{(\Delta s)^2}{2!} + \frac{d^3 \underline{r}}{ds^3} \frac{(\Delta s)^3}{3!} + \dots \quad (1.7.12)$$

Because vectors \overline{MP} and \underline{n} , $\frac{d\underline{r}}{ds}$ and \underline{n} make right angles the scalar product

$$(\overline{MP} + \ell \underline{n}) \cdot \underline{n} \quad (1.7.13)$$

yields

$$\ell = \frac{d^2 \underline{r}}{ds^2} \cdot \underline{n} \frac{(\Delta s)^2}{2!} + \frac{d^3 \underline{r}}{ds^3} \cdot \underline{n} \frac{(\Delta s)^3}{3!} + \dots \quad (1.7.14)$$

Up to members of third order ℓ is represented by the equation

$$\ell = \frac{d^2 \underline{r}}{ds^2} \cdot \underline{n} \frac{(\Delta s)^2}{1.2} \quad (1.7.15)$$

It is known from differential geometry that

$$\frac{d^2 \vec{r}}{ds^2} \cdot \vec{n} = \kappa, \quad (1.7.16)$$

where κ is the surface curvature in normal section.

Equations (1.7.15) and (1.7.16) yield

$$\ell = \kappa \frac{\Delta s^2}{2} \quad (1.7.17)$$

Let us express Δs in terms of components of the coordinate system η , ζ and ℓ (Fig. 1.7.3); axes η and ζ are located on the tangent plane Π .

$$\Delta s^2 = \eta^2 + \zeta^2 = \rho^2, \quad (1.7.18)$$

where $\rho = MP$.

It results from (1.7.17) and (1.7.18) that

$$\ell = 1/2 \kappa \rho^2 \quad (1.7.19)$$

The surface normal curvature can be expressed by principal curvatures and angle q (Fig. 1.7.3) made by MD and MP , where MD is the principal direction with principal curvature κ_I .

$$\begin{aligned} \kappa &= \kappa_I \cos^2 q + \kappa_{II} \sin^2 q = \kappa_I \cos^2(\mu - \sigma) + \\ &\quad \kappa_{II} \sin^2(\mu - \sigma) \end{aligned} \quad (1.7.20)$$

Equations (1.7.19) and (1.7.20) yield

$$2\ell = \rho^2 \left[\kappa_I \cos^2(\mu - \sigma) + \kappa_{II} \sin^2(\mu - \sigma) \right] \quad (1.7.21)$$

Figure 1.7.4 shows a plane tangent to surfaces Σ_1 and Σ_2 at point M of their contact; MD_1 and MD_2 with unit vectors $i_I^{(1)}$ and $i_I^{(2)}$ are principal directions of Σ_1 and Σ_2 with principal curvatures $\kappa_I^{(1)}$ and $\kappa_I^{(2)}$, MP defines a common normal section of surfaces Σ_1 and Σ_2 . Deflections of points of surfaces Σ_1 and Σ_2 from the tangent plane T (Fig. 1.7.3) are represented by equations

$$2\ell^{(1)} = \rho^2 \left[\kappa_I^{(1)} \cos^2(\mu - \alpha^{(1)}) + \kappa_{II}^{(1)} \sin^2(\mu - \alpha^{(1)}) \right] \quad (1.7.22)$$

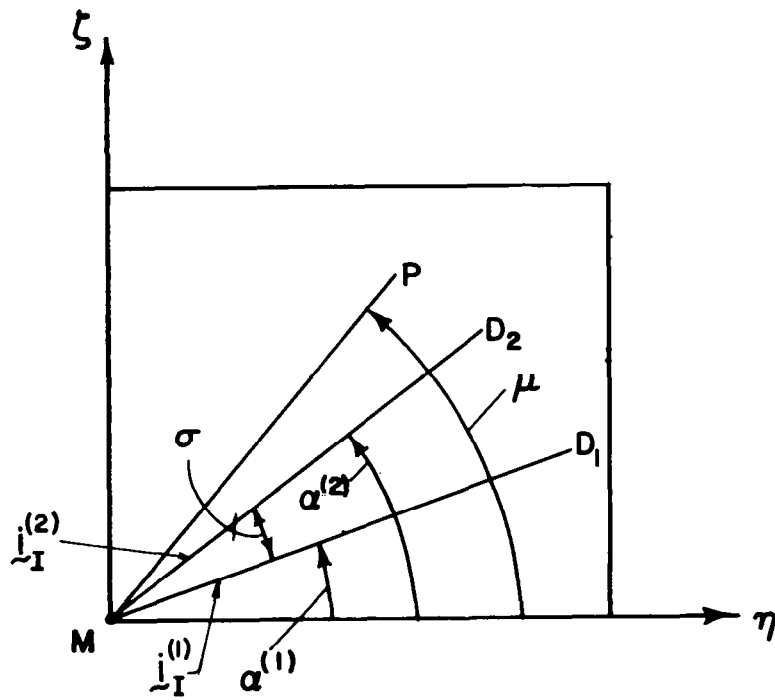


Fig. 1.7.4

Location of Contact Ellipse

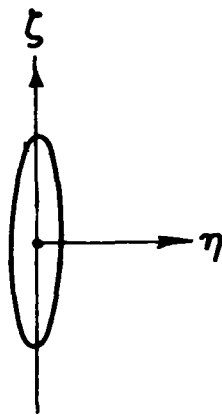


Fig. 1.7.5

$$2\lambda^{(2)} = \rho^2 \left[\kappa_I^{(2)} \cos^2(\mu - \alpha^{(2)}) + \kappa_{II}^{(1)} \sin^2(\mu - \alpha^{(2)}) \right] \quad (1.7.23)$$

At the edge of the area of deformation equation (1.7.7) must be held.

Equations (1.7.22), (1.7.23) and (1.7.7) yield

$$\rho^2 \left[\kappa_I^{(1)} \cos^2(\mu - \alpha^{(1)}) + \kappa_{II}^{(1)} \sin^2(\mu - \alpha^{(1)}) - \kappa_I^{(2)} \cos^2(\mu - \alpha^{(2)}) - \kappa_{II}^{(2)} \sin^2(\mu - \alpha^{(2)}) \right] = \pm 2\delta \quad (1.7.24)$$

Let us transform equation (1.7.24) taking into account that

$$\rho^2 = \eta^2 + \zeta^2, \quad \cos \mu = \frac{\eta}{\rho}, \quad \sin \mu = \frac{\zeta}{\rho} \quad (1.7.25)$$

It results from (1.7.24) and (1.7.25) that

$$\begin{aligned} & \eta^2 (\kappa_I^{(1)} \cos^2 \alpha^{(1)} + \kappa_{II}^{(1)} \sin^2 \alpha^{(1)} - \kappa_I^{(2)} \cos^2 \alpha^{(2)} - \kappa_{II}^{(2)} \sin^2 \alpha^{(2)}) + \\ & \zeta^2 (\kappa_I^{(1)} \sin^2 \alpha^{(1)} + \kappa_{II}^{(1)} \cos^2 \alpha^{(1)} - \kappa_I^{(2)} \sin^2 \alpha^{(2)} - \kappa_{II}^{(2)} \cos^2 \alpha^{(2)}) + \\ & \eta \zeta (g_1 \sin 2\alpha^{(1)} - g_2 \sin 2\alpha^{(2)}) = \pm 2\delta, \end{aligned} \quad (1.7.26)$$

where

$$g_1 = \kappa_I^{(1)} - \kappa_{II}^{(1)}, \quad g_2 = \kappa_I^{(2)} - \kappa_{II}^{(2)}$$

Let us designate $\alpha^{(2)} - \alpha^{(1)} = \sigma$ (Fig. 1.7.4). The angle $\alpha^{(1)}$ defining the location of MD_1 - the principal direction with principal curvature κ_I - can be chosen in an arbitrary way, particularly the way that

$$g_1 \sin 2\alpha^{(1)} - g_2 \sin 2\alpha^{(2)} = 0 \quad (1.7.27)$$

Equation (1.7.27) and equation

$$\alpha^{(2)} = \alpha^{(1)} + \sigma \quad (1.7.28)$$

yield

$$\tan 2\alpha^{(1)} = \frac{g_2 \sin 2\sigma}{g_1 - g_2 \cos 2\sigma} \quad (1.7.29)$$

It results from equations (1.7.26) and (1.7.27) that

$$B\eta^2 + A\zeta^2 = \pm \delta \quad (1.7.30)$$

Here:

$$A = \frac{1}{4} \left[\kappa_{\varepsilon}^{(1)} - \kappa_{\varepsilon}^{(2)} - (g_1^2 - 2g_1g_2 \cos 2\sigma + g_2^2)^{\frac{1}{2}} \right] \quad (1.7.31)$$

$$B = \frac{1}{4} \left[\kappa_{\varepsilon}^{(1)} - \kappa_{\varepsilon}^{(2)} + (g_1^2 - 2g_1g_2 \cos 2\sigma + g_2^2)^{\frac{1}{2}} \right], \quad (1.7.32)$$

where

$$\kappa_{\varepsilon}^{(1)} = \kappa_I^{(1)} + \kappa_{II}^{(1)}, \quad \kappa_{\varepsilon}^{(2)} = \kappa_I^{(2)} + \kappa_{II}^{(2)}$$

Equation (1.7.30) confirms that the projection of the area of deformation on the tangent plane is an ellipse with lengths of major and minor axes of $2a$ and $2b$ (Fig. 1.7.5), where

$$a = \left(\left| \frac{\delta}{A} \right| \right)^{\frac{1}{2}}, \quad b = \left(\left| \frac{\delta}{B} \right| \right)^{\frac{1}{2}} \quad (1.7.33)$$

Equations (1.7.29), (1.7.30)-(1.7.33) define the size and direction of contact ellipse with known values of δ and principal curvatures of surfaces.

Sample problem 1.7.1. Surfaces of spiral bevel gears being in point contact are considered. There are given:

$$\kappa_I^{(1)} = 0.004122047, \quad \kappa_{II}^{(1)} = -0.000292913,$$

$$\kappa_I^{(2)} = -0.001513779, \quad \kappa_{II}^{(2)} = -0.000279921,$$

the angle σ made by principal directions with $\kappa_I^{(1)}$ and $\kappa_I^{(2)}$ is equal to 12.47° . The approach of surfaces $\delta = 000787401$. It is necessary to define the size and direction of contact ellipse.

Equations (1.7.29) and (1.7.31 - 1.7.33) yield

$$\alpha^{(1)} = -7.95^\circ, \quad a = 0.539370078, \quad b = 0.035826771$$

angle $\alpha^{(1)}$ is made by axis $O\eta$ and principal direction with curvature $\kappa_I^{(1)}$. By positive value of $\alpha^{(1)}$ this angle is counted from axis $O\eta$ counter-clockwise. (Fig. 1.7.4).

2. GEOMETRY OF SPIRAL BEVEL GEARS

2.1 Introduction

Spiral bevel gears which are used in practice are normally generated with approximately conjugated tooth surfaces by using special machines and tool settings. The geometry of spiral bevel gears is not defined until these special settings are calculated; and the geometry of spiral bevel gears with all machine and tool settings is a very complicated one.

There are some important reasons why simplified mathematical models of the geometry of spiral bevel gears must be developed. These models can be applied as a basis for designers and researchers to solve the Herzian contact stress problem and define dynamic capacity and contact fatigue life, to develop the theory of lubrication of tooth surfaces. Dynamic load capacity and surface fatigue life was considered by J. Coy, D. P. Townsend, and E. Zaretzky for spur and helical gears [1]. The proposed geometric models of spiral bevel gears will enable researchers to extend this work to these gears, too.

The offered models of the geometry of spiral bevel gears are based on an assumption that tooth surfaces are conjugated ones. The aim to use special machine settings is dictated by the attempt to generate conjugated surfaces. Therefore the mentioned assumption is not in contradiction with the practice.

The basic idea of generation of conjugated surfaces of spiral bevel gears is grounded on the following principles:

(1) Two generating surfaces Σ_F and Σ_k are considered being in tangency along a line.

(2) Surfaces Σ_F and Σ_k are rigidly connected with each other in the process of an imaginary generation of surfaces Σ_1 and Σ_2 of the pinion and the member gear. It is supposed that surface Σ_F generates surface Σ_1

of pinion teeth and surface Σ_k generates surface Σ_2 of member-gear teeth.

(3) There are three axes of instantaneous rotation which correspond:

- (a) to the meshing of Σ_F and Σ_1 in the process of generation of Σ_1 ;
- (b) to the meshing of Σ_k and Σ_2 in the process of generation of Σ_2 ;
- (c) to the meshing of surfaces Σ_1 and Σ_2 . All three mentioned axes of rotation must coincide with each other.

(4) The contact of tooth surfaces Σ_1 and Σ_2 is localized because generating surfaces Σ_F and Σ_k does not coincide with each other (they have a common line only).

There are two kinds of bearing contact of spiral bevel gears applied in practice. The first one corresponds to the motion of the contact ellipse across the tooth (Fig. 2.1.1,a), the second one to the motion along the tooth (Fig. 2.1.1,b). Accordingly, two mathematical models of the geometry of spiral bevel gears corresponding to the mentioned cases will be proposed.

2.2. Geometry I: The Line of Action

Generating surfaces Σ_F and Σ_k are two cone surfaces (Fig. 2.2.1) which are in tangency along the generatrix AB.

Let us imagine that generating surfaces being rigidly connected with each other rotate about axis x_f (Fig. 2.2.2) with angular velocity $\omega^{(d)}$ ($d = F, k$) while gears 1 and 2 rotate about axes Oa and Ob with angular velocities $\omega^{(1)}$ and $\omega^{(2)}$. Axis z_f is the instantaneous axis of rotation because angular velocities $\omega^{(1)}$, $\omega^{(2)}$ and $\omega^{(d)}$ are related by the following equations

$$\omega^{(1d)} = \lambda k_f, \quad (2.2.1)$$

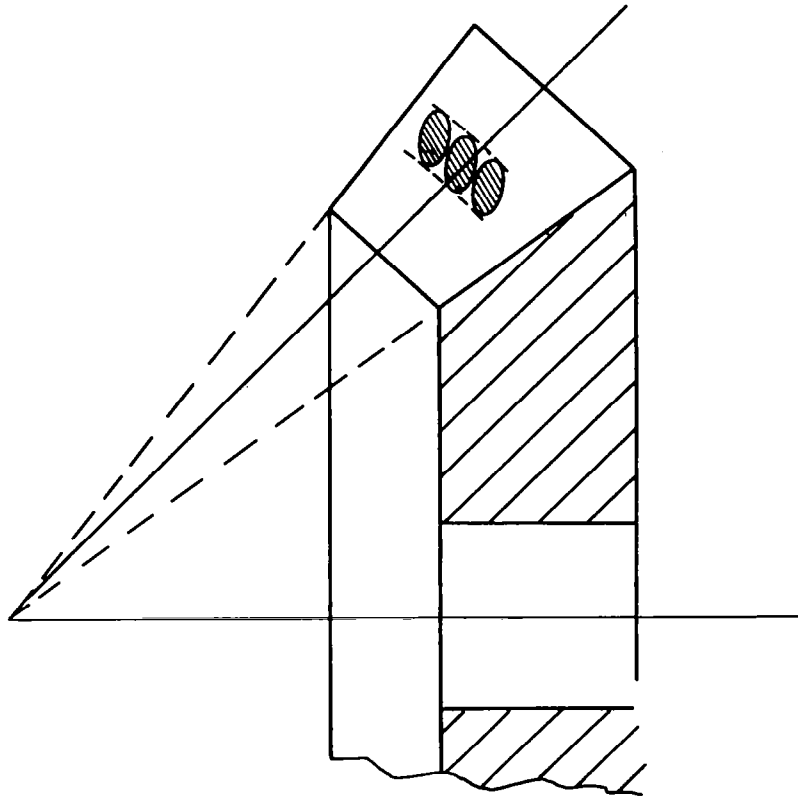
where

$$\omega^{(1d)} = \omega^{(1)} - \omega^{(d)}; \quad \omega^{(12)} = \omega^{(1d)}, \quad (2.2.2)$$

where

$$\omega^{(12)} = \omega^{(1)} - \omega^{(2)}$$

(a)



(b)

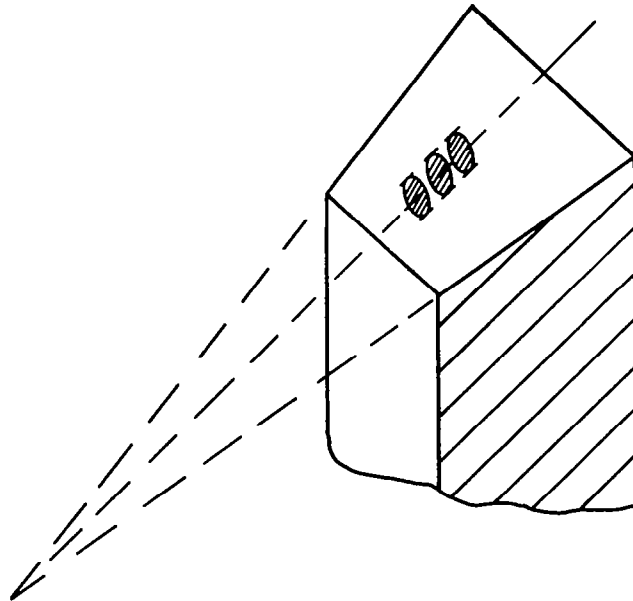


Fig. 2.1.1

Two Types of Bearing Contacts

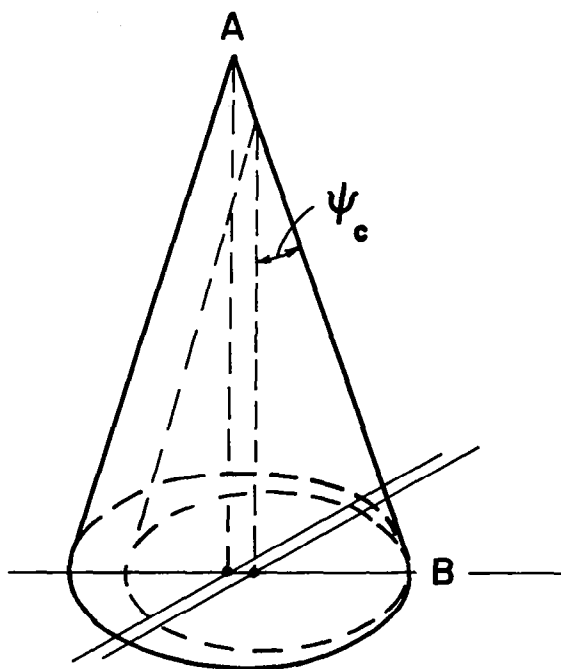


Fig. 2. 2. 1

Generating Cone Surfaces

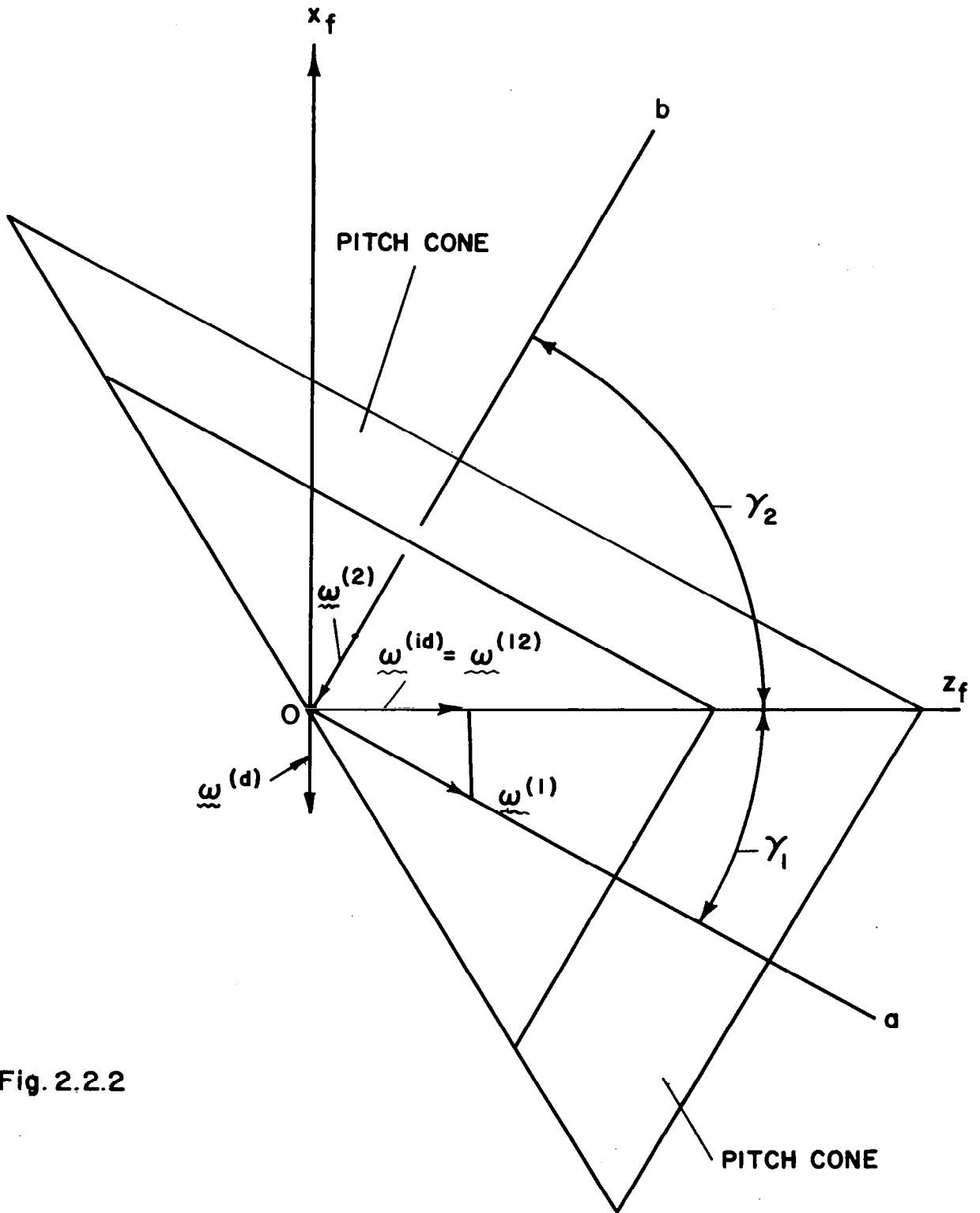


Fig. 2.2.2

Vectors $\underline{\omega}^{(1)}$, $\underline{\omega}^{(d)}$ and $\underline{\omega}^{(2)}$ are represented by the following equations

$$\underline{\omega}^{(1)} = \omega^{(1)} (-\sin \gamma_1 \underline{i}_f + \cos \gamma_1 \underline{k}_f) \quad (2.2.3)$$

$$\underline{\omega}^{(d)} = -\omega^{(d)} \underline{i}_f \quad (2.2.4)$$

$$\underline{\omega}^{(2)} = -\omega^{(2)} (\sin \gamma_2 \underline{i}_f + \cos \gamma_2 \underline{k}_f), \quad (2.2.5)$$

where γ_1 and γ_2 are pitch cone angles.

Equations (2.2.1)-(2.2.5) yield

$$\omega^{(1)} = \frac{\omega^{(d)}}{\sin \gamma_1} \quad (2.2.6)$$

$$\omega^{(2)} = \omega^{(1)} \frac{\sin \gamma_1}{\sin \gamma_2} = \frac{\omega^{(d)}}{\sin \gamma_2} \quad (2.2.7)$$

The generating surface Σ_d ($d = F, k$) can be represented by equations which are analogical to (1.5.22)

$$\begin{aligned} x_f^{(d)} &= r_d \cot \psi_c - u_d \cos \psi_c \\ y_f^{(d)} &= u_d \sin \psi_c \sin \tau_d - b_d \sin(q_d - \phi_d) \end{aligned} \quad (2.2.8)$$

$$z_f^{(d)} = u_d \sin \psi_c \cos \tau_d + b_d \cos(q_d - \phi_d),$$

where $\tau_d = \theta_d - q_d + \phi_d$

Here: (u_d, θ_d) are generating surface coordinates, ϕ_d is the angle of rotation about axis x_f ; ψ_c is the shape angle of head-cutter blades; r_d, b_d and q_d are parameters of tool settings (Fig. 1.5.4).

The surface normal is represented by equations

$$\underline{n}_f = \frac{\partial \underline{r}_f}{\partial \theta} \times \frac{\partial \underline{r}_f}{\partial u} =$$

$$\begin{vmatrix} \tilde{i}_f & \tilde{j}_f & \tilde{k}_f \\ \frac{\partial x_f}{\partial \theta} & \frac{\partial y_f}{\partial \theta} & \frac{\partial z_f}{\partial \theta} \\ \frac{\partial x_f}{\partial u} & \frac{\partial y_f}{\partial u} & \frac{\partial z_f}{\partial u} \end{vmatrix} =$$

$$u_d \sin \psi_c (\sin \psi_c \tilde{i}_f + \cos \psi_c \sin \tau_d \tilde{j}_f + \cos \psi_c \cos \tau_d \tilde{k}_f), \quad (2.2.9)$$

where $\tau_d = \theta_d - \alpha_d + \phi_d$

The surface unit normal is represented by equation

$$\begin{aligned} \tilde{n}_f &= \frac{\tilde{N}_f}{|\tilde{N}_f|} = \\ &\sin \psi_c \tilde{i}_f + \cos \psi_c \sin \tau_d \tilde{j}_f + \cos \psi_c \cos \tau_d \tilde{k}_f \\ &\text{(by } u_d \sin \psi_c \neq 0) \end{aligned} \quad (2.2.10)$$

To define the line of action of gears 1 and 2 let us imagine that all four surfaces - $\Sigma_F, \Sigma_k, \Sigma_1$ and Σ_2 - are in meshing. Surfaces Σ_F and Σ_k are rigidly connected with each other and are in tangency along the generatrix AB (Fig. 2.2.1). Surfaces Σ_F and Σ_1 are in linear contact and lines of instantaneous contact cover these surfaces. The same statement is true for surfaces Σ_k and Σ_2 . Fig. 2.2.3 shows surface Σ_d ($d = F, k$) covered with instantaneous contact lines; the location of contact lines on the surface depends on the angle ϕ_d of rotation.

Surfaces Σ_1 and Σ_2 can be in point-contact only. Contact points of these surfaces move along the common generatrix AB (Fig. 2.2.3, Fig. 2.2.1) while all four surfaces - $\Sigma_F, \Sigma_k, \Sigma_1$ and Σ_2 - are in meshing. The line of action of surfaces Σ_1 and Σ_2 is the locus of contact points represented in coordinate system S_f by equations

$$\tilde{r}_f^{(d)} = \tilde{r}_f^{(d)}(u_d, \theta_d, \phi_d) \quad (2.2.11)$$

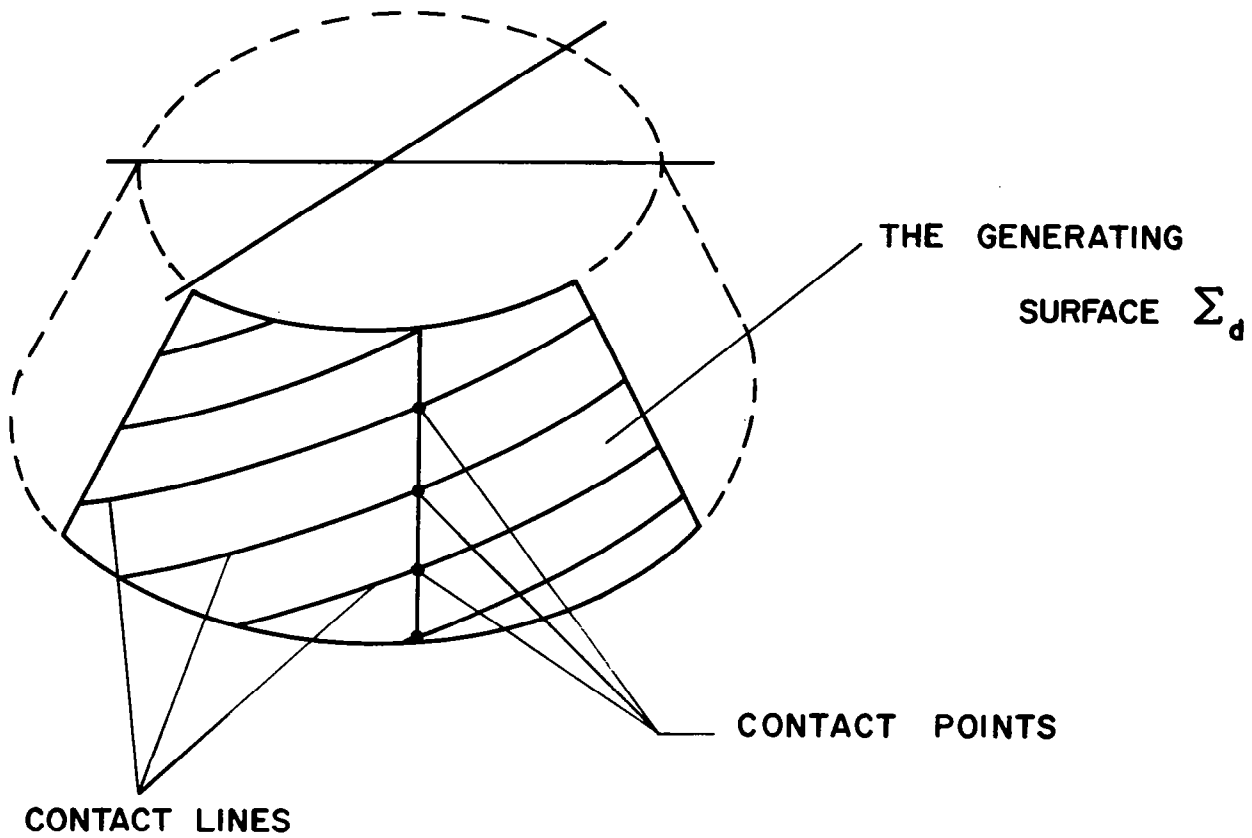


Fig. 2. 2. 3

Instantaneous Contact Lines on Generating Surface

$$\tilde{N}_f^{(F)} \tilde{V}_f^{(F1)} = f_1(u_F, \theta_F, \phi_F) = 0 \quad (2.2.12)$$

$$\tilde{N}_f^{(k)} \tilde{V}_f^{(k2)} = f_2(u_k, \theta_k, \phi_k) = 0 \quad (2.2.13)$$

Equation (2.2.11) was represented in terms of components $x_f^{(d)}$, $y_f^{(d)}$ and $z_f^{(d)}$ by equations (2.2.8). The surface normal \tilde{N}_f and unit normal \underline{n}_f were represented by equations (2.2.9) and (2.2.10).

Vector $\tilde{V}_f^{(F1)}$ is represented by equation

$$\tilde{V}_f^{(F1)} = \tilde{\omega}^{(F1)} \times \tilde{r}_f^{(F)} = \begin{vmatrix} \tilde{i}_f & \tilde{j}_f & \tilde{k}_f \\ \omega_{fx}^{(F1)} & \omega_{fy}^{(F1)} & \omega_{fz}^{(F1)} \\ x_f & y_f & z_f \end{vmatrix} \quad (2.2.14)$$

Equations (2.2.1), (2.2.3) and (2.2.4) yield that by $d = F$

$$\tilde{\omega}^{(F1)} = \tilde{\omega}^{(F)} - \tilde{\omega}^{(1)} = -\omega^{(1)} \cos \gamma_1 \tilde{k}_f = -\omega^{(F)} \cot \gamma_1 \tilde{k}_f \quad (2.2.15)$$

It results from equations (2.2.8), (2.2.9), (2.2.14) and (2.2.15) that

$$\begin{aligned} \tilde{N}_f^{(F1)} \tilde{V}_f^{(F1)} &= \omega^{(F)} \cot \gamma_1 (y_f n_{fx} - x_f n_{fy}) = \\ &\omega^{(F)} \cot \gamma_1 \left[(u_F - r_F \cot \psi_c \cos \psi_c) \sin \tau_F - \right. \\ &\left. b_F \sin \psi_c \sin(q_F - \phi_F) \right] = 0. \end{aligned} \quad (2.2.16)$$

Where $\tau_F = \theta_F - q_F + \phi_F$.

Equation (2.2.16) yields that

$$\begin{aligned} (u_F - r_F \cot \psi_c \cos \psi_c) \sin(\theta_F - q_F + \phi_F) - \\ b_F \sin \psi_c \sin(q_F - \phi_F) = 0 \end{aligned} \quad (2.2.17)$$

Similarly, equation (2.2.13) can be expressed as

$$\begin{aligned} (u_k - r_k \cot \psi_c \cos \psi_c) \sin(\theta_k - q_k + \phi_k) - \\ b_k \sin \psi_c \sin(q_k - \phi_k) = 0 \end{aligned} \quad (2.2.18)$$

At contact points of surfaces Σ_1 and Σ_2 the following equations must be observed

$$x_f = r_k \cot \psi_c - u_k \cos \psi_c = r_F \cot \psi_c - u_F \cos \psi_c \quad (2.2.19)$$

$$\left. \begin{aligned} y_f &= u_k \sin \psi_c \sin \tau_k - b_k \sin(q_k - \phi_k) = \\ u_F \sin \psi_c \sin \tau_F - b_F \sin(q_F - \phi_F) & \end{aligned} \right\} \quad (2.2.20)$$

$$\left. \begin{aligned} z_f &= u_k \sin \psi_c \cos \tau_k + b_k \cos(q_k - \phi_k) = \\ u_F \sin \psi_c \cos \tau_F + b_F \cos(q_F - \phi_F) & \end{aligned} \right\} \quad (2.2.21)$$

Here: $\tau_d = \theta_d - q_d + \phi_d$ ($d=F, k$)

Parameters u_d, τ_d ($d=F, k$) are related by equations (2.2.17) and (2.2.18); $\phi_k = \phi_F$ because generating surfaces Σ_k and Σ_F are rigidly connected and rotate with the same angular velocity.

After elimination of u_k and u_F the system of equations (2.2.17)-(2.2.21) yields a system of two equations

$$r_k - b_k \frac{\sin(q_k - \phi_d)}{\sin \tau_k} = r_F - b_F \frac{\sin(q_F - \phi_d)}{\sin \tau_F} \quad (2.2.22)$$

$$\begin{aligned} b_k \frac{\sin \theta_k}{\sin \tau_k} + \left[r_k - \frac{b_k \sin(q_k - \phi_d)}{\sin \tau_k} \right] \cos^2 \psi_c \cos \tau_k = \\ b_F \frac{\sin \theta_F}{\sin \tau_F} + \left[r_F - \frac{b_F \sin(q_F - \phi_d)}{\sin \tau_F} \right] \cos^2 \psi_c \cos \tau_F \end{aligned} \quad (2.2.23)$$

These equations will be observed for all values of ϕ_d if machine settings will satisfy the following equations

$$\phi_k = \phi_F, \theta_k - q_k = \theta_F - q_F, b_k \sin \theta_k = b_F \sin \theta_F,$$

$$r_k - \frac{b_k \sin q_k}{\cos \beta} = r_F - \frac{b_F \sin q_F}{\cos \beta}, \quad (2.2.24)$$

where $\beta = 90^\circ - (\theta_k - q_k) = 90^\circ - (\theta_F - q_F)$

The geometrical interpretation of equations (2.2.24) is represented by Fig. 2.2.4.

The line of action of surfaces Σ_1 and Σ_2 is represented by equations

$$\begin{aligned} x_f &= \left[r_d - b_d \frac{\sin(q_d - \phi_d)}{\sin \tau_d} \right] \sin \psi_c \cos \psi_c, \\ y_f &= \frac{\sin \tau_d}{\tan \psi_c} x_f, \\ z_f &= \frac{b_d \sin \theta_d}{\sin \tau_d} + \frac{\cos \tau_d}{\tan \psi_c} x_f, \end{aligned} \quad (2.2.25)$$

where

$$\tau_d = \theta_d - q_d + \phi_d, \quad d = F, k, \phi_k = \phi_F$$

Equations (2.2.25) represent coordinates of the line of action as functions $x_f(\phi_d)$, $y_f(\phi_d)$, $z_f(\phi_d)$.

2.3. Geometry I: Contact Point Path on Surface Σ_i ($i=1,2$)

Contact point path on surface Σ_i ($i=1,2$) is a locus of points of contact represented in coordinate system Σ_i rigidly connected with gear i .

Fig. 2.3.1 shows coordinate systems S_f and S_h rigidly connected with the frame and system S_1 rigidly connected with gear 1. The coordinate transformation by transition from S_f to S_1 is represented by matrix equation (Fig. 2.3.1)

$$\begin{aligned} \begin{bmatrix} r_1 \end{bmatrix} &= \begin{bmatrix} L_{1h} \end{bmatrix} \begin{bmatrix} L_{hf} \end{bmatrix} \begin{bmatrix} r_f \end{bmatrix} = \\ \begin{bmatrix} \cos \phi_1 & \sin \phi_1 & 0 \\ -\sin \phi_1 & \cos \phi_1 & 0 \\ 0 & 0 & 1 \end{bmatrix} \begin{bmatrix} \cos \gamma_1 & 0 & \sin \gamma_1 \\ 0 & 1 & 0 \\ -\sin \gamma_1 & 0 & \cos \gamma_1 \end{bmatrix} \begin{bmatrix} x_f(\phi_d) \\ y_f(\phi_d) \\ z_f(\phi_d) \end{bmatrix} &= \end{aligned}$$

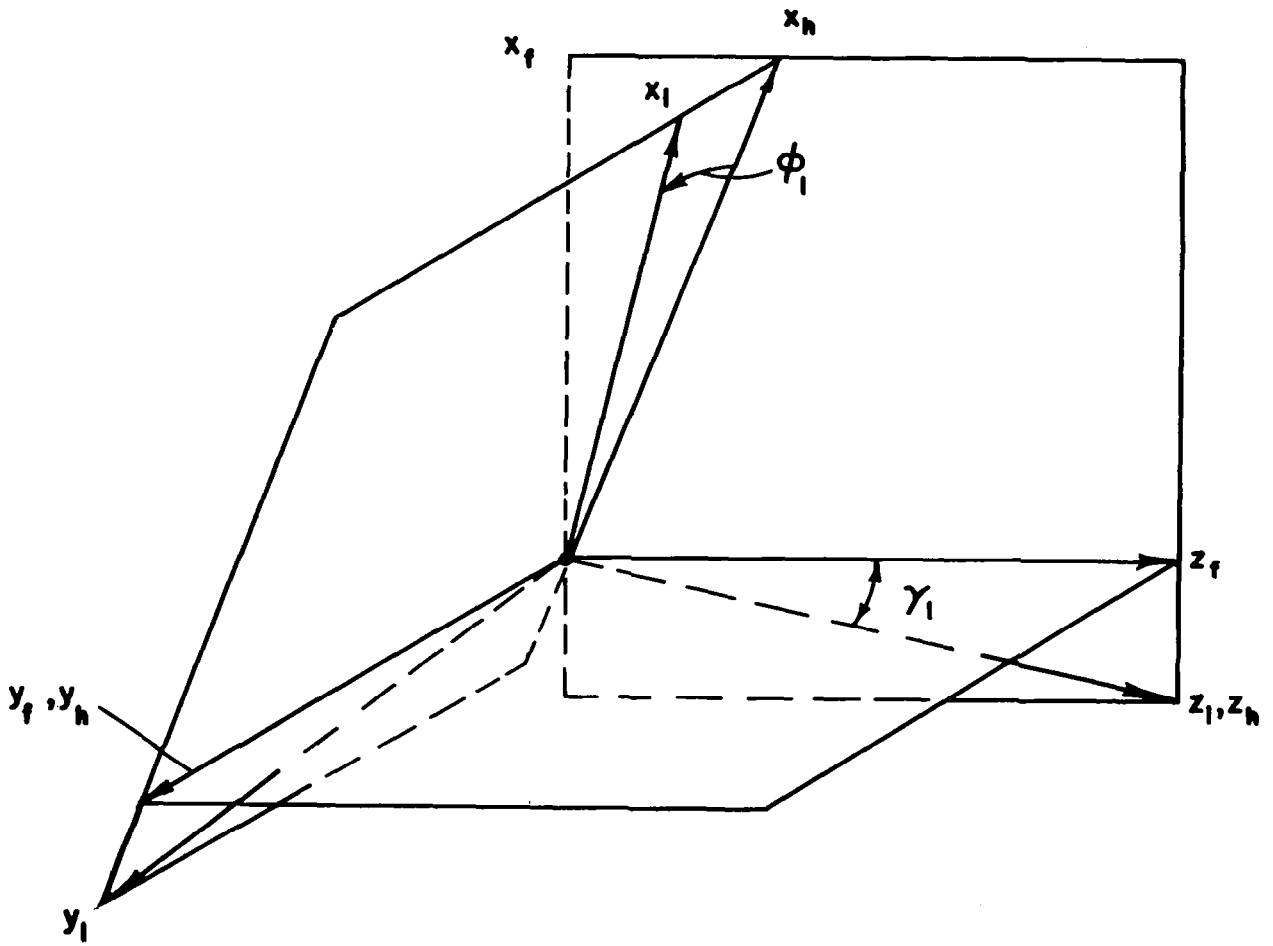


Fig. 2.3.1

Coordinate Systems Associated with Gear 1

$$\begin{aligned}
&= \begin{bmatrix} \cos \phi_1 \cos \gamma_1 & \sin \phi_1 & \cos \phi_1 \sin \gamma_1 \\ -\sin \phi_1 \cos \gamma_1 & \cos \phi_1 & -\sin \phi_1 \sin \gamma_1 \\ -\sin \gamma_1 & 0 & \cos \gamma_1 \end{bmatrix} \begin{bmatrix} x_f(\phi_d) \\ y_f(\phi_d) \\ z_f(\phi_d) \end{bmatrix} = \\
&\begin{bmatrix} x_f(\phi_d) \cos \phi_1 \cos \gamma_1 + y_f(\phi_d) \sin \phi_1 + z_f(\phi_d) \cos \phi_1 \sin \gamma_1 \\ -x_f(\phi_d) \sin \phi_1 \cos \gamma_1 + y_f(\phi_d) \cos \phi_1 - z_f(\phi_d) \sin \phi_1 \sin \gamma_1 \\ -x_f(\phi_d) \sin \gamma_1 + z_f(\phi_d) \cos \gamma_1 \end{bmatrix} \quad (2.3.1)
\end{aligned}$$

Here: $x_f(\phi_d)$, $y_f(\phi_d)$ and $z_f(\phi_d)$ are functions represented by equations (2.2.25). The angle of rotation ϕ_1 of gear 1 and the angle of rotation of generating gear are related by the equation which is analogous to equation (2.2.6)

$$\phi_1 = \frac{\phi_d}{\sin \gamma_1} \quad (2.3.2)$$

Fig. 2.3.2 shows coordinate systems S_f and S_p rigidly connected with the frame and coordinate system S_2 rigidly connected with gear 2. The coordinate transformation is represented by matrix equality

$$\begin{aligned}
\begin{bmatrix} r_2 \end{bmatrix} &= \begin{bmatrix} L_{2p} \end{bmatrix} \begin{bmatrix} L_{pf} \end{bmatrix} \begin{bmatrix} r_f \end{bmatrix} = \\
\begin{bmatrix} \cos \phi_2 & -\sin \phi_2 & 0 \\ \sin \phi_2 & \cos \phi_2 & 0 \\ 0 & 0 & 1 \end{bmatrix} \begin{bmatrix} \cos \gamma_2 & 0 & -\sin \gamma_2 \\ 0 & 1 & 0 \\ \sin \gamma_2 & 0 & \cos \gamma_2 \end{bmatrix} \begin{bmatrix} x_f(\phi_d) \\ y_f(\phi_d) \\ z_f(\phi_d) \end{bmatrix} &= \\
\begin{bmatrix} x_f(\phi_d) \cos \phi_2 \cos \gamma_2 - y_f(\phi_d) \sin \phi_2 - z_f(\phi_d) \cos \phi_2 \sin \gamma_2 \\ x_f(\phi_d) \sin \phi_2 \cos \gamma_2 + y_f(\phi_d) \cos \phi_2 - z_f(\phi_d) \sin \phi_2 \sin \gamma_2 \\ x_f(\phi_d) \sin \gamma_2 + z_f(\phi_d) \cos \gamma_2 \end{bmatrix}, \quad (2.3.3)
\end{aligned}$$

where

$$\phi_2 = \frac{\phi_d}{\sin \gamma_2} \quad (2.3.4)$$

Matrix equality (2.3.3) and equations (2.2.25) and (2.3.4) represent the contact point path on the surface Σ_2 of gear 2.

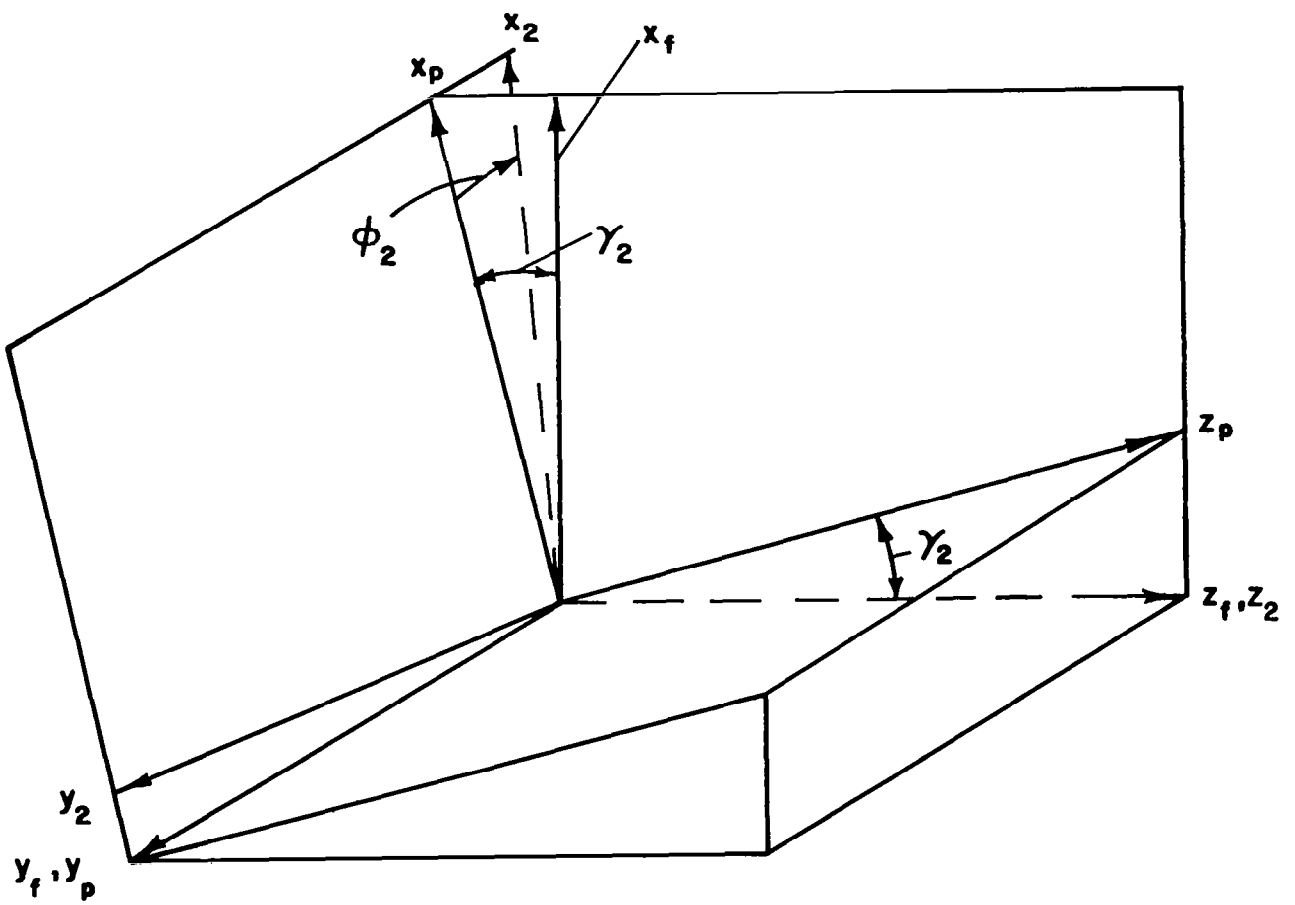


Fig. 2.3.2

Coordinate Systems Associated with Gear 2

2.4 Geometry I: The Instantaneous Contact Ellipse

The size and direction of the instantaneous contact ellipse may be obtained by the equations given in Items 1.6 and 1.7.

The solution of this problem can be divided into three stages: (1) the determination of principal curvatures of surfaces Σ_1 and Σ_2 , (2) the determination of the principal directions of surfaces Σ_1 and of Σ_2 , and (3) the determination of contact ellipse.

Principle Curvatures and Directions of Surface Σ_1

Surface Σ_1 is generated by cone surface Σ_F . Principal directions and curvatures of Σ_F are represented by the following equations (see sample problem 1.6.1):

$$\tilde{i}_I^{(F)} = \frac{\frac{\partial \tilde{r}_f}{\partial \theta}}{\left| \frac{\partial \tilde{r}_f}{\partial \theta} \right|} = \begin{bmatrix} 0 \\ \cos \tau_F \\ -\sin \tau_F \end{bmatrix} = \begin{bmatrix} 0 \\ \sin(\beta - \phi_F) \\ -\cos(\beta - \phi_F) \end{bmatrix}, \quad (2.4.1)$$

$$\kappa_I^{(F)} = -\frac{1}{u_F \tan \psi_c} = -\frac{\cos(\beta - \phi_F)}{b_F \sin \psi_c \tan \psi_c \sin(\alpha_F - \phi_F) + r_F \cos \psi_c \cos(\beta - \phi_F)} \quad (2.4.2)$$

$$\tilde{i}_{II}^{(F)} = \frac{\frac{\partial \tilde{r}}{\partial u}}{\left| \frac{\partial \tilde{r}}{\partial u} \right|} = \begin{bmatrix} -\cos \psi_c \\ \sin \psi_c \sin \tau_F \\ \sin \psi_c \cos \tau_F \end{bmatrix} = \begin{bmatrix} -\cos \psi_c \\ \sin \psi_c \cos(\beta - \phi_F) \\ \sin \psi_c \sin(\beta - \phi_F) \end{bmatrix} \quad (2.4.3)$$

$$\kappa_{II}^{(F)} = 0 \quad (2.4.4)$$

The principal curvatures and directions of Σ_1 are represented by equations analogical to equations (1.6.40)-(1.6.42)

$$\tan 2\sigma^{(1)} = \frac{2F^{(1)}}{\kappa_I^{(F)} + G^{(1)}} \quad (2.4.5)$$

$$\kappa_I^{(1)} + \kappa_{II}^{(1)} = \kappa_I^{(F)} + S^{(1)} \quad (2.4.6)$$

$$\kappa_I^{(1)} - \kappa_{II}^{(1)} = \frac{\kappa_I^{(F)} + G^{(1)}}{\cos 2\sigma^{(1)}} \quad (2.4.7)$$

Here: $\kappa_I^{(1)}$ and $\kappa_{II}^{(1)}$ are principal curvatures of surface Σ_1 ; $\sigma^{(1)}$ is the angle made by the directions of principal curvatures $\kappa_I^{(F)}$ and $\kappa_{II}^{(F)}$. Coefficients $F^{(1)}$, $S^{(1)}$ and $G^{(1)}$ are functions of ϕ_F and represented by equations

$$F^{(1)} = \frac{a_{31} a_{32}}{b_3 + V_I^{(F1)} a_{31} + V_{II}^{(F1)} a_{32}} \quad (2.4.8)$$

$$G^{(1)} = \frac{a_{31}^2 - a_{32}^2}{b_3 + V_I^{(F1)} a_{31} + V_{II}^{(F1)} a_{32}} \quad (2.4.9)$$

$$S^{(1)} = \frac{a_{31}^2 + a_{32}^2}{b_3 + V_I^{(F1)} a_{31} + V_{II}^{(F1)} a_{32}} \quad (2.4.10)$$

$$a_{31}^{(1)} = \left[\tilde{n}^{(F)} \tilde{\omega}^{(F1)} \tilde{i}_I^{(F)} \right] - \kappa_I^{(F)} V_I^{(F1)} \quad (2.4.11)$$

$$a_{32}^{(1)} = \left[\tilde{n}^{(F)} \tilde{\omega}^{(F1)} \tilde{i}_{II}^{(F)} \right] - \kappa_{II}^{(F)} V_{II}^{(F1)} \quad (2.4.12)$$

$$b_3^{(1)} = \left[\tilde{n}^{(F)} \tilde{\omega}^{(1)} \tilde{V}_{tr}^{(F)} \right] - \left[\tilde{n}^{(F)} \tilde{\omega}^{(F)} \tilde{V}_{tr}^{(1)} \right] \quad (2.4.13)$$

$$\left[\tilde{n}^{(F)} \right] = \begin{bmatrix} \sin \psi_c \\ \cos \psi_c \cos(\beta - \phi_F) \\ \cos \psi_c \sin(\beta - \phi_F) \end{bmatrix} \quad (2.4.14)$$

$$\left[\tilde{\omega}^{(F1)} \right] = \begin{bmatrix} 0 \\ 0 \\ -\omega^{(F)} \cot \gamma_1 \end{bmatrix} \quad (2.4.15)$$

To simplify equations for $\tilde{v}^{(F1)}$ and a_{31} let us note that

$$\begin{aligned}
 b_F &= r_F \frac{\cos \beta}{\sin q_F}; \quad r_F \cos(\beta - \phi_F) - b_F \sin(q_F - \phi_F) = \\
 &r_F \frac{\sin \phi_F \cos(\beta - \phi_F)}{\sin q_F}; \quad b_F \sin \psi_c \tan \psi_c \sin(q_F - \phi_F) \\
 &+ r_F \cos \psi_c \cos(\beta - \phi_F) = r_F \frac{\cos \beta \sin(q_F - \phi_F) + \cos^2 \psi_c \sin \psi_F \cos(\beta - q_F)}{\sin q_F \cos \psi_c}
 \end{aligned}$$

After that $\tilde{v}^{(F1)}$ can be represented by the following equation

$$\left[\tilde{v}^{(F1)} \right] = r_F \frac{\omega^{(F)} \cot \gamma_1 \cos \psi_c \sin \phi_F}{\sin q_F} \begin{bmatrix} \cos(\beta - \phi_F) \cos \psi_c \\ -\sin \psi_c \\ 0 \end{bmatrix} \quad (2.4.16)$$

Vectors $\tilde{i}_I^{(F)}$ and $\tilde{i}_{II}^{(F)}$ were represented by equations (2.4.1) and (2.4.3).

Equations (2.4.11)-(2.4.16), (2.4.1) and (2.4.3) yield

$$a_{31}^{(1)} = \omega^{(F)} \cot \gamma_1 \sin \psi_c \sin(\beta - \phi_F).$$

$$\frac{\cos \beta \sin(q_F - \phi_F)}{\cos \beta \sin(q_F - \phi_F) + \sin \phi_F \cos^2 \psi_c \cos(\beta - \phi_F)} \quad (2.4.17)$$

$$a_{32}^{(1)} = \omega^{(F)} \cot \gamma_1 \cos(\beta - \phi_F) \quad (2.4.18)$$

$$b_3^{(1)} = -L (\omega^{(F)})^2 \cot \gamma_1 \frac{\cos \beta \sin \psi_c}{\cos(\beta - \phi_F)} \quad (2.4.19)$$

$$V_I^{(F1)} a_{31}^{(1)} = -r_F (\omega^{(F)} \cot \gamma_1 \sin \psi_c \cos \psi_c) \cos \beta.$$

$$\frac{\sin \phi_F \sin(\beta - \phi_F) \sin(q_F - \phi_F)}{\sin q_F \left[\cos \beta \sin(q_F - \phi_F) + \cos^2 \psi_c \sin \phi_F \cos(\beta - \phi_F) \right]} \quad (2.4.20)$$

$$\begin{aligned}
& v_{II}^{(F1)} a_{32}^{(1)} = \\
& - r_F \left[\omega^{(F)} \cot \gamma_1 \cos(\beta - \phi_F) \right]^2 \frac{\sin \phi_F \cos \psi_c}{\sin \alpha_F} \quad (2.4.21)
\end{aligned}$$

Equations (2.4.2), (2.4.5)-(2.4.10) and (2.4.17)-(2.4.21) represent the principal directions and principal curvatures of surface Σ_1 . At the mean contact point the principal directions and curvatures are represented by the following equations

$$\tan 2\sigma^{(1)} = \frac{\sin \psi_c \sin 2\beta}{\frac{L}{2r_F} \tan \gamma_1 \sin 2\psi_c + \sin^2 \beta \sin^2 \psi_c - \cos^2 \beta} \quad (2.4.22)$$

$$\kappa_I^{(1)} + \kappa_{II}^{(1)} = - \frac{\cos \psi_c}{r_F} - \frac{\cot \gamma_1 (\sin^2 \beta \sin^2 \psi_c + \cos^2 \beta)}{L \sin \psi_c} \quad (2.4.23)$$

$$\kappa_I^{(1)} - \kappa_{II}^{(1)} = - \frac{\frac{\cos \psi_c}{r_F} + \frac{\cot \gamma_1 (\sin^2 \beta \sin^2 \psi_c - \cos^2 \beta)}{L \sin \psi_c}}{\cos 2\sigma^{(1)}} \quad (2.4.24)$$

Now, let us define principal curvatures and directions of surface Σ_2 generated by surface Σ_K . They are represented by equations analogical to equations (2.4.5)-(2.4.7)

$$\tan 2\sigma^{(2)} = \frac{2 F^{(2)}}{\kappa_I^{(K)} + G^{(2)}} \quad (2.4.25)$$

$$\kappa_I^{(2)} + \kappa_{II}^{(2)} = \kappa_I^{(K)} + S^{(2)} \quad (2.4.26)$$

$$\kappa_I^{(2)} - \kappa_{II}^{(2)} = \frac{\kappa_I^{(K)} + G^{(2)}}{\cos 2\sigma^{(2)}} \quad (2.4.27)$$

To define functions $F^{(2)}(\phi_k)$, $G^{(2)}(\phi_k)$ and $S^{(2)}(\phi_k)$ ($\phi_k = \phi_F$) it is sufficient to change subscripts "F" for "k" and "1" for "2" in expressions (2.4.17)-(2.4.21).

The principal curvature $\kappa_I^{(k)}$ of surface Σ_k is represented by equation analogous to (2.4.2)

$$\kappa_I^{(k)} = \frac{\cos(\beta - \phi_k)}{b_k \sin \psi_c \tan \psi_c \sin(\alpha_k - \phi_k) + r_k \cos \psi_c \cos(\beta - \phi_k)} \quad (2.4.28)$$

Equations (2.4.28), (2.4.2) and (2.2.22) yield that

$$\frac{1}{\kappa_I^{(k)}} = \frac{1}{\kappa_I^{(F)}} - \frac{r_k - r_F}{\cos \psi_c} \quad (2.4.29)$$

Equations (2.4.25)-(2.4.27) and (2.4.28) represent principal curvatures and directions of surface Σ_2 .

On the third stage of solution the size and direction of instantaneous contact ellipse is to be obtained. Equations (1.7.30)-(1.7.34) are to be applied for this aim.

2.5. GEOMETRY II: GENERATING SURFACES

Fig. 2.5.1 shows two generating surfaces Σ_k and Σ_F rigidly connected with each other. These surfaces are in tangency along their common circle C of radius r_d (Fig. 2.5.1). Surface Σ_k is a cone surface represented in the coordinate system by equations (2.2.19)-(2.2.21). Surface Σ_F is a surface of revolution. It is generated by the revolution of an arc m-m of a circle of radius ρ about axis x_a (Fig. 2.5.2,a). The arc m-m is represented in the auxiliary coordinate system $S_a(x_a, y_a, z_a)$ by equations.

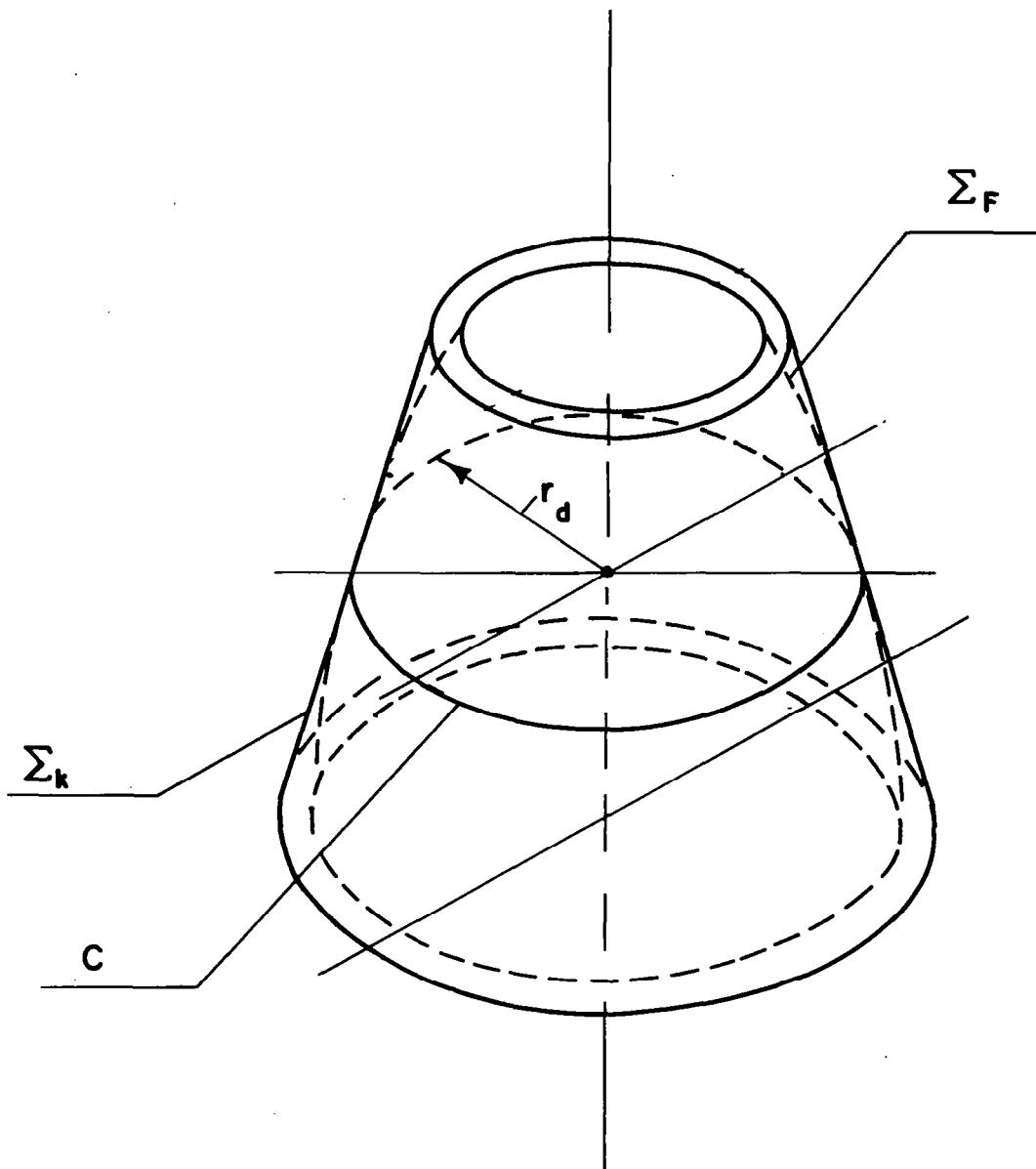


Fig. 2.5.1

Generating Surfaces: Conical Surface and Surface of Revolution

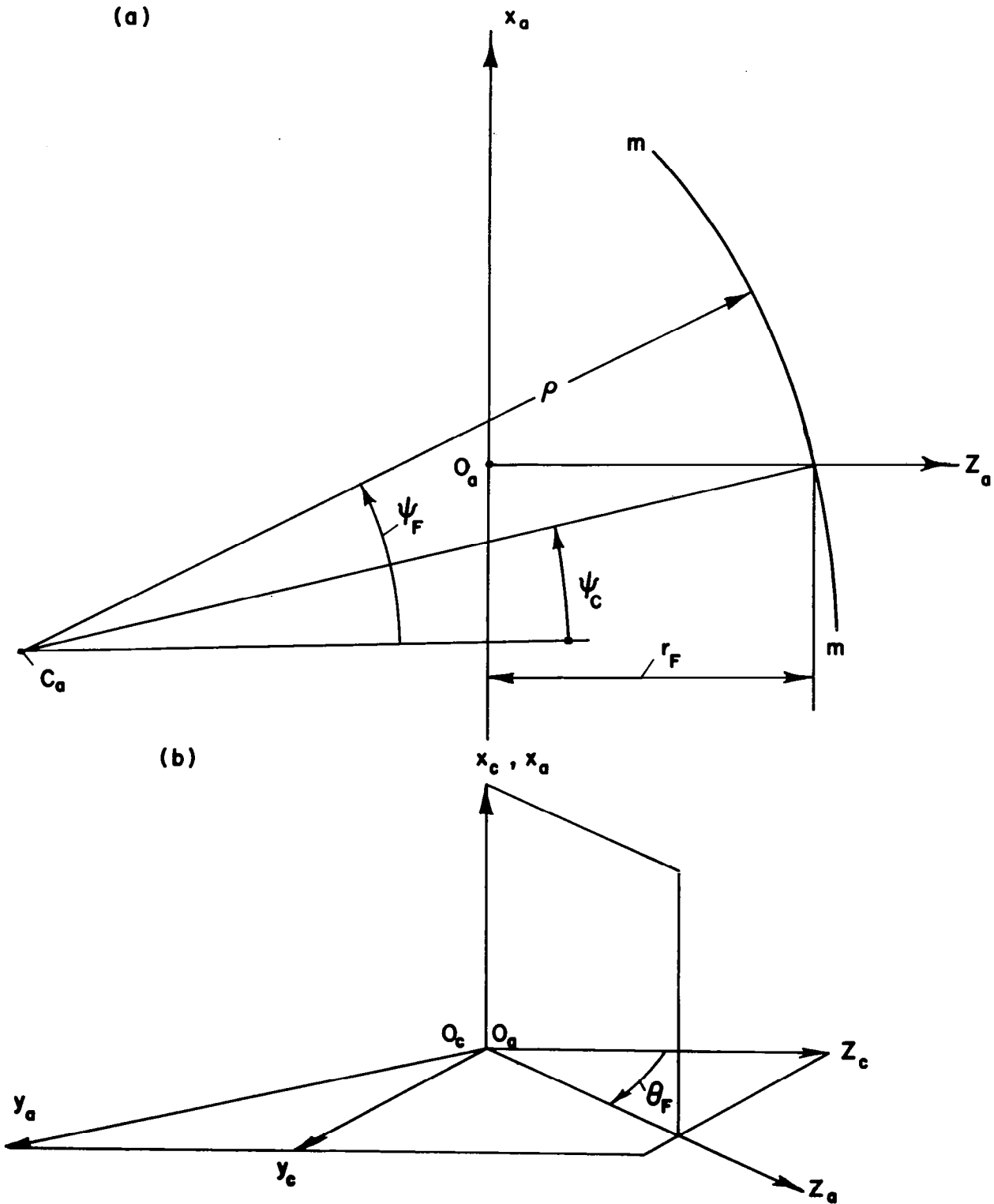


Fig. 2.5.2

$$\begin{aligned}
x_a &= \rho(\sin \psi_F - \sin \psi_c) \\
y_a &= 0 \\
z_a &= \rho(\cos \psi_F - \cos \psi_c) + r_F
\end{aligned} \tag{2.5.1}$$

Surface Σ_F is represented in coordinate system $S_c(x_c, y_c, z_c)$ by matrix equality

$$\begin{aligned}
\begin{bmatrix} r_c \\ \end{bmatrix} &= \begin{bmatrix} L_{ca} \\ \end{bmatrix} \begin{bmatrix} r_a \\ \end{bmatrix} = \\
\begin{bmatrix} 1 & 0 & 0 \\ 0 & \cos \theta_F & \sin \theta_F \\ 0 & -\sin \theta_F & \cos \theta_F \end{bmatrix} &\begin{bmatrix} x_a \\ y_a \\ z_a \end{bmatrix}
\end{aligned} \tag{2.5.2}$$

$$\begin{aligned}
x_c &= \rho(\sin \psi_F - \sin \psi_c) \\
y_c &= \left[\rho(\cos \psi_F - \cos \psi_c) + r_F \right] \sin \theta_F \\
z_c &= \left[\rho(\cos \psi_F - \cos \psi_c) + r_F \right] \cos \theta_F
\end{aligned} \tag{2.5.3}$$

Here: ψ_F and θ_F are surface Σ_F coordinates. The coordinate transformation by transition from $S_c(x_c, y_c, z_c)$ to $S_f(x_f, y_f, z_f)$ (Fig. 1.5.4) is represented by matrix equality

$$\begin{bmatrix} r_f \\ \end{bmatrix} = \begin{bmatrix} M_{fc} \\ \end{bmatrix} \begin{bmatrix} r_c \\ \end{bmatrix} \tag{2.5.4}$$

Expressions analogous to (1.5.9) and (1.5.15) yield

$$\begin{bmatrix} M_{fc} \\ \end{bmatrix} = \begin{bmatrix} 1 & 0 & 0 & 0 \\ 0 & \cos(q_F - \phi_F) & -\sin(q_F - \phi_F) & -b \sin(q_F - \phi_F) \\ 0 & \sin(q_F - \phi_F) & \cos(q_F - \phi_F) & b \cos(q_F - \phi_F) \\ 0 & 0 & 0 & 1 \end{bmatrix} \tag{2.5.5}$$

It results from expressions (2.5.3)-(2.5.5) that the generating surface Σ_F is represented in coordinate system S_f by equations

$$\begin{aligned}
x_f^{(F)} &= \rho(\sin \psi_F - \sin \psi_c) \\
y_f^{(F)} &= \left[\rho(\cos \psi_F - \cos \psi_c) + r_F \right] \sin \tau_F - b \sin(q_F - \phi_F) \\
z_f^{(F)} &= \left[\rho(\cos \psi_F - \cos \psi_c) + r \right] \cos \tau_F + b \cos(q_F - \phi_F),
\end{aligned} \tag{2.5.6}$$

where

$$\tau_F = \theta_F - (q_F - \phi_F)$$

The surface normal is represented by equation

$$\begin{aligned} \tilde{N}^{(F)} &= \frac{\partial \tilde{r}_f}{\partial \psi_F} \times \frac{\partial \tilde{r}_f}{\partial \theta_F} = \\ & \begin{vmatrix} \tilde{i}_f & \tilde{j}_f & \tilde{k}_f \\ \rho \cos \psi_F & -\rho \sin \psi_F \sin \tau_F & -\rho \sin \psi_F \cos \tau_F \\ 0 & A \cos \tau_F & -A \sin \tau_F \end{vmatrix} = \\ & A \rho \sin \psi_F \tilde{i}_f + A \rho \cos \psi_F \sin \tau_F \tilde{j}_f + A \rho \cos \psi_F \cos \tau_F \tilde{k}_f \end{aligned} \quad (2.5.7)$$

Here:

$$A = \rho(\cos \psi_F - \cos \psi_C) + r_F$$

The surface unit normal $\tilde{n}^{(F)}$ is represented by equation

$$\tilde{n}^{(F)} = \frac{\tilde{N}^{(F)}}{|\tilde{N}^{(F)}|} = \sin \psi_F \tilde{i}_f + \cos \psi_F (\sin \tau_F \tilde{j}_f + \cos \tau_F \tilde{k}_f) \quad (2.5.8)$$

The generating surface Σ_k and its unit normal are represented by equations (2.2.8) and (2.2.10) with subscript $d=k$.

By $\psi_F = \psi_C$, $r_F = r_k$, $u_k = \frac{r_k}{\sin \psi_C}$ surfaces Σ_F and Σ_k are in tangency along the circle of radius $r_k = r_F$.

2.6 Geometry II: The Line of Action

The law of meshing of surfaces Σ_k and Σ_2 was represented by the equation [see(2.2.18)]

$$\begin{aligned} & (u_k - r_k \cot \psi_C \cos \psi_C) \sin(\theta_k - q_k + \phi_k) \\ & - b_k \sin \psi_C \sin(q_k - \phi_k) = 0 \end{aligned} \quad (2.6.1)$$

At contact points of surfaces Σ_1 and Σ_2 parameter

$$u_k \sin \psi_C = r_k \quad (2.6.2)$$

Equations (2.6.1) and (2.6.2) yield

$$r_k \sin[\theta_k - (q_k - \phi_k)] - b_k \sin(q_k - \phi_k) = f(\theta_k, \phi_k) = 0 \quad (2.6.3)$$

This equation relates the surface parameter θ_k with the angle of rotation ϕ_k . By $\frac{\partial f}{\partial \theta_k} \neq 0$ this equation represents in implicit form a function $\theta_k(\phi_k)$.

Equations (2.2.8), (2.6.2) and (2.6.3) yield that the line of action can be represented that way

$$\begin{aligned} x_f = 0, \quad y_f = 0, \quad z_f &= r_k \cos[\theta_k - (q_k - \phi_k)] + \\ b_k \cos(q_k - \phi_k) &= z_f(\phi_k) \end{aligned} \quad (2.6.4)$$

where angles $[\theta - (q_k - \phi_k)]$ and $(q_k - \phi_k)$ are related by (2.6.3).

Contact point paths on surface Σ_1 and Σ_2 can be defined the same way mentioned in item 2.3.

2.7. Geometry II: The Instantaneous Contact Ellipse.

The principal curvatures and directions of surface Σ_2 generated by surface Σ_k were defined in item 2.4 by equations (2.4.20)-(2.4.21). For surface Σ_2 with geometry II coefficients $a_{31}^{(2)}$, $a_{32}^{(2)}$, $b_3^{(2)}$, $F^{(2)}$, $G^{(2)}$ and $S^{(2)}$ are represented by following equations

$$a_{31}^{(1)} = -\omega^{(k)} \cot \gamma_2 \sin \psi_c \cos \tau_k \quad (2.7.1)$$

$$a_{32}^{(2)} = -\omega^{(k)} \cot \gamma_2 \sin \tau_k \quad (2.7.2)$$

$$b_3^{(2)} = r_k (\omega^{(k)})^2 \cot \gamma_2 \sin \psi_c \left[\frac{\cos \tau_k \sin q_k + \cos \beta \cos(q_k - \phi_k)}{\sin q_k} \right] \quad (2.7.3)$$

$$F^{(2)} = \frac{a_{31} a_{32}}{b_3} = \frac{\sin q_k \cot \gamma_2 \cos \tau_k \sin \tau_k}{r_k [\cos \tau_k \sin q_k + \cos \beta \cos(q_k - \phi_k)]} \quad (2.7.4)$$

$$G^{(2)} = \frac{a_{31}^2 - a_{32}^2}{b_3} = \frac{(\sin^2 \psi_c \cos^2 \tau_k - \sin^2 \tau_k) \sin q_k \cot \gamma_2}{r_k [\cos \tau_k \sin q_k + \cos \beta \cos(q_k - \phi_k)]} \quad (2.7.5)$$

$$S^{(2)} = \frac{a_{31}^2 + a_{32}^2}{b_3} = \frac{(\sin^2 \psi_c \cos^2 \tau_k + \sin^2 \tau_k) \sin q_k \cot \gamma_2}{r_k [\cos \tau_k \sin q_k + \cos \beta \cos(q_k - \phi_k)]} \quad (2.7.6)$$

Parameters θ_k and ϕ_k are related by equation (2.6.3).

Now, let us define principal curvatures and directions of surface Σ_1 generated by Σ_F . To solve this problem we must in first define principal directions and curvatures of surface Σ_F .

It is easy to verify that principal directions of surface Σ_F correspond to $\frac{d\psi_F}{dt} = 0$ and to $\frac{d\theta_F}{dt} = 0$ and that principal curvatures are represented by equations

$$\kappa_I^{(F)} = - \frac{\cos \psi_F}{\rho(\cos \psi_F - \cos \psi_c) + r_F} \quad (2.7.7)$$

$$\kappa_{II}^{(F)} = - \frac{1}{\rho} \quad (2.7.8)$$

At the point of contact of surfaces Σ_F and Σ_1 the principal curvature is

$$\kappa_I^{(F)} = - \frac{\cos \psi_c}{r_F} \quad (2.7.9)$$

because at this point $\psi_F = \psi_c$.

Principal curvatures and directions of surface Σ_1 are represented by equations

$$\tan 2\sigma^{(1)} = \frac{2F^{(1)}}{\kappa_I^{(F)} - \kappa_{II}^{(F)} + G^{(1)}} \quad (2.7.10)$$

$$\kappa_I^{(1)} + \kappa_{II}^{(1)} = \kappa_I^{(F)} + \kappa_{II}^{(F)} + S^{(1)} \quad (2.7.11)$$

$$\kappa_I^{(1)} - \kappa_{II}^{(1)} = \frac{\kappa_I^{(F)} - \kappa_{II}^{(F)} + G^{(1)}}{\cos 2\sigma^{(1)}} \quad (2.7.12)$$

Here:

$$F^{(1)} = F^{(2)}, S^{(1)} = S^{(2)}, G^{(1)} = G^{(2)}$$

The size and direction of instantaneous contact ellipse are defined the same way which was mentioned in item 1.7.

3. METHODS TO CALCULATE GEAR-DRIVE KINEMATICAL ERRORS.

3.1. Introduction

It is well known that errors of manufacturing and assemblage of gears induce kinematical errors in gear-drives. These errors can be represented by a function

$$\Delta \phi_2 (\phi_1, \Delta Q), \quad (3.1.1)$$

where ϕ_1 is the angle of rotation of the driving gear 1,

$$\Delta Q = (\Delta q_1, \Delta q_2, \dots) \quad (3.1.2)$$

is the vector of errors;

$$\Delta \phi_2 = \phi_2^o - \phi_2 \quad (3.1.3)$$

is the kinematical error of the gear drive represented as the difference of theoretical and actual angles of rotation of the driven gear.

In this part of the report two methods to calculate the function (3.1.1) are presented: the first one is a numerical computer method and the second one is worked out as an approximate method but with a possibility to obtain relatively simple results which are in most cases in an analytical form.

3.2. The Computer Method.

In the process of motion tooth surfaces Σ_1 and Σ_2 must be in continuous tangency. It was demonstrated (see item 1.1) that following equations are to be observed (see equations (1.1.12) and (1.1.13)).

$$\underline{r}_f^{(1)}(u_1, \theta_1, \phi_1) = \underline{r}_f^{(2)}(u_2, \theta_2, \phi_2) \quad (3.2.1)$$

$$\underline{n}_f^{(1)}(u_1, \theta_1, \phi_1) = \underline{n}_f^{(2)}(u_2, \theta_2, \phi_2) \quad (3.2.2)$$

Here: $\underline{r}_f^{(i)}$ and $\underline{n}_f^{(i)}$ are the position vectors and normals of surfaces Σ_i as defined in coordinate system S_f rigidly connected with the frame; u_i, θ_i are the surface coordinates, ϕ_i are the angles of gear rotation.

Here it is assumed that errors of manufacturing and assemblage did not appear.

For gears with errors represented by vectors ΔQ_1 and ΔQ_2 following equations of tangency must be observed instead of equations (3.2.1) and (3.2.2)

$$\underline{r}_f^{(1)}(u_1, \theta_1, \phi_1, \Delta Q_1) = \underline{r}_f^{(2)}(u_2, \theta_2, \phi_2, \Delta Q_2) \quad (3.2.3)$$

$$\underline{n}_f^{(1)}(u_1, \theta_1, \phi_1, \Delta Q_1) = \underline{n}_f^{(2)}(u_2, \theta_2, \phi_2, \Delta Q_2) \quad (3.2.4)$$

Equations (3.2.3) and (3.2.4) yield the function

$$\phi_2(\phi_1, \Delta Q_1, \Delta Q_2) = \phi_2^\circ(\phi_1) + \Delta \phi_2(\phi_1, \Delta Q_1, \Delta Q_2) \quad (3.2.5)$$

Here: $\phi_2^\circ(\phi_1)$ is the theoretical function yielded by equations (3.2.1) and (3.2.2).

Equations (3.2.3) and (3.2.4) also yield the functions

$$u_i(\phi_1, \Delta Q_1, \Delta Q_2), \theta_i(\phi_1, \Delta Q_1, \Delta Q_2) \quad (i=1,2) \quad (3.2.6)$$

Functions

$$\underline{r}_i(u_i, \theta_i), u_i(\phi_1, \Delta Q_1, \Delta Q_2), \theta_i(\phi_1, \Delta Q_1, \Delta Q_2) \quad (i=1,2) \quad (3.2.7)$$

represent the path of contact points on surface Σ_i corresponding to gear meshing with errors of manufacturing and assemblage.

Functions

$$\underline{r}_i(u_i, \theta_i), u_i^\circ(\phi_1), \theta_i^\circ(\phi_1) \quad (3.2.8)$$

represent the path of contact point on surface Σ_i correspondent to the meshing without errors. Comparison of functions (3.2.8) and (3.2.7) yields the change of contact point path induced by errors.

Let us consider the detailed solution of equations (3.2.1)-(3.2.2) and (3.2.3)-(3.2.4).

Vector-equations (3.2.1) and (3.2.2) yield only five independent scalar equations because $|\tilde{n}_f^{(1)}| = |\tilde{n}_f^{(2)}|$:

$$f_j(u_1, \theta_1, \phi_1, u_2, \theta_2, \phi_2^o) = 0 \quad (j=1,2,\dots,5) \quad (3.2.9)$$

It is assumed that

$$\{f_1, f_2, f_3, f_4, f_5\} \in C^1$$

and that the system of equations (3.2.9) is satisfied by a set of parameters

$$P = (u_1^*, \theta_1^*, \phi_1^*, u_2^*, \theta_2^*, \phi_2^*) \quad (3.2.10)$$

and surfaces Σ_1 and Σ_2 are in tangency at a point M_0 . Surfaces Σ_1 and Σ_2 will be in point contact in the neighborhood of M_0 if by the set of parameters P the following inequality is held

$$\frac{D(f_1, f_2, f_3, f_4, f_5)}{D(u_1, \theta_1, u_2, \theta_2, \phi_2^o)} = \frac{\begin{vmatrix} \frac{\partial f_1}{\partial u_1} & \frac{\partial f_1}{\partial \theta_1} & \frac{\partial f_1}{\partial u_2} & \frac{\partial f_1}{\partial \theta_2} & \frac{\partial f_1}{\partial \phi_2^o} \\ \frac{\partial f_2}{\partial u_1} & \frac{\partial f_2}{\partial \theta_1} & \frac{\partial f_2}{\partial u_2} & \frac{\partial f_2}{\partial \theta_2} & \frac{\partial f_2}{\partial \phi_2^o} \\ \frac{\partial f_3}{\partial u_1} & \frac{\partial f_3}{\partial \theta_1} & \frac{\partial f_3}{\partial u_2} & \frac{\partial f_3}{\partial \theta_2} & \frac{\partial f_3}{\partial \phi_2^o} \\ \frac{\partial f_4}{\partial u_1} & \frac{\partial f_4}{\partial \theta_1} & \frac{\partial f_4}{\partial u_2} & \frac{\partial f_4}{\partial \theta_2} & \frac{\partial f_4}{\partial \phi_2^o} \\ \frac{\partial f_5}{\partial u_1} & \frac{\partial f_5}{\partial \theta_1} & \frac{\partial f_5}{\partial u_2} & \frac{\partial f_5}{\partial \theta_2} & \frac{\partial f_5}{\partial \phi_2^o} \end{vmatrix}}{\begin{vmatrix} \frac{\partial f_5}{\partial u_1} & \frac{\partial f_5}{\partial \theta_1} & \frac{\partial f_5}{\partial u_2} & \frac{\partial f_5}{\partial \theta_2} & \frac{\partial f_5}{\partial \phi_2^o} \end{vmatrix}} \neq 0 \quad (3.2.11)$$

Then in the neighborhood of P equations (3.2.9) provide functions

$$\{u_1(\phi_1), \theta_1(\phi_1), u_2(\phi_1), \theta_2(\phi_1), \phi_2^o(\phi_1)\} \in C^1 \quad (3.2.12)$$

Function $\phi_2^o(\phi_1)$ represents the ideal law of motion transformation.

Mostly, $\phi_2^o(\phi_1)$ is a linear function.

Equations (3.2.3)-(3.2.4) also yield a system of five independent equations

$$\psi_j(u_1, \theta_1, \phi_1, u_2, \theta_2, \phi_2, \Delta Q) = 0 \quad (3.2.13)$$

By the same value of ϕ_1 this system is satisfied by a set of parameters

$$P' = (u_1^{**}, \theta_1^{**}, \phi_1^*, u_2^{**}, \theta_2^{**}, \phi_2^{**}) \quad (3.2.14)$$

which is different from the set P represented by (3.2.10).

System of equations (3.2.13) can yield functions

$$u_1(\phi_1, \Delta Q), \theta_1(\phi_1, \Delta Q), u_2(\phi_1, \Delta Q), \theta_2(\phi_1, \Delta Q), \phi_2(\phi_1, \Delta Q) \in C^1 \quad (3.2.15)$$

in the neighborhood of P' if at P' the following inequality is held

$$\frac{D(\psi_1, \psi_2, \psi_3, \psi_4, \psi_5)}{D(u_1, \theta_1, u_2, \theta_2, \phi_2)} \neq 0 \quad (3.2.16)$$

Function $\phi_2(\phi_1, \Delta Q)$ represents the real law of motion transformation. Kinematical errors of the gear-drive are represented by function

$$\Delta\phi_2 = \phi_2^o(\phi_1) - \phi_2(\phi_1, \Delta Q) \quad (3.2.17)$$

The demonstrated method can provide not only the kinematical errors induced by errors ΔQ but new contact point path on the surface Σ_i , too. (see functions (3.2.7)).

The solution of a system of five non-linear equations is a hard problem and needs iterations. To save computer time a more effective way of solution was recently proposed by F. Litvin and YE. Gutman [12]. The principle of this method follows:

The system of equations (3.2.13) can be represented as follows

$$f_1(u_1, \theta_1, \phi_1, u_2, \theta_2, \phi_2, A, H_1, H_2) = 0 \quad (3.2.18)$$

$$f_2(u_1, \theta_1, \phi_1, u_2, \theta_2, \phi_2, A, H_1, H_2) = 0 \quad (3.2.19)$$

$$f_3(u_1, \theta_1, \phi_1, u_2, \theta_2, \phi_2, A, H_1, H_2) = 0 \quad (3.2.20)$$

$$f_4(u_1, \theta_1, \phi_1, u_2, \theta_2, \phi_2) = 0 \quad (3.2.21)$$

$$f_5(u_1, \theta_1, \phi_1, u_2, \theta_2, \phi_2) = 0 \quad (3.2.22)$$

Equations (3.2.18)-(3.2.20) are yielded by vector equation (3.2.3) and equations (3.2.21)-(3.2.22) by vector equation (3.2.4). Parameters A, H_1 and H_2 are linear measurements which represent the shortest distance between gear axes of rotation and axial settings of gears (Fig. 3.2.1).

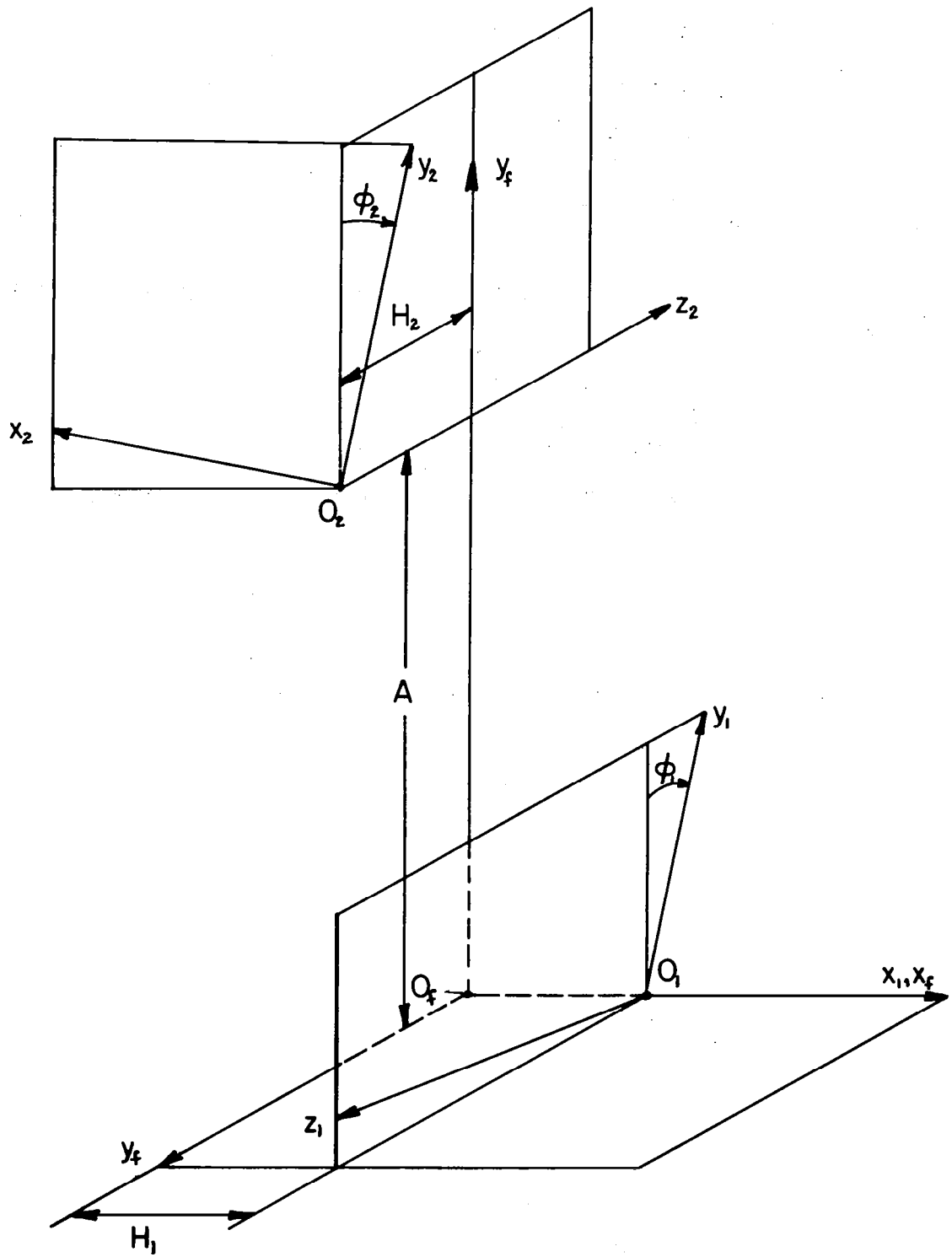


FIG. 3.2.I

Axial Settings of Gears: H_1 , H_2 and A

Let us suppose that points $M_1(u_1, \theta_1)$ and $M_2(u_2, \theta_2)$ of surfaces Σ_1 and Σ_2 are chosen. By a set of given parameters $(u_1, \theta_1, u_2, \theta_2)$ system of equations (3.2.21) and (3.2.22) becomes a system of two equations in two unknowns which may be expressed as

$$F_1(\phi_1, \phi_2) = 0 \quad (3.2.23)$$

$$F_2(\phi_1, \phi_2) = 0 \quad (3.2.24)$$

After that a system of three equations must be solved

$$A - K_1(u_1, \theta_1, \phi_1, u_2, \theta_2, \phi_2) = 0 \quad (3.2.25)$$

$$H_1 - K_2(u_1, \theta_1, \phi_1, u_2, \theta_2, \phi_2) = 0 \quad (3.2.26)$$

$$H_2 - K_3(u_1, \theta_1, \phi_1, u_2, \theta_2, \phi_2) = 0 \quad (3.2.27)$$

The method of solution of the two systems of equations (3.2.23)-(3.2.23) and (3.2.24)-(3.2.26) is an iterative procedure. By computation one of four varied parameters $(u_1, \theta_1, u_2, \theta_2)$ is fixed and the three others must be changed that way that two mentioned above systems of equations are to be satisfied.

The advantage of the proposed method is the opportunity to divide the system (3.2.18)-(3.2.22) of five equations into two subsystems -- of two and one of three equations - and solve them separately

3.3. Approximate Method

Accuracy of gear drives investigated by the above computer method can be defined as a rule only numerically and this is a certain disadvantage of this method. Therefore, in addition to the computer method an approximate method with the opportunity to obtain results analytically is proposed.

Figure 3.3.1 shows two surfaces Σ_1 and Σ_2 which are in tangency at point M. Points M_1 and M_2 of these surfaces coincide with each other at M, position vectors $\underline{r}_f^{(1)}$ and $\underline{r}_f^{(2)}$ drqwn from O_f and surface unit normals $\underline{n}_f^{(1)}$ and $\underline{n}_f^{(2)}$ coincide at M, too. Surfaces Σ_1 and Σ_2 rotate about axes I-I and II-II and angles of rotation ϕ_1 and ϕ_2° correspond to the positions of surfaces shown in Fig. 3.3.1. It is supposed initially that Σ_1 and Σ_2 are manufactured and assembled without errors. Due to errors surfaces Σ_1 and Σ_2 cannot be in tangency by the same values of ϕ_1 and ϕ_2° - either a clearance will appear between these surfaces or the surfaces will interfere with each other. Figure 3.3.2 shows that surfaces Σ_1 and Σ_2 are not in tangency: points M_1 and M_2 do not coincide with each other, $\underline{r}_f^{(1)} \neq \underline{r}_f^{(2)}$ and $\underline{n}_f^{(1)} \neq \underline{n}_f^{(2)}$. To get surfaces Σ_1 and Σ_2 in tangency it is sufficient to rotate one of the surfaces by an additional small angle. It is more preferable to hold the position of surface Σ_1 and to rotate surface Σ_2 until it contacts Σ_1 . Then the additional angle of rotation $\Delta\phi_2$ will represent the change of theoretical value ϕ_2° induced by errors of manufacturing and assemblage. It can be predicted that $\Delta\phi_2$ is a function of the vector $\Delta\tilde{Q}$ and changes in the process of motion. So

$$\Delta\phi_2 = f(\phi_1, \Delta\tilde{Q}). \quad (3.3.1)$$

The definition of function (3.3.1) can be based on the equations of kinematical relations discussed in Item 1.1.

Because tooth surfaces Σ_1 and Σ_2 are to be in continuous contact the following vector equations must be observed

$$\underline{dr}_f^{(1)} = \underline{dr}_f^{(2)} \quad (3.3.2)$$

$$\underline{dn}_f^{(1)} = \underline{dn}_f^{(2)} \quad (3.3.3)$$

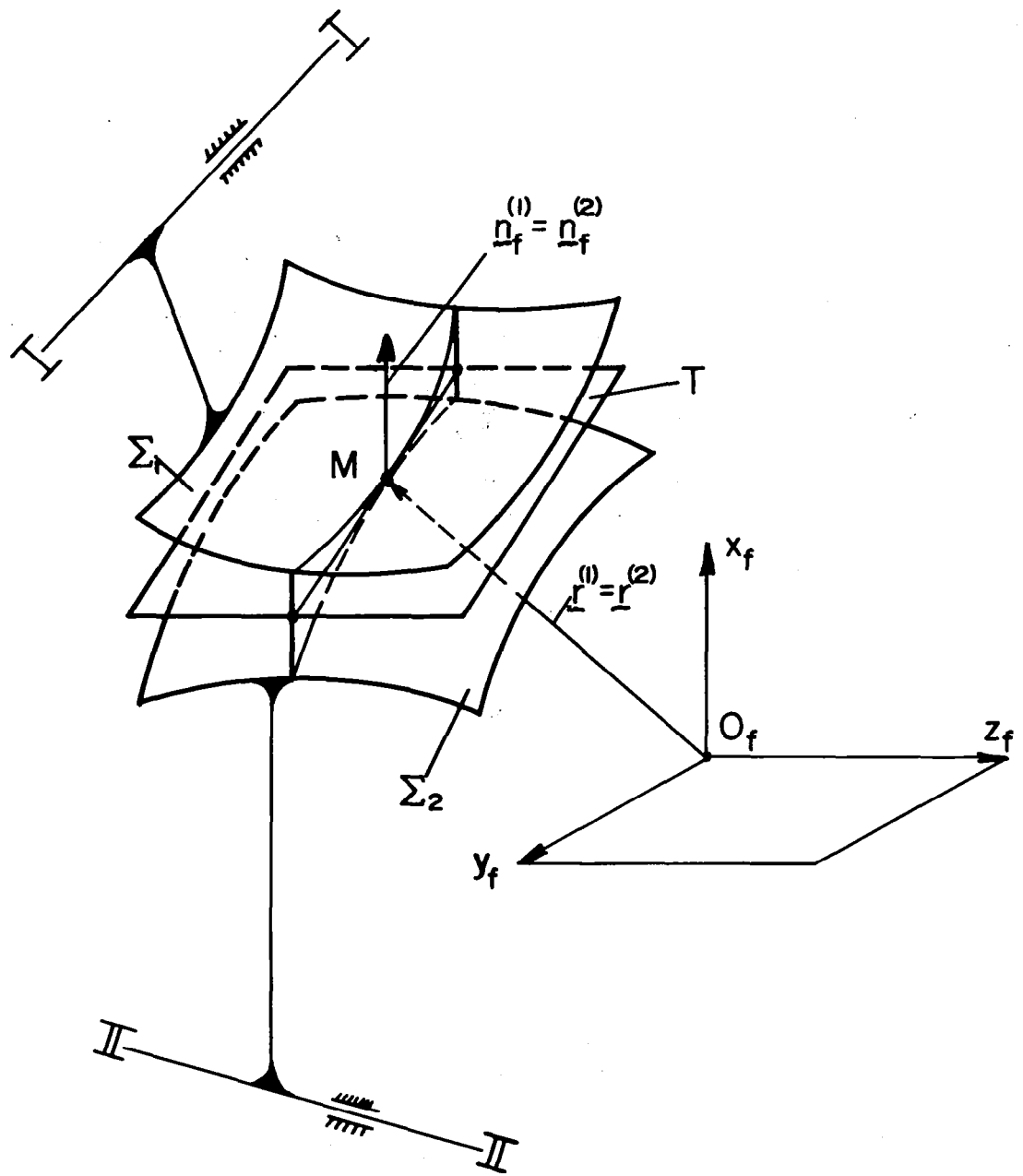


FIG. 3.3.1

Contacting Tooth Surfaces

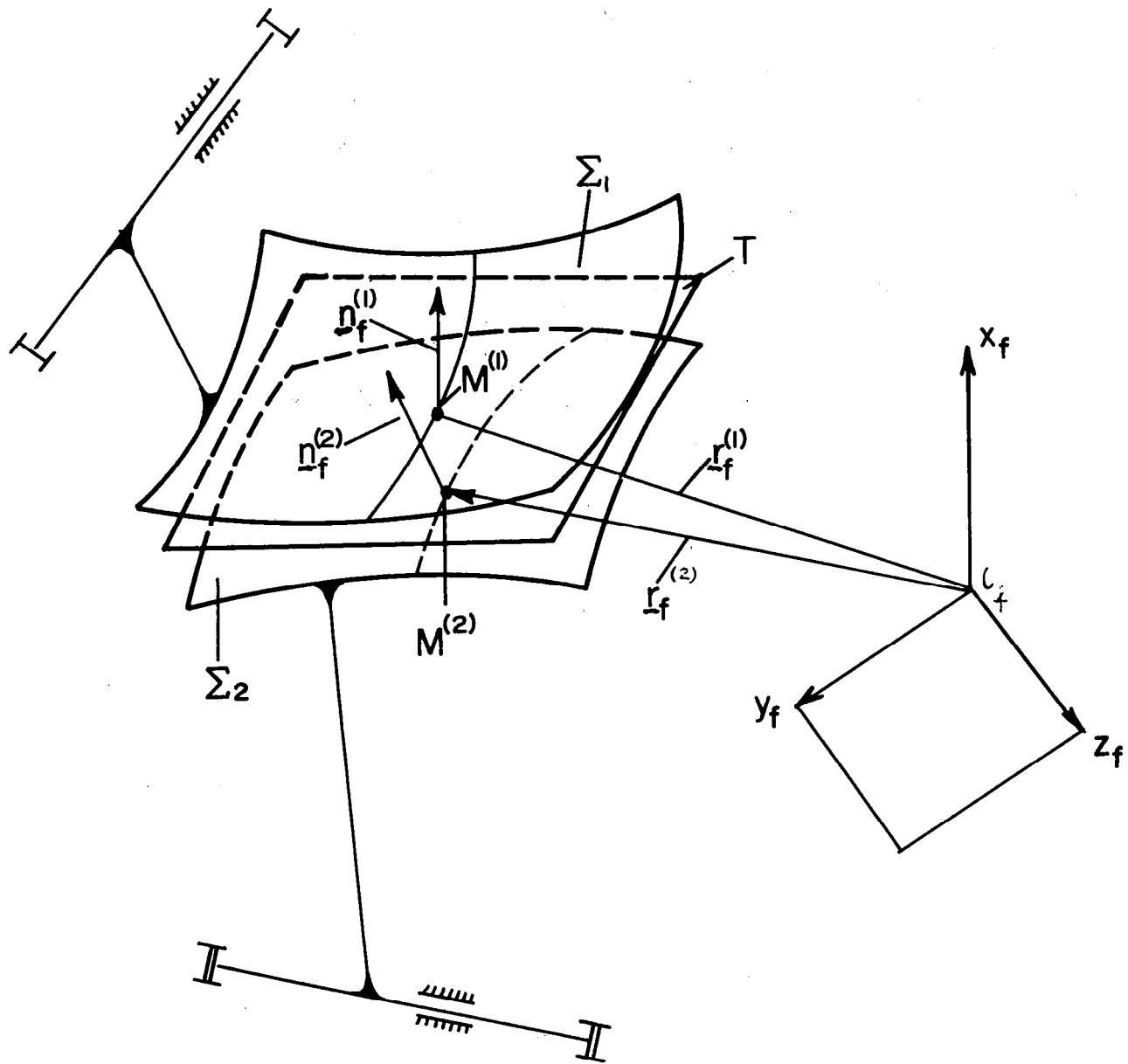


FIG. 3.3.2

Tooth Surfaces with Clearance Induced by Errors

It results from equations (3.3.2) and (3.3.3) that

$$ds_{\sim tr}^{(1)} + ds_{\sim r}^{(1)} = ds_{\sim tr}^{(2)} + ds_{\sim r}^{(2)} \quad (3.3.4)$$

$$dn_{\sim tr}^{(1)} + dn_{\sim r}^{(1)} = dn_{\sim tr}^{(2)} + dn_{\sim r}^{(2)} \quad (3.3.5)$$

Here: $ds_{\sim tr}^{(i)}$ is the displacement of the contact point of surface Σ_i ($i=1,2$) in transfer motion (with the surface); $ds_{\sim r}^{(i)}$ is the contact point displacement in relative motion (relative to the surface); notations of $dn_{\sim tr}^{(i)}$ and $dn_{\sim r}^{(i)}$ have the same meanings for the tip of the unit normal vectors; subscript "f" is dropped for simplification.

Equations (3.3.4) and (3.3.5) are similar to equations (1.1.35) and (1.1.36).

Errors of manufacturing and assemblage induce that the theoretical contact point changes its position. To hold surfaces in tangency following equations must be observed:

$$ds_{\sim tr}^{(1)} + ds_{\sim r}^{(1)} + ds_{\sim q}^{(1)} = ds_{\sim tr}^{(2)} + ds_{\sim r}^{(2)} + ds_{\sim q}^{(2)} \quad (3.3.6)$$

$$dn_{\sim tr}^{(1)} + dn_{\sim r}^{(1)} + dn_{\sim q}^{(1)} = dn_{\sim tr}^{(2)} + dn_{\sim r}^{(2)} + dn_{\sim q}^{(2)} \quad (3.3.7)$$

Here: the subscript "q" corresponds to the displacement induced by errors. It is necessary to emphasize that not only angular errors but linear errors also induce $dn_{\sim q}^{(i)}$.

It was mentioned above that interference of surfaces or their clearance can be compensated by rotation of surface Σ_2 only. Therefore, $ds_{\sim tr}^{(1)}=0$ and $dn_{\sim tr}^{(1)}=0$ and

$$ds_{\sim r}^{(1)} + ds_{\sim q}^{(1)} = ds_{\sim tr}^{(2)} + ds_{\sim r}^{(2)} + ds_{\sim q}^{(2)} \quad (3.3.8)$$

$$dn_{\sim r}^{(1)} + dn_{\sim q}^{(1)} = dn_{\sim tr}^{(2)} + dn_{\sim r}^{(2)} + dn_{\sim q}^{(2)} \quad (3.3.9)$$

It was demonstrated in item 1.1 that

$$\underline{ds}_{tr}^{(2)} = d\phi^{(2)} \times \underline{\rho}^{(2)} \quad (3.3.10)$$

where

$$\underline{\rho}^{(2)} = \overline{N^{(2)}M^{(2)}}$$

is a vector drawn from an arbitrary point $N^{(2)}$ of axis rotation to the contact point $M^{(2)}$. (Fig. 1.2.1).

Then, (see item 1.1),

$$\underline{dn}_{tr}^{(i)} = d\phi^{(i)} \times \underline{n}^{(i)} \quad (3.3.11)$$

Here: vector $d\phi^{(i)}$ is similar to vector $\underline{\omega}^{(i)}$ and is directed along the axis of rotation according to the direction of rotation

$$d\phi^{(i)} = \underline{\omega}^{(i)} dt, \quad (3.3.12)$$

where t is time.

Let us compose following scalar products

$$\underline{n} \cdot (\underline{ds}_r^{(1)} + \underline{ds}_q^{(1)}) = \underline{n} \cdot (\underline{ds}_{tr}^{(2)} + \underline{ds}_r^{(2)} + \underline{ds}_q^{(2)}) \quad (3.3.13)$$

$$\underline{n} \cdot (\underline{dn}_r^{(1)} + \underline{dn}_q^{(1)}) = \underline{n} \cdot (\underline{dn}_{tr}^{(2)} + \underline{dn}_r^{(2)} + \underline{dn}_q^{(2)}), \quad (3.3.14)$$

where \underline{n} is the common unit normal of surfaces.

Vectors $\underline{ds}_r^{(1)}$ and $\underline{ds}_r^{(2)}$ belong to the common tangent plane T (Fig. 3.3.1). Therefore,

$$\underline{n} \cdot \underline{ds}_r^{(i)} = 0 \quad (i=1,2) \quad (3.3.15)$$

Equations (3.3.13), (3.3.10) and (3.3.15) yield

$$\left[d\phi^{(2)} \underline{\rho}^{(2)} \underline{n} \right] = \left(\underline{ds}_q^{(1)} - \underline{ds}_q^{(2)} \right) \cdot \underline{n} \quad (3.3.16)$$

It is easy to be verified that both parts of equation (3.3.14) are equal to zero identically. Indeed, vectors $\underline{dn}_r^{(i)}$ belong to the tangent plane and therefore

$$\vec{n} \cdot d\vec{n}_r^{(i)} = 0 \quad (3.3.17)$$

It results from equation (3.3.11) that

$$\vec{n} \cdot d\vec{n}_{tr}^{(2)} = \left[\vec{n} \quad d\phi^{(2)} \vec{n} \right] = 0 \quad (3.3.18)$$

Vector $d\vec{n}_q^{(i)}$ ($i=1,2$) can be represented the expression

$$d\vec{n}_q^{(i)} = d\delta_q^{(i)} \times \vec{n} \quad (3.3.19)$$

where $d\delta_q^{(i)}$ is a vector represented by the angular error.

Therefore

$$\vec{n} \cdot d\vec{n}_q^{(i)} = \left[\vec{n} \quad d\delta_q^{(i)} \vec{n} \right] = 0 \quad (3.3.20)$$

Equation (3.3.16) is the basic equation for the determination of kinematical errors of gear drives. Its application will be demonstrated in the following items.

3.4. Kinematical Errors of Spiral Bevel Gears Induced by Their Eccentricity

Gear eccentricity occurs when a gear's geometrical axis does not coincide with its axis of rotation (Fig. 3.4.1). By rotation the geometrical axis of a gear generates a cylindrical surface of radius Δe . The vector of eccentricity Δe is represented by a vector of constant magnitude which rotates about gear axis.

The initial position of vector Δe (the position at the beginning of motion) is given by the angle α and its current position by angle $(\phi + \alpha)$ (Fig. 3.4.2).

Fig. 3.4.2 shows coordinate systems $S_1(x_1, y_1, z_1)$ and S_f rigidly connected with gear 1 and the frame; the coordinate system S_h is an auxiliary one which is also rigidly connected with the frame. The driving gear 1 rotates about axis z_h . The position of Δe_1 in coordinate system S_1 is given by the angle α_1 made by Δe_1 and axis x_1 . The current position of Δe_1 in coordinate

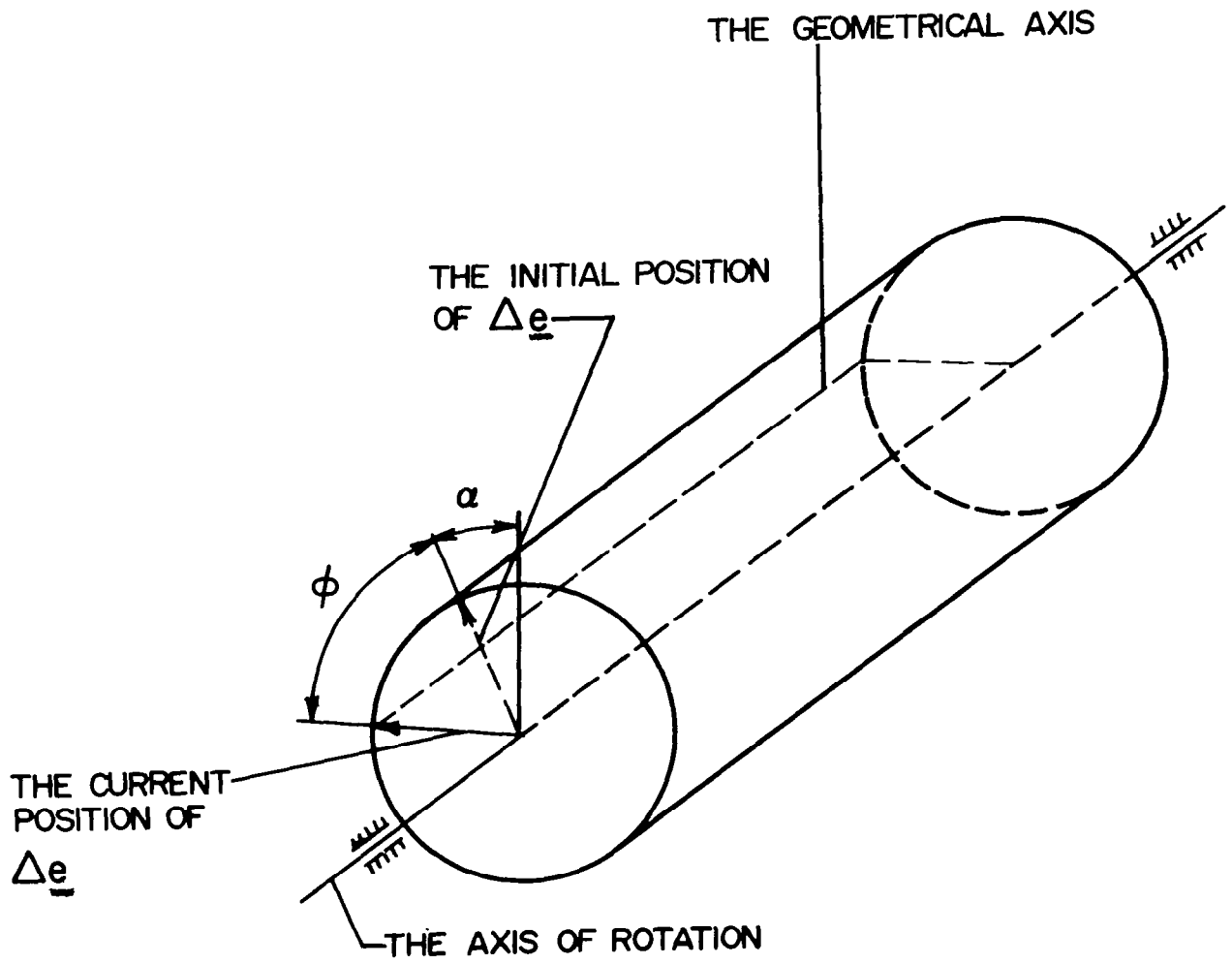


FIG. 3.4.1

Cylinder Generated by Geometrical Axis of Eccentric Gear

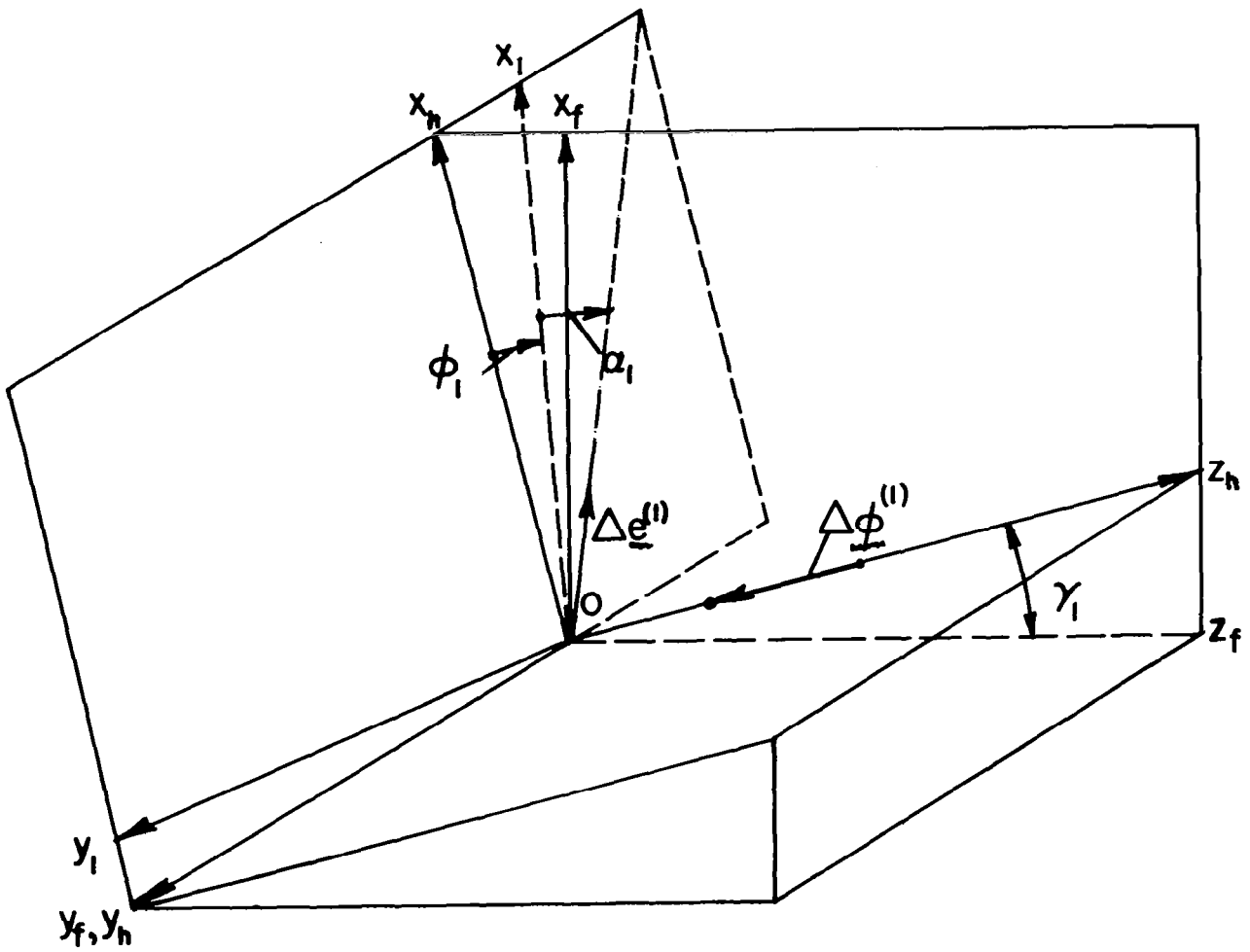


FIG. 3.4.2

Coordinate Systems Associated with Gear 1

system S_f (or S_h) is defined by the angle $(\phi_1 + \alpha_1)$. Vector $\Delta \underline{e}_f^{(1)}$ is represented by the matrix equation

$$\begin{aligned} \left[\Delta \underline{e}_f^{(1)} \right] &= \left[L_{fh} \right] \left[\Delta \underline{e}_h^{(1)} \right] = \\ &\begin{bmatrix} \cos \gamma_1 & 0 & \sin \gamma_1 \\ 0 & 1 & 0 \\ -\sin \gamma_1 & 0 & \cos \gamma_1 \end{bmatrix} \begin{bmatrix} \Delta e_1 \cos(\phi_1 + \alpha_1) \\ -\Delta e_1 \sin(\phi_1 + \alpha_1) \\ 0 \end{bmatrix} \end{aligned} \quad (3.4.1)$$

Matrix equality (3.4.1) yields

$$\left[\Delta \underline{e}_f^{(1)} \right] = \begin{bmatrix} \Delta e_1 \cos(\phi_1 + \alpha_1) \cos \gamma_1 \\ -\Delta e_1 \sin(\phi_1 + \alpha_1) \\ -\Delta e_1 \cos(\phi_1 + \alpha_1) \sin \gamma_1 \end{bmatrix} \quad (3.4.2)$$

The vector of eccentricity of the driven gear 2 $\Delta \underline{e}^{(2)}$ can be defined the same way. Fig. 3.4.3 shows coordinate systems S_2 and S_f rigidly connected with gear 2 and the frame. Coordinate system S_p is also rigidly connected with the frame.

Vector $\Delta \underline{e}^{(2)}$ is represented by the matrix equation

$$\begin{aligned} \left[\Delta \underline{e}_f^{(2)} \right] &= \left[L_{fp} \right] \left[\Delta \underline{e}_p^{(2)} \right] = \\ &\begin{bmatrix} \cos \gamma_2 & 0 & -\sin \gamma_2 \\ 0 & 1 & 0 \\ \sin \gamma_2 & 0 & \cos \gamma_2 \end{bmatrix} \begin{bmatrix} \Delta e_2 \cos(\phi_2 + \alpha_2) \\ \Delta e_2 \sin(\phi_2 + \alpha_2) \\ 0 \end{bmatrix} \end{aligned} \quad (3.4.3)$$

It results from matrix equality (3.4.3) that

$$\left[\Delta \underline{e}_f^{(2)} \right] = \begin{bmatrix} \Delta e_2 \cos(\phi_2 + \alpha_2) \cos \gamma_2 \\ \Delta e_2 \sin(\phi_2 + \alpha_2) \\ \Delta e_2 \cos(\phi_2 + \alpha_2) \sin \gamma_2 \end{bmatrix} \quad (3.4.4)$$

Kinematical errors induced by gear's eccentricities are defined by an equation similar to (3.3.16):

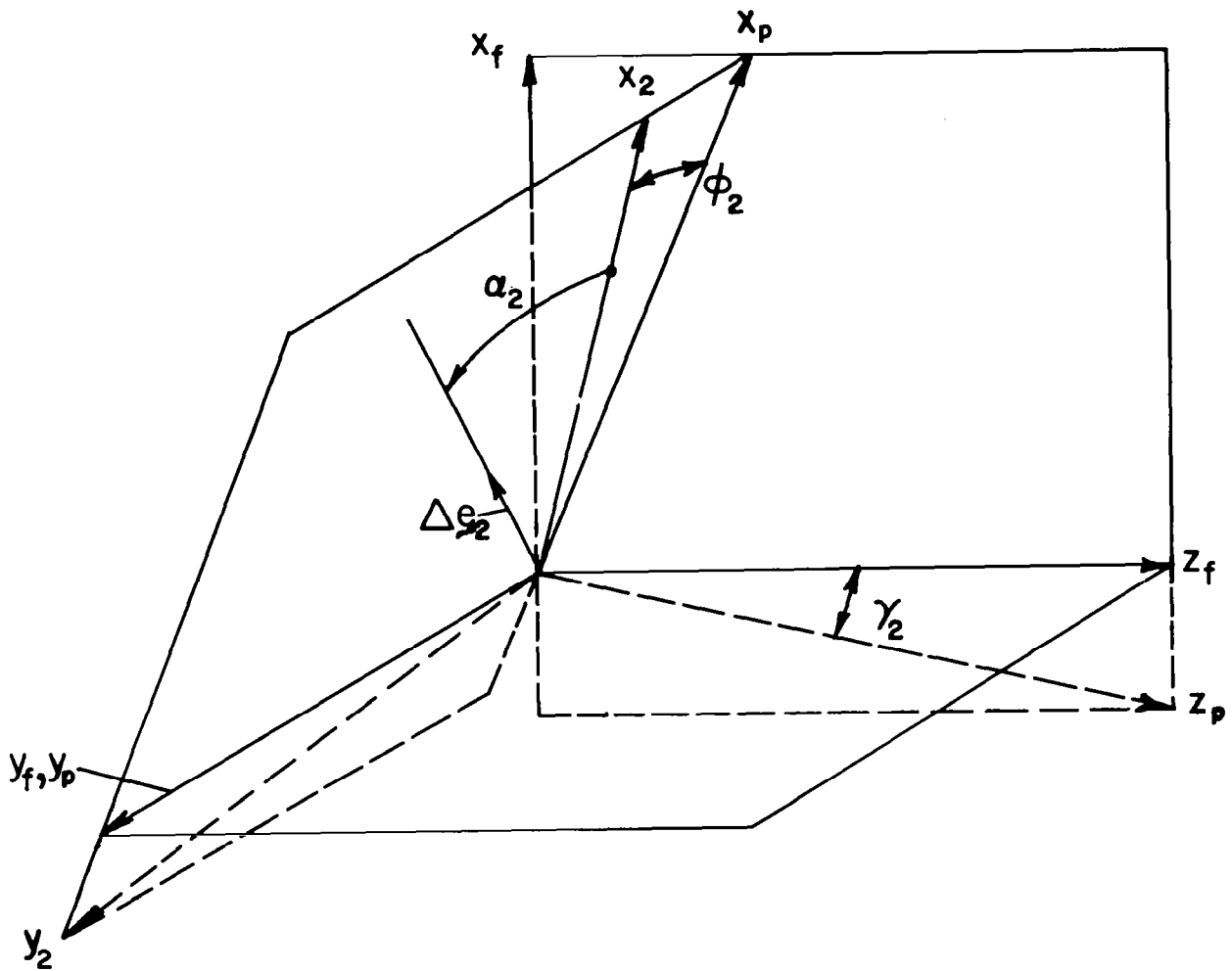


FIG 3.4.3

Coordinate Systems Associated with Gear 2

$$\left[\Delta \phi_f^{(2)} \rho_f^{(2)} n_f \right] = \left(\Delta e_f^{(1)} - \Delta e_f^{(2)} \right) \cdot n_f, \quad (3.4.5)$$

where $\Delta e_f^{(1)}$ and $\Delta e_f^{(2)}$ are represented by matrices (3.4.2) and (3.4.4); $\Delta \phi_f^{(2)}$ (Fig. 3.4.3) is represented by matrix

$$\left[\Delta \phi_f^{(2)} \right] = \left[L_{fp} \right] \left[\Delta \phi_p^{(2)} \right] = \begin{bmatrix} \cos \gamma_2 & 0 & -\sin \gamma_2 \\ 0 & 1 & 0 \\ \sin \gamma_2 & 0 & \cos \gamma_2 \end{bmatrix} \begin{bmatrix} 0 \\ 0 \\ \Delta \phi_2 \end{bmatrix} = \begin{bmatrix} -\Delta \phi_2 \sin \gamma_2 \\ 0 \\ \Delta \phi_2 \cos \gamma_2 \end{bmatrix} \quad (3.4.6)$$

Vector $\rho_f^{(2)}$ represents the position vector of a point which belongs to the line of action and n_f represents the unit normal of the contacting surfaces at their point of tangency.

Equations (3.4.5) and (3.4.6) yield

$$\Delta \phi_2 = \frac{n_x \Sigma \Delta e_x + n_y \Sigma \Delta e_y + n_z \Sigma \Delta e_z}{-y \cos \gamma_2 n_x + (x \cos \gamma_2 + z \sin \gamma_2) n_y - y \sin \gamma_2 n_z} \quad (3.4.7)$$

Here: $\Sigma \Delta e_x = \Delta e_x^{(1)} - \Delta e_x^{(2)}$, $\Sigma \Delta e_y = \Delta e_y^{(1)} - \Delta e_y^{(2)}$, $\Sigma \Delta e_z = \Delta e_z^{(1)} - \Delta e_z^{(2)}$. The subscript "f" was dropped in equation (3.4.7). The unit normal was represented by equations (2.2.10)

$$\begin{aligned} n_f &= \sin \psi_c i_{cf} + \cos \psi_c \sin \tau_d j_{df} + \cos \psi_c \cos \tau_d k_{df} = \\ &= \sin \psi_c i_{cf} + \cos \psi_c \left[\cos(\beta - \phi_d) j_{df} + \sin(\beta - \phi_d) k_{df} \right] = \\ &= \sin \psi_c i_{cf} + \cos \psi_c \left[\cos(\beta - \phi_1 \sin \gamma_1) j_{df} + \sin(\beta - \phi_1 \sin \gamma_1) k_{df} \right] \end{aligned} \quad (3.4.8)$$

Equations (3.4.7) by $\phi_1=0$ represent the surface unit normal at the point of intersection of the tooth surface with the generatrix of the pitch cone.

Coordinates x, y, z of a current point of line action were represented:

(a) by equations (2.2.25) for spiral bevel gears with geometry I; (b) by equations (2.6.4) for spiral bevel gears with geometry II.

In the process of meshing of one pair of teeth the angle of rotation ϕ_1 changes in the interval $[-\pi/N_1, \pi/N_1]$, where N_1 is the number of teeth of gear 1. Considering $\phi_1 \sin \gamma_1$ as negligible the unit surface normal can be represented by the equation

$$\vec{n}_f = \sin \psi_c \vec{i}_f + \cos \psi_c (\cos \beta \vec{j}_f + \sin \beta \vec{k}_f) \quad (3.4.9)$$

With the same assumption for $\phi_1 \sin \gamma_1$ it can be taken that

$$x_f = 0, y_f = 0, z_f = L \quad (3.4.10)$$

Equations (3.4.7), (3.4.9) and (3.4.10) yield

$$\Delta\phi_2(\phi_1) = \frac{n_x \Sigma \Delta e_x + n_y \Sigma \Delta e_y + n_z \Sigma \Delta e_z}{L \sin \gamma_2 \cos \psi_c \cos \beta} \quad (3.4.11)$$

Here:

$$\begin{aligned} n_x \Sigma \Delta e_x + n_y \Sigma \Delta e_y + n_z \Sigma \Delta e_z = & a_1 \sin(\phi_1 + \alpha_1) + b_1 \cos(\phi_1 + \alpha_1) \\ & + a_2 \sin(\phi_2 + \alpha_2) + b_2 \cos(\phi_2 + \alpha_2) \end{aligned} \quad (3.4.12)$$

Here:

$$\begin{aligned} a_1 &= -\Delta e_1 \cos \psi_c \cos \beta ; & b_1 &= \Delta e_1 (\cos \gamma_1 \sin \psi_c - \sin \gamma_1 \cos \psi_c \sin \beta) \\ a_2 &= -\Delta e_2 \cos \psi_c \cos \beta ; & b_2 &= -\Delta e_2 (\cos \gamma_2 \sin \psi_c + \sin \gamma_2 \cos \psi_c \sin \beta) \\ \phi_2 &= \phi_1 \frac{N_1}{N_2} \end{aligned} \quad (3.4.13)$$

It results from equations (3.4.12) that kinematical errors of spiral bevel gears can be represented as the sum of four harmonics. The period of two harmonics coincides with the period of revolution of gear 1; the period of the other two harmonics coincides with the period of revolution of driven gear (of gear 2).

The function $\Delta\phi_2(\phi_1)$ as defined by equation (3.4.11) is a smoothed function. In reality this function breaks by changing teeth in meshing. This break can be discovered if the function $\Delta\phi_2(\phi_1)$ is defined by equation (3.4.7).

Equation (3.4.11) can be applied for spur gears, too. By $L \sin \gamma_2 = r_2$, $\beta = 0$, $\sin \gamma_1 = \sin \gamma_2 = 0$ equations (3.4.11) and (3.4.12) yield:

$$\Delta \phi_2(\phi_1) = \frac{\Delta e_1 \sin(\psi_c - \phi_1 - \alpha_1) + \Delta e_2 \sin(\psi_c + \alpha_2 + \phi_1)}{r_2 \cos \psi_c}, \quad (3.4.14)$$

where r_2 is the pitch radius of gear 2.

Parameters α_1 and α_2 influence the distribution of function $\Delta \phi_2(\phi_1)$ in the positive and negative areas. For a drive with $N_1 = N_2$, $\alpha_2 = \pi + \alpha_1$ and $\Delta e_2 = \Delta e_1$ the function $\Delta \phi_2(\phi_1) \equiv 0$. In other words, kinematical errors induced by eccentricities Δe_1 and Δe_2 are compensated completely.

3.5 Kinematical Errors Induced by Misalignment

There are following kinds of misalignment (Fig. 2.2.2): (a) displacement of a gear in direction of positive or negative axis x_f ; (b) axial displacement of gear 1 in direction of its axis $0a$; (c) axial displacement of gear 2 in direction of axis $0b$; (d) an error of the angle made by axes $0a$ and $0b$.

Let us suppose that gear 1 is displaced in the direction of negative axis x_f by

$$\Delta s_q^{(1)} = -\Delta A i_f \quad (3.5.1)$$

Equations (3.3.16) and (3.5.1) yield

$$\left[\Delta \phi_{\rho}^{(2)} \right]_{\underline{n}} = -\Delta s_q^{(1)} \underline{n} \quad (3.5.2)$$

It results from (3.5.2) that

$$\Delta \phi_2(\phi_d) = \frac{-\Delta A \sin \psi_c}{-y \cos \gamma_2 n_x + (x \cos \gamma_2 + z \sin \gamma_2) n_y - y \sin \gamma_2 n_z} \quad (3.5.3)$$

Here: $\phi_d = \phi_1 \sin \gamma_1 = \phi_2 \sin \gamma_2$ is the angle of rotation of the generating gear; x, y, z are coordinates of the line of action represented by equations (2.2.25) and (2.6.4) for spiral bevel gears with geometry I and II, respectively.

Now, let us consider a case when gear 1 is displaced in the direction of negative axis y_f at

$$\Delta \underline{s}_q^{(1)} = - \Delta E \underline{j}_f \quad (3.5.4)$$

By analogy with equation (3.5.3) it will be

$$\Delta \phi_2(\phi_d) = \frac{\Delta E n_y}{-y \cos \gamma_2 n_x + (x \cos \gamma_2 + z \sin \gamma_2) n_y - y \sin \gamma_2 n_z} \quad (3.5.5)$$

The variation of the angle made by gear axes Oa and Ob can be represented as a result of rotation of one of the gears about axis y_f , for instance, gear 1. The vector of rotation is

$$\Delta \underline{\delta} = \Delta \delta \underline{j}_f \quad (3.5.6)$$

and the displacement of contact point is represented by equation

$$\Delta \underline{s}_q^{(1)} = \Delta \delta \times \underline{\rho}, \quad (3.5.7)$$

where $\underline{\rho}$ is the radius-vector drawn from o_f to the point of action.

Kinematical errors induced by $\Delta \underline{s}_q^{(1)}$ are represented by equation

$$\left[\Delta \underline{\phi}^{(2)} \underline{\rho} \underline{n} \right] = \left[\Delta \underline{\delta} \underline{\rho} \underline{n} \right] \quad (3.5.8)$$

Equation (3.5.8) yields

$$\Delta \phi_2(\phi_d) = \frac{(z n_x - x n_z) \Delta \delta}{-y \cos \gamma_2 n_x + (x \cos \gamma_2 + z \sin \gamma_2) n_y - y \sin \gamma_2 n_z} \quad (3.5.9)$$

Equations (3.5.3), (3.5.5) and (3.5.9) can be simplified for spiral bevel gears with geometry II taking into account that in this case $x = 0$,

$y=0$ (see equations (2.6.4)).

Equations proposed in this item can be applied for approximate determination of kinematical errors induced by incorrect methods of generation of spiral bevel gears and for determination of machine settings to compensate such errors.

It was mentioned in item 2.1 that a correct meshing of spiral bevel gears can be gotten by coinciding three axes of instantaneous rotation. In reality these axes do not coincide and therefore kinematical errors represented by equation (3.5.9) appear by $\Delta\delta$ equal to the sum of dedendum angles of the two gears.

To compensate these errors corrections of machine settings for cutting the pinion are used. These corrections are pinion displacements represented by equation

$$\Delta \underset{\sim}{s}_q^{(1)} = \Delta E \underset{\sim}{j}_f + \Delta L \underset{\sim}{k}_f, \quad (3.5.10)$$

where ΔE and ΔL are algebraic values.

Equations (3.3.15) and (3.5.10) yield

$$\Delta\phi_2(\phi_d) = \frac{\Delta E n_y + \Delta L n_z}{-y \cos \gamma_2 n_x + (x \cos \gamma_2 + z \sin \gamma_2) n_y - y \sin \gamma_2 n_z} \quad (3.5.11)$$

To compensate kinematical errors (3.5.9) the following function

$$f(\phi_d) = \frac{\Delta E n_y + \Delta L n_z - (z n_x - x n_z) \Delta\delta}{-y \cos \gamma_2 n_x + (x \cos \gamma_2 + z \sin \gamma_2) n_y - y \sin \gamma_2 n_z} \quad (3.5.12)$$

must be minimized.

Let us represent function $f(\phi_d)$ as a difference of two functions as follows:

$$f(\phi_d) = f_1(\phi_d) - f_2(d) \quad (3.5.13)$$

Here

$$f_2(\phi_d) = \frac{(z n_x - x n_z) \Delta \delta}{-y \cos \gamma_2 n_x + (x \cos \gamma_2 + z \sin \gamma_2) n_y - y \sin \gamma_2 n_z} \quad (3.5.14)$$

is the function of errors, and

$$f_1(\phi_d) = \frac{\Delta E n_y + \Delta L n_z}{-y \cos \gamma_2 n_x + (x \cos \gamma_2 + z \sin \gamma_2) n_y - y \sin \gamma_2 n_z} \quad (3.5.15)$$

is the compensating function which is applied in order to compensate the kinematical errors induced by $\Delta \delta$ as a result of an incorrect method of gear generation.

Let us define derivatives $\frac{df_1}{d\phi_d}$ and $\frac{df_2}{d\phi_d}$ at the main contact point at which $y=0$, $x=0$, $z=L$ for gears with geometry I and geometry II.

Geometry I. Projections of the surface unit normal were represented by equations (2.2.10)

$$\begin{aligned} n_x &= \sin \psi_c \\ n_y &= \cos \psi_c \sin(\theta_d - q_d + \phi_d) \\ n_z &= \cos \psi_c \cos(\theta_d - q_d + \phi_d) \end{aligned} \quad (3.5.16)$$

where ψ_c , θ_d and q_d are constant parameters and $\theta_d - q_d = 90^\circ - \beta$.

Coordinates of contact point were represented by equations (2.2.25)

$$\begin{aligned} x &= \left[r_d - b_d \frac{\sin(q_d - \phi_d)}{\cos(\beta - \phi_d)} \right] \sin \psi_c \cos \psi_c \\ y &= \frac{\cos(\beta - \phi_d)}{\tan \psi_c} \\ z &= \frac{b_d \sin \theta_d}{\cos(\beta - \phi_d)} + \frac{\sin(\beta - \phi_d)}{\tan \psi_c} x \end{aligned} \quad (3.5.17)$$

At the main contact point $\phi_d=0$, $x=y=0$, $z=L$. Equations (3.5.16) and (3.5.17) yield that at the main contact point

$$\frac{dn_x}{d\phi_d} = 0, \quad \frac{dn_y}{d\phi_d} = \cos \psi_c \sin \beta, \quad \frac{dn_z}{d\phi_d} = -\cos \psi_c \cos \beta \quad (3.5.18)$$

$$\frac{dx}{d\phi_d} = \frac{b_d \sin \theta_d}{\cos^2 \beta} \sin \psi_c \cos \psi_c = \frac{L}{\cos \beta} \sin \psi_c \cos \psi_c \quad (3.5.19)$$

$$\frac{dy}{d\phi_d} = L \cos^2 \psi_c \quad (3.5.20)$$

$$\frac{dz}{d\phi_d} = -L \sin^2 \psi_c \tan \beta \quad (3.5.21)$$

At the main contact point the derivative $\frac{df_2}{d\phi_d}$ is represented by equation

$$\frac{df_2}{d\phi_d} = \left\{ \frac{\frac{dz}{d\phi_d} n_x - \frac{dx}{d\phi_d} n_z}{L \sin \gamma_2 n_y} - \frac{n_x \left[\cos \gamma_2 \left(-\frac{dy}{d\phi_d} n_x + \frac{dx}{d\phi_d} n_y \right) + \sin \gamma_2 \left(\frac{dz}{d\phi_d} n_y + z \frac{dn_y}{d\phi_d} - \frac{dy}{d\phi_d} n_z \right) \right]}{L \sin^2 \gamma_2 n_y^2} \right\} \Delta \delta \quad (3.5.22)$$

Equations (3.5.22), (3.5.16) and (3.5.19)-(3.5.21) yield

$$\frac{df_2}{d\phi_d} = -\frac{\tan \beta \tan \psi_c}{\sin \gamma_2 \cos \beta} \Delta \delta \quad (3.5.23)$$

Equation (3.5.15), (3.5.16) and (3.5.19)-(3.5.21) yield that

$$\frac{df_1}{d\phi_d} = \frac{\Delta E \frac{dn_y}{d\phi_d} + \Delta L \frac{dn_z}{d\phi_d}}{L \sin \gamma_2 n_y} = \frac{\Delta E \sin \beta - \Delta L \cos \beta}{L \sin \gamma_2 \cos \beta} \quad (3.5.24)$$

Kinematical errors will be compensated in the neighborhood of the main contact point if

$$\frac{\partial f}{\partial \phi_d} = \frac{\partial f_1}{\partial \phi_d} - \frac{\partial f_2}{\partial \phi_d} = 0 \quad (3.5.25)$$

This requirement is satisfied by

$$\frac{\Delta E \sin \beta - \Delta L \cos \beta}{L} + \Delta \delta \tan \beta \tan \psi_c = 0 \quad (3.5.26)$$

A requirement that functions $f_1(\phi_d)$ and $f_2(\phi_d)$ must be equal at the main contact point yields

$$\frac{\Delta E \cos \beta + \Delta L \sin \beta}{L} - \Delta \delta \tan \psi_c = 0 \quad (3.5.27)$$

It results from equations (3.5.26) and (3.5.27) that

$$\frac{\Delta E}{L} = \frac{\tan \psi_c \cos 2\beta}{\cos \beta} \Delta \delta \quad (3.5.28)$$

$$\frac{\Delta L}{L} = 2 \tan \psi_c \sin \beta \Delta \delta \quad (3.5.29)$$

Equations (3.5.28) and (3.5.29) provide approximate magnitudes of machine settings for spiral bevel gears.

For spiral bevel gears with geometry II functions (3.5.14) and (3.5.15) will be the following ones.

$$f_2(\phi_d) = \frac{\Delta \delta n_x}{\sin \gamma_2 n_y} = \frac{\tan \psi_c}{\sin \gamma_2 \cos \beta} \Delta \delta \quad (3.5.30)$$

$$\frac{df_2}{d\phi_d} = - \frac{\cot q_d \tan \psi_c}{\cos \beta} \Delta \delta \quad (3.5.31)$$

$$f_1(\phi_d) = \frac{\Delta E n_y + \Delta L n_z}{z \sin \gamma_2 n_y} = \frac{\Delta E \cos \beta + \Delta L \sin \beta}{L \sin \gamma_2 \cos \beta} \quad (3.5.32)$$

$$\frac{df_1}{d\phi_d} = \frac{1}{L \sin \gamma_2} \left[\Delta L \left(\frac{\cot q_d}{\cos \beta \sin \beta} - 1 \right) - \Delta E \cot \beta \right] \quad (3.5.33)$$

Requirements that at the main contact point

$$f_1(\phi_d) = f_2(\phi_d) , \quad \frac{df_1}{d\phi_d} = \frac{df_2}{d\phi_d}$$

yield

$$\frac{\Delta E}{L} = (\cos \beta - \sin \beta \tan q_d) \tan \psi_c \Delta \delta \quad (3.5.34)$$

$$\frac{\Delta L}{L} = (\sin \beta + \cos \beta \tan q_d) \tan \psi_c \Delta \delta \quad (3.5.35)$$

4. CONCLUSION

- a. General kinematic relations for conjugate gear tooth surfaces are proposed. The proposed equations relate the motions of: (a) points of contact and (b) surface unit normals. The equations above are applied to define: (a) relations between principal curvatures and directions for two gear tooth surfaces which are in mesh, (b) kinematical errors induced by errors of manufacturing and assemblage.
- b. Two mathematical models of geometry of spiral bevel gears are proposed. Models above correspond to the motion of contact point across and along the tooth surface.
- c. The bearing contact of spiral bevel gears for both models is determined. A computer program for this has been worked out.
- d. Method to investigate kinematical errors of spiral bevel gears is worked out.

LIST OF SYMBOLS

Section 1

a	half the length of major axis
A	auxiliary function used in Eq. (1.7.30) represented by Eq. (1.7.31)
b	half the length of the minor axis
B	auxiliary function defined by Eq. (1.7.32)
C	shortest distance between axis of rotation
f_i	elastic deformation of surface Σ_i
$g_1 = \kappa_I^{(1)} - \kappa_{II}^{(1)}$	auxiliary function to determine size of contact ellipse
$g_2 = \kappa_I^{(2)} - \kappa_{II}^{(2)}$	auxiliary function to determine size of contact ellipse
λ_i	distance of point N from tangent plane t-t
$[L_{ij}]$	projection transformation matrix
M_o	point of contact of tooth surfaces
$[M_{ij}]$	coordinate transformation matrix; transformation from S_j to S_i
$\tilde{n}_{abs}^{(i)}$	absolute velocity of the end of unit normal
$\tilde{n}_i(u_i, \theta_i)$	unit normal vector to surface Σ_i
$(\tilde{n}_x^{(i)}, \tilde{n}_y^{(i)}, \tilde{n}_z^{(i)})$	projections of $\tilde{n}^{(i)}$ in coordinate system S_f
$\dot{\tilde{n}}_r^{(i)}$	relative velocity of the end of unit normal vector \tilde{n}_i
$\dot{\tilde{n}}_{tr}^{(i)}$	transfer velocity of the end of unit normal vector \tilde{n}_i
N	a point on surface Σ_1
N_1	new position of point N after displacement
N_2	final position of point N after displacement and elastic deformation
N'	point on surface 2
N'_2	final position of N' after displacement and elastic deformation

N_i	normal vector to surface Σ_i
$r_i(u_i, \theta_i)$	position vector describing surface Σ_i with surface coordinate (u_i, θ_i)
$S_i(x_i, y_i, z_i)$	coordinate system i
$t-t$	tangent plane to surface Σ_1 and Σ_2
$\tilde{v}_{abs}^{(i)}$	absolute velocity of contact point on surface Σ_i
$\tilde{v}_r^{(i)}$	relative velocity of contact point on surface Σ_i
$\tilde{v}_{tr}^{(i)}$	transfer velocity of contact point on surface Σ_i
$V_1^{(i)}$	transfer velocities of points on surface Σ_i in coordinate system 1
$V_1^{(21)} = V_1^{(2)} - V_1^{(1)}$	relative velocity of point 2 with respect to point 1
$(x_f^{(i)}, y_f^{(i)}, z_f^{(i)})$	Cartesian coordinates of contact point on surface Σ_i as expressed in coordinate system S_f
$\alpha^{(1)}$	angle made by axis η and $i_I^{(1)}$
$\alpha^{(2)}$	angle made by axis η and $i_I^{(2)}$
γ	angle of crossing of axis of rotation
δ	approach of surface Σ_1 and Σ_2
δ_1	displacement of surface Σ_1 when Σ_1 and Σ_2 are in meshing
δ_2	displacement of surface Σ_2
$(\hat{i}_I^{(1)}, \hat{i}_{II}^{(1)})$	unit vectors along principal direction of surface Σ_1
$(\hat{i}_I^{(2)}, \hat{i}_{II}^{(2)})$	unit vector along principal direction of surface Σ_2
$\kappa_I^{(1)}, \kappa_{II}^{(1)}$	principal curvatures of surface Σ_1
$\kappa_I^{(2)}, \kappa_{II}^{(2)}$	principal curvatures of surface Σ_2
$\kappa_\varepsilon^{(1)} = \kappa_I^{(1)} + \kappa_{II}^{(1)}$	auxiliary function
$\kappa_\varepsilon^{(2)} = \kappa_{II}^{(2)} + \kappa_I^{(2)}$	auxiliary function
ρ	distance of points N and N' from point M_0
σ	angle between $\hat{i}_I^{(1)}$ and $\hat{i}_{II}^{(1)}$

Σ_i	surface i
ϕ_i	angle of rotation of gear i
$\omega_f^{(i)}$	angular velocity of surface Σ_i

Section 2 (i = 1, 2) (d = f, k)

$a_{31}^{(1)}$	auxiliary function defined by Eq. (2.4.11)
$a_{32}^{(1)}$	auxiliary function defined by Eq. (2.4.12)
$b_3^{(1)}$	auxiliary function defined by Eq. (2.4.13)
b_d	a parameter of tool setting
$F^{(i)}$	auxiliary function used to compute the principal direction of surface Σ_i
$G^{(i)}$	auxiliary function used to compute the principal curvatures of surface Σ_i
$[L_{ij}]$	projection transformation matrix
$[M_{ij}]$	coordinate transformation matrix; transformation from S_j to S_i
\tilde{n}_f	surface unit normal
$N_f^{(d)}$	surface normal to surface d
q_d	a parameter of tool setting
$r_f^{(d)}$	locus of contact point on surface d
r_d	a parameter of tool setting
$S^{(i)}$	auxiliary function used to compute principal curvature of surface Σ_i
$S_a(x_a, y_a, z_a)$	auxiliary coordinate system
$S_c(x_c, y_c, z_c)$	coordinate system used to represent surface Σ_F in geometry II
S_h	coordinate system rigidly connected with frame
S_i	coordinate system rigidly connected with gear i
u_d	generating surface coordinate

$V_f^{(F1)}$	relative velocity of a contact point on surface Σ_F with respect to contact point on surface Σ_1
$V_f^{(K2)}$	relative velocity of a contact point on surface Σ_K with respect to contact point on surface Σ_2
(x_f, y_f, z_f)	coordinates of the line of action of surface Σ_i
$(x_f^{(d)}, y_f^{(d)}, z_f^{(d)})$	components of the equations of the generating surface $\Sigma_{(d)}$
β	$90^\circ - (\theta_d - q_d)$ see Eq. (2.2.24)
γ_i	half of pitch cone angles of gear i
θ_d	generating surface coordinate
$i_I^{(d)}$	unit vector representing the first principal direction of surface d
$i_{II}^{(d)}$	unit vector representing the second principal direction of surface d
$\kappa_I^{(d)}$	principal curvature I of surface d
$\kappa_{II}^{(d)}$	principal curvature of II of surface d
$\sigma^{(i)}$	angle between $i_I^{(d)}$ and D_i positive clockwise
Σ_d	tool surface d
Σ_i	generated surface of pinion and gear
τ_d	$\theta_d - (q_d - \phi_d)$ auxiliary function
ϕ_d	angle of rotation of generating surface about axis x_f
ϕ_i	angle of rotation of gear i
ψ_c	shape angle of head-cutter blades
$\omega^{(dl)}$	relative angular velocity of contact point on surface d with respect to contact point on surface l
$\omega^{(d)}$	angular velocity of surface d
$\omega^{(i)}$	angular velocity of gear i

Section 3

ΔA	gear displacement
ΔE	machine setting
$\Delta e^{(i)}$	eccentricity vector of gear i
ΔL	machine setting
M_i	contact point on surface Σ_i
$\underline{n}_f^{(i)}$	unit normal vector of surface Σ_i
$\Delta \underline{Q}$	vector of errors
Q_i	components of vector of errors
$\underline{x}_f^{(i)}$	position vector of point on surface Σ_i
$d\underline{S}_q^{(i)}$	displacement vector of contact point due to kinematical errors
α_i	angular position of eccentricity vector
$\Delta \delta$	sum of dedendum angles of gears 1 and 2
Σ_i	surface i
$\Delta \phi_2$	kinematical error function
ϕ_2°	theoretical value of gear 2 angle of rotation
ϕ_2	actual value of gear 2 angle of rotation

REFERENCES

1. J. Coy, D. P. Townsend and E. **Zaretsky**, "Dynamic Capacity and **Surface Fatigue Life for Spur and Helical Gears**," ASME, Journal of Lubrication Technology, Vol. 98, No. 2, April 1966, pp. 267-276.
2. F. Litvin, Theory of Gearing, Second Edition, Nauka, 1968 (in Russian).
3. F. Litvin, "Die Beziehungen zwischen den Krümmungen der Zahnoberflächen bei räumlichen Verzahnungen," ZAMM, 49 (1969), Heft 11, Seite 685-690.
4. F. Litvin, "The Synthesis of Approximate Meshing for Spatial Gears," Journal of Mechanisms, Vol. 4, 1969, Pergamon Press, pp. 187-191.
5. F. Litvin, "An Analysis of Undercut Conditions and of Appearance of Contact Lines Envelope Conditions of Gears, ASME Transactions, Journal of Mechanical Design, July 1978, pp. 423-432.
6. F. Litvin, K. Petrov and V. Ganshin, "The Effects of Geometric Parameters of Hypoid and Spiroid Gears on Their Quality Characteristics," ASME Transactions, Journal of Engineering for Industry, February 1974, pp. 330-334.
7. F. Litvin, N. Krylov and M. Erichov, "Generation of Tooth Surfaces by Two-Parameter Enveloping," Mechanism and Machine Theory, Vol. 10, 1975, Pergamon Press, pp. 365-373.
8. M. Baxter, "Exact Determination of Tooth Surfaces for Spiral Bevel and Hypoid Gears," AGMA Paper #139.02, October 1966.
9. E. Wildhaber, "Surface Curvature - A Tool for Engineers," Industrial Mathematics, Vol. 5, 1954, pp. 31-116.
10. M. Baxter, "Second-Order Surface Generation," Industrial Mathematics, Vol. 23, Part 2, 1973, pp. 85-106.
11. M. Baxter, "Effect of Misalignment on Tooth Action of Bevel and Hypoid Gears," ASME Paper #61-MD-20.
12. F. Litvin and Ye. Gutman, "Methods of Synthesis and Analysis for Hypoid Gear Drives of 'Formate' and 'Helixform'," P. 1, P. 2, P. 3, Transactions of the ASME, Journal of Mechanical Design, Vol. 103, January 1981, pp. 83-102.
13. F. Litvin and Ye. Gutman, "A Method of Local Synthesis of Gears Grounded on the Connections Between the Principal and Geodetic Curvatures of Surfaces," Transactions of the ASME, Journal of Mechanical Design, Vol. 103, 1981, pp. 102-113.

1. Report No. NASA CR-3553	2. Government Accession No.	3. Recipient's Catalog No.	
4. Title and Subtitle MATHEMATICAL MODELS FOR THE SYNTHESIS AND OPTIMIZATION OF SPIRAL BEVEL GEAR TOOTH SURFACES		5. Report Date June 1982	6. Performing Organization Code
		8. Performing Organization Report No. None	10. Work Unit No.
7. Author(s) F. L. Litvin, Pernez Rahman, and Robert N. Goldrich		11. Contract or Grant No. NAG-348	13. Type of Report and Period Covered Contractor Report
9. Performing Organization Name and Address University of Illinois at Chicago Circle Dept. of Materials Engineering Box 4348 Chicago, Illinois 60680		14. Sponsoring Agency Code 511-58-12	
		12. Sponsoring Agency Name and Address National Aeronautics and Space Administration Washington, D.C. 20546	
15. Supplementary Notes Final report. Project Manager, John J. Coy, Propulsion Laboratory, AVRADCOM Research and Technology Laboratories, NASA Lewis Research Center, Cleveland, Ohio 44135.			
16. Abstract Spiral bevel gears have widespread applications in the transmission systems of aircraft. Major requirements in the field of helicopter transmissions are: (a) improved life and reliability, (b) reduction in overall weight (i.e., a large power to weight ratio) without compromising the strength and efficiency during the service life, (c) reduction in the transmission noise. The first two parts of this report deal with tooth contact geometry. In this report, a novel approach to the study of the geometry of spiral bevel gears and to their rational design is proposed. The nonconjugate tooth surfaces of spiral bevel gears are, in theory, replaced (or approximated) by conjugated tooth surfaces. These surfaces can be generated: (a) by two conical surfaces and (b) by a conical surface and a revolution. Although these conjugated tooth surfaces are simpler than the actual ones, the determination of their principal curvatures and directions is still a complicated problem. Therefore, a new approach, to the solution of these is proposed in this report. In this approach, direct relationships between the principal curvatures and directions of the tool surface and those of the generated gear surface are obtained. With the aid of these analytical tools, the Hertzian contact problem for conjugate tooth surfaces can be solved. These results are eventually useful in determining compressive load capacity and surface fatigue life of spiral bevel gears. In the third part of this report, a general theory of kinematical errors exerted by manufacturing and assembly errors is developed. This theory is used to determine the analytical relationship between gear misalignments and kinematical errors. This is important to the study of noise and vibration in geared systems.			
17. Key Words (Suggested by Author(s)) Gears Mechanism Optimization Transmissions		18. Distribution Statement Unclassified - unlimited STAR Category 37	
19. Security Classif. (of this report) Unclassified	20. Security Classif. (of this page) Unclassified	21. No. of Pages 121	22. Price* A06